DISSERTATION

VALVE INTERSTITIAL CELL PHENOTYPES AND SIGNALING PATHWAYS INVOLVED WITH CANINE MYXOMATOUS DEGENERATIVE MITRAL VALVE DISEASE

Submitted by

Sirilak Disatian

Department of Clinical Sciences

In partial fulfillment of the requirements

For the Degree of Doctor of Philosophy

Colorado State University

Fort Collins, Colorado

Summer 2008

UMI Number: 3332723

Copyright 2008 by
Disatian, Sirilak

All rights reserved.

INFORMATION TO USERS

The quality of this reproduction is dependent upon the quality of the copy submitted. Broken or indistinct print, colored or poor quality illustrations and photographs, print bleed-through, substandard margins, and improper alignment can adversely affect reproduction.

In the unlikely event that the author did not send a complete manuscript and there are missing pages, these will be noted. Also, if unauthorized copyright material had to be removed, a note will indicate the deletion.

UMI®

UMI Microform 3332723
Copyright 2008 by ProQuest LLC.
All rights reserved. This microform edition is protected against unauthorized copying under Title 17, United States Code.

ProQuest LLC
789 E. Eisenhower Parkway
PO Box 1346
Ann Arbor, MI 48106-1346

Copyright by Sirilak Disatian 2008

All Rights Reserved

COLORADO STATE UNIVERSITY

May 30, 2008

WE HERE BY RECOMMEND THAT THE DISSERTATION PREPARED UNDER OUR SUPERVISION BY SIRILAK DISATIAN ENTITILED VALVE INTERSTITIAL CELL PHENOTYPES AND SIGNALING PATHWAYS INVOLVED WITH CANINE MYXOMATOUS DEGENERATIVE MITRAL VALVE DISEASE BE ACCEPTED AS FULFILLING IN PART REQUIREMENTS FOR THE DEGREE OF DOCTOR OF PHILOSOPHY.

Committee on Graduate Work

Janice M. Bright

Eric Mohnet

E.J. Ehrhart

Advisor: E. Christopher Orton

Department Head/Director

ABSTRACT OF DISSERTATION

VALVE INTERSTITIAL CELL PHENOTYPES AND SIGNALING PATHWAYS INVOLVED WITH CANINE MYXOMATOUS DEGENERATIVE MITRAL VALVE DISEASE

Myxomatous mitral valve disease is a common naturally-occurring heart disease of dogs that is pathologically similar to myxomatous mitral valve disease in humans. Thus, the first hypothesis of this dissertation is that interstitial cell phenotype transformation recently described in human myxomatous valves also occurs in dogs with myxomatous mitral valves and correlates with disease severity. Normal and early-, intermediate-, and late-stage myxomatous canine mitral valves were examined by histology and immunohistochemistry for cytoskeletal (vimentin, desmin, smooth muscle α-actin, smooth muscle myosin, and non-muscle myosin), collagenolytic (MMP-1, MMP-13), cell surface (CD-31, CD-45, CD-68) and proliferation (Ki-67) proteins. Normal canine mitral valve interstitial cells were positive for vimentin, but negative for α-actin, desmin, and non-muscle myosin (i.e. fibroblast phenotype). Interstitial cells from myxomatous valves showed increased positive staining for α-actin and desmin, but were negative for smooth muscle myosin (i.e. myofibroblast phenotype). Positive staining cells first appeared as cellular clusters in the subendocardial region of the *lamina atrialis* and extended into deeper layers with increasing severity. Interstitial cells from myxomatous valves showed positive staining for non-muscle myosin

(i.e. activated mesenchymal cell phenotype). Positive staining cells increased with disease severity and were dispersed throughout the valve layers. Expression of MMP-1 and MMP-13 increased in myxomatous mitral valves and correlated with disease severity. Interstitial cellularity increased dramatically in degenerative mitral valves however Ki-67 staining was only mildly increased. In conclusion, two patterns of interstitial cell phenotype transformation were identified in dogs with myxomatous mitral valve disease and both correlated with disease severity. Myofibroblast transformation characterized by positive staining for α-actin and desmin occurred in cellular clusters primarily in the *lamina atrialis*. Mesenchymal cell activation characterized by positive staining to non-muscle myosin occurred throughout the valve.

Myxomatous mitral valve disease in dogs shares similar pathological lesions to serotonin induced heart valve disease in humans. The second hypothesis of this dissertation is that serotonin signaling and its closely associated signaling pathways including mitogen activated protein kinases/extracellular signal-regulated kinases (MAPK/ERK), and transforming growth factor β1 (TGFβ1) play a role in canine myxomatous mitral valve disease. Septal mitral valve leaflets from dogs affected by late-stage myxomatous disease and healthy dogs were collected. Immunohistochemistry and Western blot analyses were performed to determine the expression of target proteins involved in serotonin, MAPK/ERK, and TGFβ1 signaling pathways in canine normal and myxomatous mitral valves. Both immuohistochemistry and Western blotting demonstrated the up-regulation of $5HT_{2B}$ receptor, phosphorylated ERK1/2, and TGFβ1 receptor I and II, latent TGFβ1 and tryptophan hydroxylase 1 (TPH1) in myxomatous mitral valves; whereas, the expression of serotonin transporter (SERT) was down-regulated in myxomatous valves compared to normal valves.

In conclusion, serotonin and its cross linking pathways including MAPK/ERK and TGFβ1 may have roles in pathogenesis of canine myxomatous mitral valve disease. This study provides preliminary data for further studies investigating exact roles of these signaling transduction pathways in pathogenesis of myxomatous mitral valve disease in dogs.

Sirilak Disatian
Clinical Sciences Department
Colorado State University
Fort Collins, CO 80523
Summer 2008

ACKNOWLEDGEMENTS

First of all, I would like to gratefully thank Dr. E Chistopher Orton my advisor for all of his guidance, patience and support during my doctoral work. I would also like to thank my committee members Dr. Janice M Bright, Dr. Eric Monnet and Dr. EJ Ehrhart for their comments and guidance on this dissertation. In addition, I am very grateful to Anandamahidol foundation for the scholarship they awarded me. My thanks also go to Dr. Leigh Griffiths for teaching me the Western blotting method. Without his help, I would never have been able to finish my study. I would also like to acknowledge Dennis J Madden, all pathology staff, and Dr. Nicole Wilkerson for helping me to find and collect canine mitral valve tissues for using in this study. Special thanks to Dr. Kenneth F Reardon for his kindness by allowing me to use the CCD camera in his laboratory. Most importantly, I would like to thank my parents and my brother for their love, support and encouragement. At last, I would like to specially thank Auttapol Suebpongsakorn for cheering me up and standing by me through all good and bad times.

TABLE OF CONTENTS

LIST OF TABLES

LIST OF FIGURES

LIST OF ABBREVIATIONS

MVD	Myxomatous degenerative mitral valve disease
VIC	Valve interstitial cell
α-actin	Alpha smooth muscle actin
ECM	extracellular matix
MMP	matrix metalloproteinases
5-HT	5-hydroxytryptamine
MAPK	mitogen activated protein kinases
ERK	extracellular signaling kinases
TPH	tryptophan hydroxylase
SERT	serotonin transporter
TGF β	transforming growth factor β

CHAPTER 1

INTRODUCTION

Myxomatous degenerative mitral valve disease (MVD) is a common cardiac disease in dogs. At present, the etiology of this disease is unclear. Valve interstitial cells (VIC), the major cell type in heart valves, are implicated in several heart valve diseases. VIC have been characterized by two phenotypes, a 'quiescent' or 'fibroblast' phenotype and 'activated' or 'myofibroblast' phenotype. Because of an increased expression of the activated phenotype in human myxomatous degenerative mitral valves, this phenotype has been suspected to mediate pathological changes associated with MVD in humans. Studies investigating VIC phenotype in canine degenerative heart valves have yet to be reported. In addition, the spatial and temporal course of phenotype transformation of VIC during the progression of degeneration is not well established. Thus, the present study was undertaken to test the hypotheses that transformation of VIC occur in canine myxomatous degenerative mitral valve tissue and that the pattern of distribution depends on the stage of degeneration. In order to address these hypotheses, we used the cytoskeleton markers including vimentin, desmin, α-smooth muscle actin (α-actin) and non-muscle embryonic myosin to follow changes of VIC phenotype within the canine degenerative mitral valve tissues. To evaluate a role of these transformed VIC as a mediator of extracellular matrix (ECM) remodeling in canine degenerative valves, the expression of collagenase enzymes (MMP-1 and MMP-13) was reviewed.

Previous studies have established a role of serotonin or 5-hydroxytryptamine (5-HT) in human carcinoid heart valve disease and anorexigen drug (i.e. Fen/Phen) heart valve disease. Because of similarities between serotonin-mediated heart valve diseases and canine MVD, we hypothesized that paracrine-autocrine serotonin signaling might also play a role in canine MVD. Mitogen activated protein kinases (MAPK) signaling, a downstream signaling pathway of serotonin signaling, has reported to have mitogenic effects on different cells of mesenchymal origin. We hypothesized that MAPK signaling would mediate serotonin signaling in canine heart valves as well. Thus, we studied the expression of receptors and effector proteins involved in serotonin-MAPK signaling pathway in dogs affected by MVD. Tryptophan hydroxylase 1 (TPH1) is the rate-limiting enzyme in serotonin synthesis. Thus expression of TPH1 in diseased valve would be a necessary for serotonin to function as a paracrine or autocrine mediator of degenerative heart disease. Serotonin transporter (SERT) is necessary for reuptake and metabolism of serotonin. Thus, alternations in SERT expression could influence the pathogenesis of degenerative mitral valve disease. Lastly, transforming growth factor β1 (TGFβ1) signaling has been closely linked to serotonin signaling in mediating cell phenotype transformation, cell proliferation and alterations in the extracellular matrix in cultures mesenchymal cells. We thus hypothesized that TGFβ signaling might also be playing a role in naturally occurring canine mitral valve disease.

CHAPTER 2

LITERATURE REVIEW

Myxomatous degenerative mitral valve disease (MVD) is the most common cardiac disease in dogs (Whitney, 1974). It accounts for approximately 75 percent of the cardiovascular diseases seen in dogs (Delweiler and Patterson, 1965; Das and Tashijan, 1965). This degenerative disease is also known as mitral valve prolapse, endocardiosis, chronic degenerative valvular disease, chronic valvular disease, chronic valvular fibrosis, and acquired mitral regurgitation/insufficiency. The prevalence of MVD in dogs is age related. It was found that 58 percent of dogs aged 9 years old and older had marked pathologic changes of MVD (Whitney, 1974). Small breed dogs including Miniature poodles, Cocker spaniels, Miniature schnauzers, Dachshunds, Pomeranians, Chihuahuas, Pekingese, Fox terriers, and Boston terriers are predisposed to this disease. Cavalier King Charles spaniel breed is especially prone to MVD. This breed of dogs tends to develop disease earlier in life. It has been reported that 50 percent of Cavaliers have a murmur secondary to mitral regurgitation by the age of 5-6 years (Darke, 1987). In addition, degenerative lesions tend to progress faster in Cavaliers than the other breeds of dogs. It has been found that approximately 15-20% of Cavaliers develop the advanced disease before they are 10 years of age (Haggstrom, 1996). Generally, the prevalence and severity of MVD in young dogs do not show a gender-dependent difference (Olsen et al, 1999). However, in advancing age, male dogs are affected

more frequently and severely than female dogs (Buchanan, 1977). In addition, the disease progression in male dogs is faster than in female dogs.

Mitral valve function and architecture

Gross morphology

The canine mitral valve is comprised of septal (anterior) leaflet, parietal (posterior) leaflet and small commissural cusps positioned between two leaflets. Entire valve complex consists of valve annulus, leaflets, chordae tendineae, and papillary muscles (Fig. 2.1). Both leaflets and cusps connect to papillary muscles by chordae tendineae. Leaflets have chordae tendineae from both papillary muscles; on the other hand, commissural cusps have only chordae from one papillary muscle attached to them. Leaflet borders are rough and opaque called the 'rough zone'. Remaining portions of the leaflet are transparent called the 'clear zone'. Mitral valve annulus is a fibrous ring that lies between the left atrium and left ventricle.

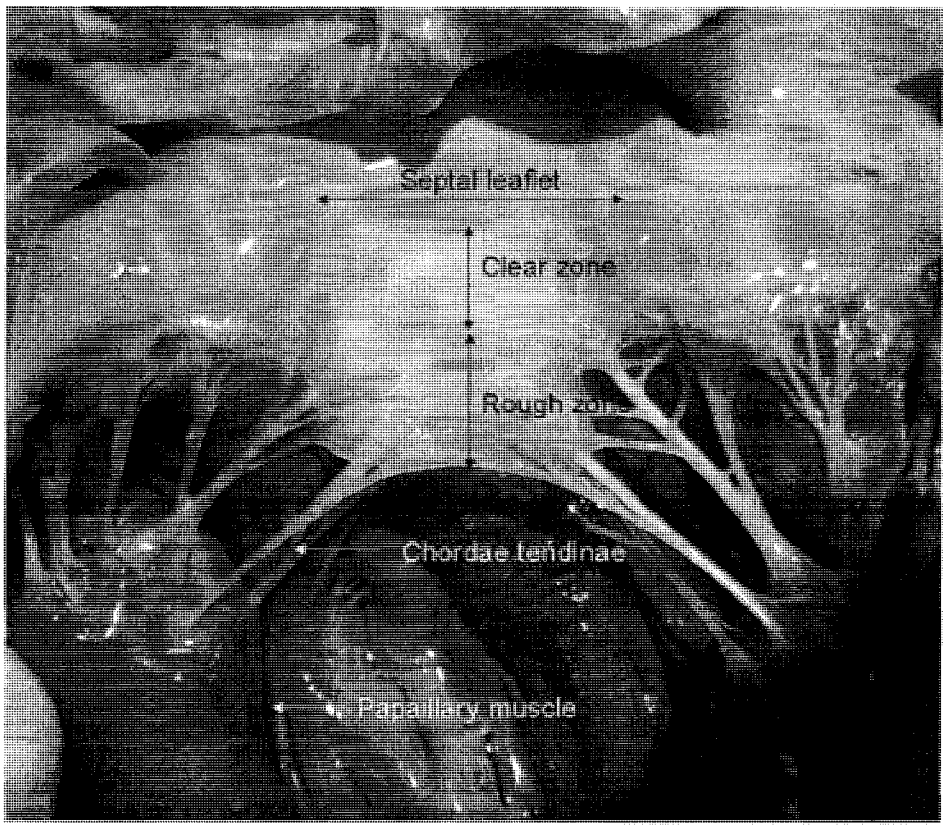

Figure 2.1: Illustration demonstrates canine mitral valve complex: valve annulus, leaflet, chordae tendineae, and papillary muscle.

Normal histology of mitral valve

Mitral valve is a complex layered structure comprised of valvular endothelial cells (VEC), valvular interstitial cells (VIC) and extracellular matrix (ECM). Each layer of valve leaflet is enriched in a specific ECM component which has a different function in accommoding shape and dimension of valve leaflet during cardiac cycle. The normal mitral valve leaflets consist of three layers as follows (Fig. 2.2):

1) *Atrialis* is comprised of an endothelial cell layer and abundant elastic fibers. The atrialis layer forms the contact aspect to the leaflet. This layer continues with the endocardium of the atrium.

2) *Spongiosa* is composed of loosely arranged collagen and proteoglycans. It lies between atrialis and fibrosa layers.

3) *Fibrosa* is a basic supportive component of the mitral leaflet. It is composed predominantly of collagen fibers. It continues with chordae tendineae and the fibrous tissue of the annulus (in case of parietal leaflet) or the aortic mitral intervalvular fibrosa (in case of septal leaflet).

Chordae tendineae, structures that connect valve leaflets and cusps to papillary muscles are composed of two distinct layers including 1) central fibrous core, a layer of densely packed collagen bundles and 2) a thin layer of loose collagen and elastic fibers. The outer surface of chordae tendineae is completely covered by a single continuous layer of endothelial cells.

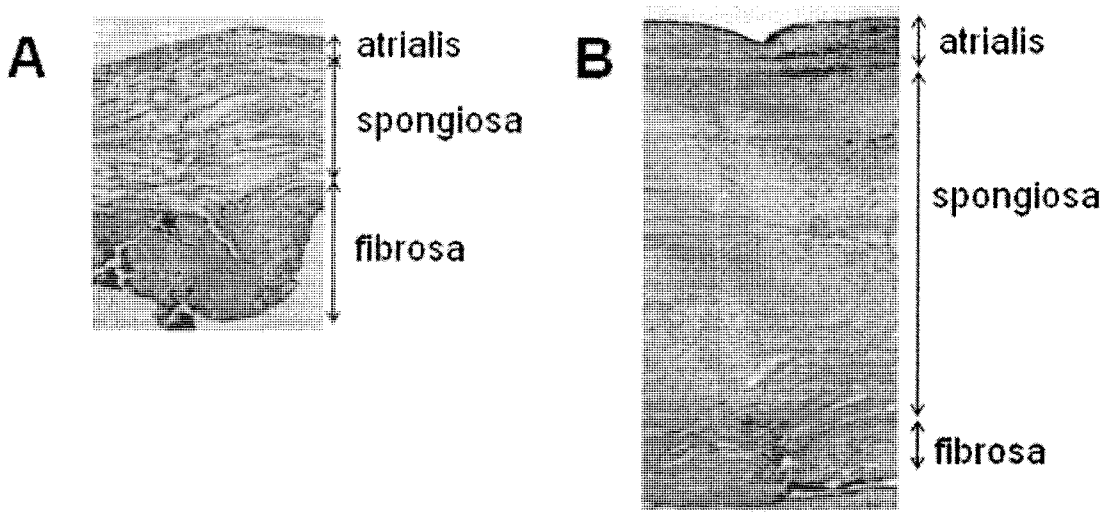

Figure 2.2: Morphological features of canine normal (A) and degenerative mitral valves (B). Original magnification x100. The normal mitral valve leaflets consist of three layers including the atrialis, spongiosa, and fibrosa layers. The myxomatous degenerative mitral valve appears with valve structure disorganization and increased in glycosaminoglycan accumulation.

Normal function of the mitral valve complex

The closure of the mitral valve normally occurs secondary to the coordination of each component within the mitral valve complex. During left atrial systole, blood flows through the mitral orifice. This creates a negative pressure area within the inflow tract and causes the tip of leaflets close to each other. The early valve closure occurs when the left atrial pressure decreases below left ventricular pressure. With the help of papillary muscles, mitral valve leaflets move together at the onset of ventricular systole. When systole proceeds, increasing pressure in left ventricle causes firm coaptation of the valve leaflets. Normality, chordae tendineae, papillary muscles as well as the supportive action of coapted valve leaflets limit the protrusion of valve leaflets back into the left atrium during ventricular systole.

Pathology of myxomatous degenerative mitral valve

Gross pathology

The common macroscopic appearance of degenerative mitral valve leaflets is characterized by thickened and enlarged leaflets with rolling up edges and elongated chordae tendineae (Das and Tashjihan, 1965; Kvat et al 2000). Pathologic changes of MVD primarily start at the free edge of valve leaflets and are apparently pronounced in areas where chordae tendineae insert. With disease progression, degenerative lesions spread from the margin into the other parts of valve leaflets. In the late stage of degeneration, valve leaflets become opaque, thicken and bulge. In addition, the chordae tendineae are elongated and thick particularly at the proximal portion. Ruptured chordae tendineae may be found (Fig. 2.3).

Figure 2.3: Illustration demonstrates the gross morphology of canine myxomatous degenerative mitral valve with chordal rupture (arrow)

Whitney (1975) classified myxomatous degenerative mitral valves into 4 types which were then modified by Kogure (1980) into 3 categories as follow.

Class I (Whitney's group 1 and 2): Small discrete and large coalescent nodules along the edge of leaflets and rough zone area. No chordal thickening.

Class II (Whitney's group 3): Thickening with plaque-like deformity all over the rough zone of leaflets and proximal portion of the chordae tendineae. No chordal rupture.

Class III (Whitney's group 4): Severe thickening all over valve leaflets (rough zone and clear zone) with elongation and occasional rupture of chordae tendineae.

Other morphologic alterations involved in dogs affected by MVD include left atrial enlargement, dilatation of mitral valve annulus, hypertrophy of the left ventricle, jet impact lesions in the left atrium, and endomyocardial tears.

Histopathology

Histological findings of MVD include deposition of glycosaminoglycans (GAG), and fragmentation of collagen bundles and elastic fibers. The study by Kogure (1980) determined that the deposition of GAG primarily appears in the spongiosa layer. As the disease progresses, the collagen bundles in the fibrosa layer become fragmented, coiled, and disorganized. The accumulation of GAG increases and invades the fibrosa layer displacing fragments of disrupted collagen within this layer. In the late stage of degeneration, the distinction between leaflet layers disappears. In addition, the disposition of GAG is visible in the chordae tendineae. Secondary fibrosis may be seen in the atrialis and ventricularis layers in severely affected valves.

Electronmicroscopic lesions

Low magnification scanning electron microscope has revealed marked thickening and swelling of the free edge of valve leaflets and swelling of the chordae tendineae at the area which they attach to the ventricular side of the leaflet (Corcoran et al, 2004). Marked damage in area close to the free edge of the valve was demonstrated at high magnification. Endothelial damage was also detected extending from valve leaflets to the proximal part of the chordae tendineae. Transmission electron microscope demonstrated disorganized matrix structure including collagen fiber degeneration, excessive GAG accumulation and elastic fiber fragmentation. Lysis of valve interstitial cells was also seen (Black et al, 2005).

Canine myxomatous degenerative mitral valve disease

Pathophysiology

The physiologic abnormality of canine MVD results from improper coaptation of mitral valve leaflets during ventricular systole. The severity of disease generally depends on the size of the regurgitant orifice and the aortic impedance to ejection blood. During the early stage of degeneration, the mitral valve remains competent and no hemodynamic alterations occur. Once, the mitral valve is incompetent, the forward flow into the systemic circulation decreases accompanied with the augmented regurgitant flow backward to the left atrium. At the first stage of mitral regurgitation, the left ventricle responds to the reduction of forward flow by increasing total stroke volume. These events occur secondary to activation of renin-angiotensin-aldosterone (RAAS) system and Frank-Staring mechanisms. As the regurgitant volume increases, the heart increases the total stroke volume by increasing contractility and heart rate to compensate for the loss of forward flow. These events are regulated by

sympathetic nervous system. Both left atrium and left ventricle dilate as a result of remodeling to accommodate a larger stroke volume. In an attempt to maintain ventricular function and normalize wall stress, the thickness of ventricular wall also increases. When severe mitral regurgitation develops over a long period of time, the left atrial chamber becomes more compliant resulting in a more powerful contraction to provide an adequate ventricular filling volume. Finally, as the disease progresses into a cardiac decompensated stage, left ventricular contractility decreases and end-systolic volume gradually increases, thereby contributing to cardiac dysfunction. While the left ventricular end-diastolic and end-systolic volumes increase, the pressure in left atrium also increases. An increase in atrial pressure results in pulmonary vein congestion and ultimately contributing to pulmonary edema accompanied with signs of left sided heart failure.

As mentioned previously, not only sympathetic nervous system (Ware et al, 1990) but also renin-angiotensin-aldosterone system (RAAS) is stimulated in dogs with mitral regurgitation (Sisson et al, 1999). A decrease of cardiac output in diseased heart leads to a reduction in renal blood flow resulting in a decrease in delivery of sodium chloride to the renal juxtaglomerular apparatus (JGA). This fall in sodium delivery causes the JGA to release renin. Renin induces the conversion of angiotensinogen into angiotensin I. Then, angiotensin converting enzyme (ACE) converts angiotensin I into angiotensin II. This angiotensin II initiates several events such as 1) stimulate vasoconstriction resulting in an increased resistance to flow from left ventricle, 2) stimulate vasopressin release causing in decreased urine production as well as increased blood volume retention and 3) increase production of aldersterone leading to increased sodium retention, decreased urine production, and increased blood volume. Therefore, the excessive stimulation of this RAAS system in

dogs affected by MVD can worsen the cardiac dysfunction and lead to left sided congestive heart failure. Other complications of mitral regurgitation include bronchial compression secondary to enlarged left atrium, cardiac arrhythmias such as supraventricular tachyarrhythmias (e.g. atrial premature complexes, paroxysmal atrial tachycardia, atrial fibrillation) and ventricular arrhythmias which perhaps occur due to dilated and overworked left atrium or ventricle, rupture of the major chordae tendineae causing abruptly increased regurgitant volume, augmented left atrial pressure, worsening pulmonary edema and ultimately acute left sided heart failure. Left atrial rupture is another possible complication of mitral regurgitation that can cause cardiac temponade, hypotension, and possibly death.

Current therapy

Currently, there are no clinical studies in veterinary medicine to suggest that any drugs or any treatments can slow the progression of MVD (Kittleson, 1998). The definitive treatment for mitral regurgitation in human patients is surgical repair or replacement of damaged valves (Braunwald, 1997). However, in veterinary medicine, mitral valve surgery has been performed in just a few hospital case dogs secondary to the expense of cardiac bypass surgery (Boggs et al, 1996; Orton et al. 2005; Griffiths et al, 2004). Presently, medical treatment goals of dogs affected by MVD are to reduce the severity of mitral regurgitation, to prevent or decrease pulmonary congestion, to maintain cardiac output, and to manage complications such as cardiac arrhythmias (Sisson et al, 1988). Overall current treatment objectives are to decrease the effect of circulatory disturbances and to improve quality of life rather than to treat the actual valve lesions.

Because data obtained in human patients with asymptomatic left ventricular systolic dysfunction showed that early intervention with ACE inhibitors may delay development of congestive heart failure (The SOLVD investigators, 1992), several veterinarians increase their interests in using ACE inhibitors as cardioprotective therapy to postpone or prevent congestive heart failure in dogs affected by early mitral valve disease. However, a recent Scandinavian study of 229 asymptomatic Cavalier King Charles spaniels with mild mitral valve regurgitation has shown that long term ACE inhibitor administration did not delay the onset of congestive heart failure in asymptomatic dogs with mild mitral regurgitation (Kvart et al, 2002). Administration of ACE inhibitors also failed to improve left ventricular remodeling and function in an experimentally induced mitral regurgitation dog model (Dell'Italia, 2002; Perry et al, 2002). Although ACE inhibitors have no significant effect upon onset of heart failure and cardiac remodeling, in symptomatic dogs these drugs have been demonstrated to improve clinical signs and increased survival times (The IMPROVE study group, 1995; The COVE study group, 1995). Beta-blockers are other drugs being used by some veterinary cardiologists as cardioprotective agents for dogs affected by MVD. These drugs protected the heart from effects of sympathetic nervous system such as controlling heart rate and reducing contraction force. The long-term administration of beta-blockers e.g. carvedilol and atenolol has been shown to improve hemodynamic, contractile function, and renal function in chronic iatrogenic mitral regurgitation experimental dogs (Uechi et al, 2002). However, a benefit of beta-blockers in improving myocardial function and reducing cardiac remodeling has not yet been demonstrated in dogs with spontaneous mitral valve regurgitation, particularly in case of asymptomatic dogs affected by mild mitral regurgitation.

Thus, the efficacy of this group of drugs in dogs with spontaneous heart valve diseases is uncertain and need further studies to clarify.

Etiology

Presently, the etiology of MVD in dogs is unknown, but the fact that some breeds are more prone to this disease than others suggests that genetic factors may have a role. Two studies in Cavalier King Charles spaniels and Dachshund families indicate that MVD is hereditary disease. A study of 107 (54 female, 53 male) Cavalier King Charles spaniels offspring from 8 parents (1 sire, 7 dams) demonstrated a strong correlation between parental MVD status and the presence as well as the intensity of cardiac murmurs in offspring at 5 years of age (Sweson et al, 1996). Another study of 18 Dachshund families also showed strong correlation between the mean parental mitral valve prolapse severity (the leaflet protrusion in millimeters assessed from two dimensional echocardiography) and the mean mitral valve prolapse severity in the litters (Olsen et al 1999).

Repeated high impact on mitral valve leaflets has been thought to be the cause of slowly progressive myxomatous degeneration (Pederson, 2000). This idea is supported by the gross lesion of MVD which usually occur primarily at the area of valve apposition. Repeated high impact on mitral valve leaflets may cause mechanical injury to the surface of valve leaflets influencing the synthesis and release of vasoactive substances such as endothelin-I from the valve endothelial cells. A recent study provided evidence that endothelin is one of vasoactive factors involved in the pathogenesis of MVD (Mow and Pederson, 1999). By autoradiography, a high density of endothelin receptors was demonstrated in degenerative mitral valve leaflets; on the other hand, normal leaflets and normal area on diseased valves

showed a low density of endothelin receptors. In addition, the endothelin receptor density within and on leaflets was directly related to the diseased severity supporting that endothelin plays a pathogenic role in degenerative process of MVD. Damage to valve endothelial cells might also influence the synthesis and release of nitric oxide. A study investigating the expression of nitric oxide synthase in canine mitral valve leaflets demonstrated an increase NADPH-d[1] activity areas of mitral valve affected by MVD. This NADPH-d activity suggests an increase expression of nitric oxide synthase and nitric oxide synthesis. In addition, the NADPH-d activity i.e. nitric oxide synthesis in endothelium is correlated with degree of mucopolysaccharide deposition and collagen degeneration. These findings suggest that nitric oxide plays a role in the pathogenesis of MVD in dogs (Olsen et al, 2003).

Several researchers have speculated that renin-angiotensin-aldosterone system (RAAS) might have a role in pathogenesis of MVD. RAAS including angiotensin II and angiotensin converting enzyme play an important role in fibrous tissue formation which is also a major pathologic change of MVD. However, autoradiographic study in canine myxomatous mitral valves showed no expression of angiotensin II receptor and angiotensin converting enzyme in both canine normal and myxomatous degenerative mitral valve leaflets suggesting that RAAS does not have an important role in pathogenesis of MVD (Mow and Pedersen, 1999b).

In humans, MVD has been speculated to be associated with a generalized connective tissue disorder (Glesby and Pyeritz, 1989). Similarly, dog breeds prone to connective tissue disorders such as intervertebral disc disease, tracheal collapse, and cruciate ligament rupture seem to be predisposed to MVD compared to other populations of dogs (Buchanan, 1977). The myxomatous degeneration of mitral valve often occurs together with arteriosclerosis of

[1] NADPH-d is the reduced from of nicotinamide-adenine dinucleotide phosphate diaphorase

intramural arteries. One study has shown that dogs affected by MVD have significantly more arterial changes i.e. arteriosclerosis in the myocardium, lung, and kidney than control dogs. This finding suggests the relationship between MVD and vascular changes in intramural arteries (Falk et al, 2006). Lesions similar to MVD including GAG disposition and elastic fiber fragmentation have been described in arteriosclerotic pulmonary artery in 7 Cavalier King Charles spaniels (Karlstam et al, 2000) suggesting that MVD and arteriosclerosis may share pathogenic mechanisms or that both of these conditions are part of one disease such as a generalized connective tissue disorders.

Abnormalities of ECM have been suggested to predispose to MVD (Haggstrom, 1996). Several studies in humans (Mow and Pederson, 1999a; Ahkhtar et al, 1999; Johnson and Caulfield, 1983) investigating abnormalities of degenerative mitral valve have reported marked deposition of GAG, fragmentation of collagen bundles, accumulation of fragmented elastic fibers as well as secondary fibrosis. GAG are hydrophilic molecules with a high negative charge. More GAG deposition increase hydrated gel formation resulting in swelling and changes of loose connective tissue in degenerative mitral valves. Collagen is the major ECM in the mitral valve. Defective or the degenerative collagen fiber may be involved in weakening of the valve tissue in degenerative mitral valves (King et al, 1982). It has been speculated that MVD may occur secondary to an inherited collagen defect. However, the study of gene segregation in human mitral valves indicates that mitral valve prolapse does not arise from a defect of genes encoding major collagen types in human mitral valve including collagen type I, III, and V (Wordsworth et al, 1989).

Human mitral valve prolapse is known to be associated with hypomagnesemia. A low magnesium status has also been found in 50% of Cavalier King Charles spaniels affected by

MVD (Pedersen and Mow, 1998). However, the specific role of a low magnesium status in canine MVD is currently unclear.

A previous electron microscope study (Black et al 2005) and an immunohistochemistry study (Zimmerman and Orton, 2004) showed that the phenotype of valve interstitial cells is different in dogs with degenerative mitral valve disease compared to unaffected dogs. Therefore, several researchers speculate that changes in VIC phenotype may have a role in pathogenesis of MVD.

Valve interstitial cell

Valve interstitial cell phenotype

Valve interstitial cell (VIC) is the major cell type in the heart valve. (Schurch, 1998) VIC is a heterogenous and dynamic cell type which is thought to maintain valve structure and function in normal valves and to regulate valve repair as well as remodeling in diseased valve. VIC have ability to produce ECM, chemokines, and catabolic enzymes such as matrix metalloproteinases (MMP) as well as their tissue inhibitors (TIMP). VIC have several unique characteristics which are different from those described in fibroblasts from other tissue types (Taylor et al, 2000). It has been demonstrated that VIC isolated from aortic, pulmonary, mitral and tricuspid valve expressed some molecular components differently from each other indicating that VIC from different types of valve may have a specific functional roles (Roy et al, 2000). Recently, Liu et al (2007) classified VIC into 5 phenotypes including 1) embryonic progenitor endothelial/mesenchymal cells: the progenitor phenotype that mediates valve formation during embryonic time of life; 2) quiescent VIC: the VIC phenotype that normally maintains valve structure and function; 3) activated VIC or myofibroblast: a phenotype that

has a role in pathological process of valve disease and injury; 4) progenitor VIC or valvular stem cells: a phenotype that may be a source of VIC during remodeling process; and 5) osteoblastic VIC: a phenotype that regulates chondrogenesis and osteogenesis. However, most researchers still identify VIC into 2 phenotypes: quiescent fibroblast and activated myofibroblast (Taylor et al, 2003; Mulholland and Gotlieb, 1996; Rabkin-Aikawa et al, 2004). VIC are quiescent and display a fibroblast like phenotype in normal mitral valves. Recent work suggests that a fibroblast phenotype in human mitral valve is characterized by immunoreactivity to vimentin (intermediate filament) but not α smooth muscle actin (α-actin; microfilament) or SM1 (differentiated smooth muscle myosin heavy chain isoforms) (Rabkin et al, 2001). This quiescent phenotype is thought to be a matrix regulator that has the ability to secrete and synthesize ECM in normal conditions. Activated VIC or myofibroblast phenotype has characteristics of both fibroblast and smooth muscle cells (Schmitt-Graff, 1994). However, myofibroblast VIC are different from smooth muscle cells because myofibroblast VIC have incomplete basement membrane whereas smooth muscle cells generally have intact basement membrane (Lester et al, 1988). A protein marker used to detect myofibroblast VIC is α-actin, the cytoskeleton protein which is normally not found in quiescent VIC (Taylor et al, 2000). Myofibroblast VIC are thought to have a role in the pathological condition of the heart valve because the differentiation of VIC into myofibroblast is related to several features involved to ECM remodeling, a major process associated to pathogenesis of several heart valve diseases (Mulholand and Gotlieb, 1996). The association between the expression of the myofibroblast VIC and catabolic enzymes in diseased and developmental valves suggests a role for this cell phenotype as a regulator of ECM remodeling (Rabkin et al, 2001; Taylor et al, 2000; Aikawa et al 2006, Rabkin et al,

2002). In several types of tissues, myofibroblasts have the ability to secrete higher levels of ECM and cytokines compared to their quiescent phenotype (Tomasek et al, 2002; Serini and Gabbiani, 1999; Larsen et al, 2004; Johnson et al, 1992). However, the quantitative study evaluating the level of ECM and cytokine production between myofibroblast VIC and quiescent VIC is yet to be definitely established. Further study is required to clarify the secretory properties of this activated VIC.

In addition to secretory properties, the myofibroblast VIC also have a contractile property. Numerous bundles of actin filaments within the myofibroblast VIC alter cellular stiffness and confer contractile features to this cell phenotype (Powell et al, 1999; Ronnov-Jessen and Peterson, 1996). The contractile property of the myofibroblast VIC can cause tissue remodeling by exerting extensive forces on the ECM. The ability of VIC to contract collagen gels has been demonstrated in cultured porcine aortic valve cells (Walker et al, 2004). Due to their contractile property, the myofibroblast VIC are also suspected to act as a valve tone supporter, particularly in weak pathological valves (Black et al, 2005). However, to date, the role of the myofibroblast VIC in contractile mechanisms in valve tissues, remain unclear, particularly in diseased valves.

VIC also play a role in valve repair. In organ culture, VIC respond to valve injury by proliferation and accumulating at the wound edge to cover the area of injury (Lester et al, 1992). Using *in vitro* wound repair model, Gotlieb et al (1999) has shown that VIC can migrate and suggested that VIC migration is another key process in valvular wound repair. Interestingly, the 'myofibroblast VIC' is a phenotype that mostly appears at the wound site (Tamura et al, 2000; Lester et al, 1999). Thus, the myofibroblast VIC have been suggested to be a key phenotype involved in valvular wound repair (Durbin and Gotlieb, 2002).

Non-muscle myosin (SMemb) or myosin heavy chain B (MHC-B) is a muscle protein that has been used as a marker to identify the activated cell phenotype. Non-muscle myosin is an embryonic isoform of muscle myosin heavy chain abundantly expressed in embryonic and dedifferentiated smooth muscle cells. The expression of non-muscle myosin is normally down-regulated during the development, but re-expressed in disease (Kuro-o et al, 1991) or in tissue injury (Aikawa et al, 1997). Muscle cells that express non-muscle myosin are also called 'undifferentiated' or 'synthetic state' smooth muscle cells because these cells have ability similar to the 'synthetic smooth muscle cells' in culture which express few myosin filaments, but abundance of organelles involved in protein synthesis, such as rough endoplasmic reticulum and free ribosomes (Kuro-o et al, 1991; Chamley-campbell; 1985).

Non-muscle myosin has been used as a molecular marker to identify abnormally proliferating cells particularly in the formation of vascular lesions such as arteriosclerosis (Kuro-o et al, 1991) or atherosclerosis (Aikawa et al, 1993) as well as several types of glomerular diseases (Hiroi et al, 1996). It has been suggested that non-muscle myosin may be used as a marker of activated cells since fibroblasts expressing non-muscle myosin have been demonstrated in several pathological tissues including hypertrophied hearts (Shiojima et al, 1999), kidneys with glomerulonephritis (Hiroi et al, 1996) and rejected cardiac allografts (Suzuki et al, 1996). Since non-muscle myosin may play an important role in interstitial cell activation, several researchers have shown interest in non-muscle myosin as a marker of activated phenotype of VIC. VIC expressed non-muscle myosin have been demonstrated in human myxomatous valves (Rabkin et al, 2001), developmental tissue engineering valves (Rabkin et al, 2002), and fetal valves (Aikawa et al, 2006). However, at present the

functional aspects and roles of VIC expressing non-muscle myosin is unclear and still needs further study.

Valve interstitial cell and catabolic enzymes

Matrix metalloproteinases (MMP) are a large family of zinc dependent proteolytic enzyme responsible for ECM remodeling in both normal and pathological process in several tissues (Hey, 1981; Birkedal-Hansen, 1995). Increased MMP activity can alter the balance between ECM synthesis and degradation resulting in changes of the overall tissue morphology and mechanical properties of pathological tissues (Stetler-Stevenson, 1996; Vu et al, 1998). MMP are produced by several types of cells including fibroblasts, smooth muscle cells, myocytes, and endothelial cells (Stetler-Stevenson, 1996; Dollery et al, 1995). At present, 20 MMP are known. They are divided into four groups: collagenases (MMP-1, MMP-8, and MMP-13), gelatinases (MMP-2, and MMP-9), stromalysin (MMP-3, MMP-7, MMP-10, MMP-11, and MMP-12) and membrane type MMP (MT1-MMP, MT2-MMP, MT3-MMP, and MT4-MMP). All MMP, with the exception of MT-MMP, are secreted into the extracellular space in a pro-enzyme state (pro-MMP). Activation of pro-MMP is achieved through enzymatic cleavage of the pro-peptide domain by serine proteases (e.g. plasmin) and other MMP species. The MMP activity is regulated by endogenous inhibitors called tissue inhibitors of metalloproteinases (TIMP). TIMP are often produced from the same cells that release MMP. At present, four TIMP are known (TIMP-1, -2, -3, -4). TIMP are able to inhibit the function of MMP by forming a complex with MMP in a 1:1 ratio (Stricklin et al, 1983).

Each MMP has ability to cleave a specific type of ECM. Interstitial collagenases (MMP-1, MMP-8, and MMP-13) are involved in the first step of collagen degradation by breakdown of the native helix of the fibrillar collagen network (Bashey et al, 1967). Gelatinases (MMP-2, and MMP-9) cleave a number of substrates including gelatin, elastin, proteoglycans, collagen and fragments of collagen cleaved by interstitial collagenases (Krane et al, 1996). The balance between TIMP and MMP is important in the remodeling of normal and pathological tissues. In normal tissues, MMP are expressed at very low levels. When tissues require remodeling, MMP are rapidly induced and activated.

Human heart valves have a specific pattern of expression MMP and TIMP expressions that vary among different types of valves. MMP-1 can be found in all four types of heart valves (aortic, pulmonic, mitral, and tricuspid), while MMP-2 is expressed minimally in aortic and pulmonic valves. MMP-3 and MMP-9 are not found in any type of heart valve. TIMP-1 and TIMP-2 are expressed in all valve leaflets but TIMP-3 can be found only in tricuspid valve (Dreger et al, 2002). Synthesis of MMP-2, MMP-9 and TIMP-1 mRNA was found in human valves affected by degenerative disease suggesting the role of MMP, particularly MMP-2 and MMP-9 in the remodeling of heart valves with degenerative disease (Soini et al, 2001). This finding is supported by Rabkin et al (2001) who reported an increase in expression of collagenases (MMP-1 and MMP-13), gelatinases (MMP-2 and MMP-9) and elastases (cathepsins S and K) in human degenerative mitral valve tissues. The enzymatic activity of MMP-2 and MMP-9 in degenerative valves has been demonstrated by gelatin zymography study supporting a role for these MMP in pathologic changes of degenerative valves (Togashi et al, 2007).

MMP are likely secreted by the myofibroblast VIC since expression of MMP and their mRNA signals were strongly correlated with the expression of the myofibroblast VIC in human degenerative valves (Rabkin et al, 2001; Soini et al, 2001). Because of these findings, myofibroblast have been implicated as a mediator of MVD. However, studies demonstrating the co-localization of myofibroblast VIC and catabolic enzymes as well as their inhibitors have not been performed. Thus, a role of the myofibroblast VIC as a major source of catabolic enzymes and as a mediator of pathological changes associated with MVD is still uncertain.

Possible mechanisms of valve interstitial cell transformation

Presently, little is known about the mechanisms of alteration of VIC phenotype from the quiescent VIC to the myofibroblast VIC. One factor that has been suspected to have a role in VIC differentiation is transforming growth factor beta 1 (TGFβ1). TGFβ1 is a growth factor belonging to TGFβ superfamily, a family of peptide that regulates biological functions in several organ systems. Currently, there are three isoforms of TGFβ in mammalian tissues including TGFβ1, 2 and 3. Major sources of TGFβ1 in human body are platelets, bone and serum (Wakefield et al, 1988). All of these sources contain latent form of TGFβ1. Mostly, TGFβ1 is secreted from cells in latent form. The latent TGFβ1 has been divided into 2 forms: "small latent complex" that contains only latent-associated peptide (LAP) and the TGFβ homodimer and "large latent complex" which is comprised of small latent complex and latent TGFβ binding protein (LTBP). Mature TGFβ must be cleaved and released from the latent complex to allow binding to receptors. The TGFβ superfamily signals through a family of cell surface serine-threonine kinase receptors. These receptors are divided into two

subfamilies including receptor I (RI) and receptor II (RII). TGFβ RI and TGFβ RII are both required for signaling. To activate the TGFβ signaling pathway, the TGFβ combines to TGFβ RII. The complex of TGFβ and TGFβ RII phosphorylate and activate TGFβ RI. The activated TGFβ RI activates the Smad pathway that in turn activates transcription of specific genes in nucleus. The Smad pathway activated by TGFβ1 regulates many cellular events including inhibition of cell proliferation, stimulation of ECM production, and controlling cellular differentiation. In wound and several tissues, TGFβ1 can trigger mesenchymal cells to differentiate into myofibroblasts and can regulate myofibroblast phenotype activity through transcription of α-actin, collagen, MMP and other cytokines (Roberts and Sporn, 1996). Previous studies demonstrate a dose dependent effect of TGFβ1 in increasing the α-actin expression within cultured aortic VIC suggesting a role of TGFβ1 in activating VIC phenotype transformation (Cushing et al, 2005; Walker et al, 2004).

Local tissue stress is another factor thought to induce VIC transformation to an activated or myofibroblast phenotype. One study demonstrated that VIC responded to local tissue force or stress by altering their cellular stiffness and biosynthesis of matrix components (i.e. increased α-actin content and collagen synthesis) (Merryman et al, 2006). In an *in vitro* study modeling circumferential cyclic stretch, a 15% strain applied for a period of 48 hours in an *ex vivo* bioreactor showed an increased expression of α-actin in stretched leaflets when compared to the fresh leaflets (Balachandran et al, 2006).

The serotonin signaling pathway has been implicated in VIC transformation. In sheep aortic VIC cultures, serotonin can induce TGFβ1 mRNA production and increase TGFβ1 activity. Because TGFβ1 is associated with VIC transformation in culture cells, serotonin transduction may be involved with VIC transformation secondary to TGFβ1 mechanisms

(Jian et al, 2002). Several lines of evidence implicate serotonin in pathogenesis of heart valve diseases.

Serotonin signaling transductions and heart valve diseases

Serotonin or 5-hydroxytryptamine (5-HT) was first recognized as a powerful vasoconstrictor in blood serum. The essential amino acid tryptophan is the precursor of serotonin. Approximately 95% of serotonin in the body is produced by enterochromaffin cells in the intestine. The rest is synthesized in the raphe nuclei of the brain, the neuroendothelial cells in the lungs and a few other discrete sites. Tryptophan hydroxylase (TPH) is the key enzyme of serotonin synthesis. This enzyme is responsible for transferring a hydroxyl group to the benzyl ring of tryptophan and form amino acid 5-hydroxytryptophan which is then converted into serotonin by decarboxylation with amino acid decarboxylases. Currently, two isoforms of enzyme tryptophan hydroxylase have been found including a 'peripheral isoform' (TPH1) which is mostly expressed in peripheral tissues and a 'central isoform' (TPH2) which is the predominant isoform in the central nervous system. After release, serotonin is normally taken up and stored by a number of cell types including platelets.

The serotonergic system is known to modulate mood, emotion, sleep and appetite. Generally, serotonin is implicated in the control of numerous behavioral and physiological functions. Hence, studies of serotonin are mostly focused on its roles in the nervous system. Recently, several researchers have increased their interest in function of serotonin in other organ systems since serotonin receptors are increasingly found in several tissues besides the brain.

Different biological actions of serotonin are mediated by types of receptors. Presently, serotonin receptors are divided into seven distinct classes (5-HT_1 to 5-HT_7). $5HT_2$ family has been reported to be involved in regulating cardiac structure as well as cardiac differentiation and proliferation during development (Nebigil et al, 2000). The disruption of the $5HT_{2B}$ receptor gene in mice caused abnormalities of cardiac structure and cardiac function (Nebigil et al, 2001). Serotonin receptors are also presented in human cardiac valves suggesting the potential of VIC to respond to serotonin (Fitzgerald et al, 2000). Currently, serotonin is suspected to be one factor involved in several heart valve diseases. High levels of serotonin in circulation are thought to be associated with carcinoid disease in people (Rajamannan et al, 2001). Rats administered serotonin for long term developed pathological changes of aortic valves that are similar to those described in human carcinoid disease (Gustafsson et al, 2005). In addition, fenflulamine, a serotonergic drug, has been reported to mediate human heart valve disease by increasing the plasma serotonin and stimulating serotonin signaling pathway (Rothman et al, 2000). Cavalier King Charles spaniel, a breed with high incidence of MVD, is also affected by giant platelet syndrome (Cowan et al, 2004). Several researchers suggested that these giant platelets may contain high levels of serotonin which may contribute to MVD in Cavalier King Charles spaniel.

The $5HT_2$ receptor family consists of 3 subtypes including $5HT_{2A}$, $5HT_{2B}$ and $5HT_{2C}$ receptors (Leysen, 2004). These receptor subtypes share a close amino acid sequence but have different pharmacological profiles. The predominant subtypes of $5HT_2$ that have been found in human heart valves are $5HT_{2A}$ and $5HT_{2B}$ (Fitzgerald et al, 2000). Since $5HT_2$ receptor family is predominantly found in heart valves, it has been suggested that this family of serotonin receptor may be involved in pathogenesis of heart valve diseases. A recent study

showed that the activation of $5HT_{2B}$ receptors is necessary to initiate heart valve disease-mediated by serotonergic medications (Rothman et al, 2000). A study in rats study showed an increased number of cells expressing $5HT_{2B}$ receptor in leaflets with spontaneous mitral valvulopathy suggesting the role of $5HT_{2B}$ receptor in pathogenesis (Elangbam et al, 2006). In addition, present work by whole tissue microarray analysis has demonstrated an up-regulation of $5HT_{2B}$ receptor gene in canine degenerative mitral valve tissues suggesting that $5HT_{2B}$ receptor and serotonin signaling transduction might have an important role in pathogenesis of canine MVD (Oyama and Chittur, 2006).

The 5-HT_2 receptors are G-protein coupled receptors which are linked to Gαq subtype. To activate signal transduction, serotonin binds to receptors which subsequently activate phospholipase C, induce phosphatidylinositol (PI) hydrolysis creating inositol triphosphate (IP_3) and 1,2-diacylglycerol (DAG). The accumulation of IP_3 initiates internal Ca^{2+} releasing. Both DAG and Ca^{2+} are necessary for activating protein kinase C (PKC). This PKC activates several downstream effectors and cross talk to other signaling pathways. Mitogen-activated protein kinases (MAPK) signaling is one pathway linked to serotonin transduction signaling. The MAPK signaling pathway normally controls gene expressions involved in cell proliferation and differentiation (Cano and Mahadevan, 1995). MAPK signaling pathways have been classified into three subfamilies including extracellular-signal regulated kinases (ERK), ERK1 and ERK2 (also known as $p44^{mapk}$, and $p42^{mapk}$, respectively), c-Jun N-terminal kinase (JNK) and p38 kinase. The ERK pathway has been reported to be the downstream of the $5HT_{2B}$ receptor (Launays et al, 1996). Generally, the ERK are phosphorylated and activated by threonine and tyrosine protein kinases called MAPKK/MEK which are activated by effectors such as PKC. Phosphorylated ERK have

ability to phosphorylate several transcription factors regulating the expression of genes associated with cell mitogenesis. The mitogenic effect of serotonin via $5HT_{2B}$ receptors and MAPK-ERK1/2 pathways has been reported in transfected fibroblasts (Nebigil et al, 2000). A similar finding was also found in the study of cultured sheep aortic valve cells (Xu et al, 2002). Norfenfluramine, a serotonergic drug can activate the MAPK cascade in cells expressing recombinant $5HT_{2B}$ receptors (Rothman et al, 2000). Taken together, these findings suggest the mitogenic action of the $5HT_{2B}$ receptor is mediated by MAPK pathway in cultured cells. However, in tissues particularly in heart valve tissues, mechanisms of cell proliferation stimulated by serotonin/MAPK signaling transduction are unclear and further studies are required to clarify.

Serotonin is also thought to be involved with ECM secretion during diseased process (Hafizi et al, 2000). However, a previous study demonstrated that an increased ECM synthesis (collagen and GAG) in VIC cultures supplemented by serotonin is secondary to TGFβ1 and not a direct effect of serotonin itself because ECM production stimulated by serotonin was significantly decreased by the TGFβ1 blocking antibody (Jian et al, 2002). This finding suggests that serotonin associated valve diseases may be mediated by TGFβ1. Roles of serotonin signaling transduction in ECM production and remodeling in naturally-occurring canine myxomatous mitral valve disease are unclear.

After release, serotonin is normally taken up inside a cell via serotonin transporter (SERT). Platelets are major components in the periphery that has a function to uptake serotonin via SERT. SERT is a transmembrane protein which spans the bilayer 12 times (12 transmembrane domains) and that both amino acid and carboxy termini are intracellular. SERT is a sodium-dependent transporter which has a major function to move serotonin from

outside a cell into inside the cell for vesicular repackaging or metabolism via monoamine oxidase. SERT has been suggested to have a role in decreasing the effect of serotonin transduction by reducing the amount of serotonin at the serotonin-receptor reaction site. The study of human fetal heart cell cultures demonstrated that the blockade of serotonin uptake by paroxetine decreased the effect of serotonin in stimulating heart cell proliferation (Sari et al, 2003). Another previous study showed that patients using dexfenflulamine, a serotonin uptake inhibitor have high circulating serotonin levels. An increase of serotonin has been thought to enhance the transduction of serotonin signaling and increase the risk to develop pulmonary hypertension (Eddahibi et al, 2001; Abenhaim et al, 1996). A similar result has been demonstrated in the study of human VIC culture showing that SERT inhibitors, dexfenfluramine and fluoxetine enhance serotonin-mediated signal transduction in VIC by blocking SERT (Connolly et al, 2007). A study in mice demonstrated the expression of SERT mRNA and protein within mouse valvular tissues (Mekontso-Dessap et al, 2006). In addition, this study showed that SERT knocked out mice developed cardiac and valvular fibrosis. The result of this study suggests that SERT has a role in preventing the development of heart valve diseases in mice. Since the canine MVD may have diseased process similar to that in mice, it is reasonable to speculate that SERT may have roles in MVD similar to that described in valvulopathy in mice.

Methodological consideration

Immunohistochemical staining

Immunohistochemistry is a method to visualize the distribution and localization specific proteins of interest within cells or tissues. This technique has been used since the 1940s when Coons and colleagues published their paper describing the identification of tissue antigens using a direct fluorescence method (Coon et al, 1941). Generally, a protocol of immunohistochemistry consists of the following steps: First, the application of primary antibody to bind the specific antigen. Second, an enzyme-conjugated secondary antibody is then applied to bind the antibody-antigen complex. Third, the antibody-antigen reaction is visualized by the enzyme-specific substrate and chromogen. Several immunohistochemical staining procedures have been used including direct horse radish peroxidase, the peroxidase-anti peroxidase, the avidin-biotin complex and the alkaline phosphatase-anti alkaline phosphatase. All of these methods typically take 2 to 4 hours to perform. Recently, new rapid immunohistochemical techniques have been developed. EnVision™ is one of these newly developed systems which can be used to stain tissues in a shorter time compared to the older methods such as avidin biotin complex (ABC) system (Kammerer et al, 2001). The envision system is a two-step method which is based on a horse radish peroxidase labeled polymer conjugated with secondary antibodies. This technique is highly sensitive offering an enhanced signal generating system to detect antigens by using a low titer of primary antibodies.

Western blot analysis

Western blotting (Towbin et al, 1979) is a protein/protein hybridization method used to detect the specific protein of interest in a complex mixture of proteins. Basically, whole tissue or cell culture samples are first broken down by mechanical methods such as homogenization, sonication and manual grinding or by chemical method such as enzymatic, detergent and organic solvent treatment. Proteins in mixture samples are then separate using sodium dodecyl sulfate-polyarylamide gel electrophoresis (SDS-PAGE). With this method, sampled proteins are denatured and coated with negatively charged SDS. The SDS generally provides an approximately uniform mass:charge ratio for most proteins in the sample. Proteins migrating in an electric field to the positively charged electrode are then separated by their molecular weight on the polyacrylamide gel. After electrophoresis, separated protein molecules are immobilized onto a transfer membrane typically nitrocellulose or polyvinyldifluoride (PVDF). Proteins of interest on the transfer membrane are probed using antibodies specific to them. The antigen-antibody complex is then detected by a secondary antibody conjugated with enzyme such as alkaline phosphatase or horseradish peroxidase. Most commonly, a horseradish peroxidase linked secondary antibody is used in combination with a chemiluminescent agent. The reaction product produces luminescence in proportion to the amount of proteins. The resulting signal is measured using a camera laminator or a high contrast, high-sensitivity X-ray film.

REFERENCES

1. Abenhaim L, Moride Y, Brenot F, et al. Appetite-suppressant drugs and the risk of pulmonary hypertension. International primary pulmonary hypertension study group. N Engl J Med 1996;335:609-616
2. Aikawa M, Sivam PN, Kuro-o M, et al. Human smooth muscle myosin heavy chain isoforms as molecular markers for vascular development and atherosclerosis. Circ Res 1993;73(6):1000-1012
3. Aikawa M, Sakomura Y, Ueda M, et al. Redifferentiation of smooth muscle cells after coronary angioplasty determined via myosin heavy chain expression. Circulation 1997;96:82-90
4. Aikawa E, Whittaker P, Farber M, et al. Human semilunar cardiac valve remodeling by activated cells from fetus to adult: implications for postnatal adaptation, pathology, and tissue engineering. Circulation 2006;113:1344-1352
5. Akhtar S, Meek KM, James V. Ultrastructure abnormalities in proteoglycans, collagen fibrils and elastic fibers in normal and myxomatous mitral valve and chordae tendinae. Cardio Physio 1999;8:191-201
6. Balachandran K , Konduri S, Sucosky P, et al. An ex vivo study of the biological properties of porcine aortic valves in response to circumferential cyclic stretch. Ann Biomed Eng 2006;34:1655-1665
7. Bashey RI, Torii S, Angrist A. Age-related collagen and elastin content of heart valves. J Gerontol 1967;22:203-208
8. Birkedal-Hansen H. Proteolytic remodeling of extracellular matrix. Curr Opin Cell Biol 1995;7:728-735

9. Black A, French AT, Dukes-McEwan J, Corcoran B. Ultrastructural morphologic evaluation of the phenotypic of valvular interstitial cells in dogs with myxomatous degeneration of the mitral valve. Am J Vet Res 2005;66:1408-1414

10. Boggs LS, Dewan SJ, Ballard SE. Mitral valve reconstruction in a toy breed dog. J Am Vet Med Assoc 1996;209:1872

11. Braunwald E. Valvular heart disease. *In* Braunwald E ed. Heart disease, A Textbook of Cardiovascular Medicine, 5th edition, Philadelphia: WB Saunders, 1997;1007-1072

12. Buchanan JW. Chronic valvular disease (endocardiosis) in dogs. Adv Vet Sci Comp Med 1977;21:75-106

13. Cano E, Mahadevan LC. Parallel signal processing among mammalian MAPKs. Trends Biochem Sci 1995;20:117-122

14. Chamley-campbell J, Campbell GR, Ross R. The smooth muscle cell in culture. Physiol Rev. 1985;260:1959-1966

15. Connolly JM, Blamey C, Oyama M, et al. Dexfenfluramine and fluoxetine increase serotonin-mediated signal transduction in mitral valve cells via serotonin transporter blockade, not direct serotonin receptor signaling. Proceeding of the 4th biennial meeting of the society for heart valve disease 2007;157

16. Coon AH, Creech HJ, Jones RN. Immunological properties of an antibody containing a fluorescent group. Proc Soc Exp Biol Med 1941;47:200-202

17. Corcoran BM, Black A, Anderson H, et al. Identification of surface morphologic changes in the mitral valve leaflets and chordae tendineae of dogs with myxomatous degeneration. Am J Vet Res 2004;65(2):198-206

18. Cowan SM, Bartges JW, Gompf RE, et al. Giant platelet disorder in the Cavalier King Charles Spaniel. Exp Hematol 2004;32:344-350

19. Cushing MC, Liao JT, Anseth KS. Activation of valvular interstitial cells is mediated by transforming growth factor beta 1 interactions with matrix molecules. Matrix Biol 2005;24:428-437

20. Darke PG. Valvular incompetence in cavalier King Charles spaniels. Vet Rec 1987;120:365-366

21. Das KM, Tashijan RJ. Chronic mitral valve disease in the dogs. Vet Med Small Anim Clin 1965;60:1209-1216

22. Delweiler DK, Patterson DF. The prevalence and types of cardiovascular disease in dogs. Ann NY Acad Sci 1965;127:481-516

23. Dell'Italia LJ. The renin-angiotensin system in mitral regurgitation: atypical example of tissue activation. Curr Cardiol Rep 2002;4(2):97-103

24. Dollery CM, McEwan JR, Henny AM. Matrix metalloproteinases and cardiovascular disease. Circ Res 1995;77863-868

25. Dreger SA, Taylor PM, Allen SP, et al. Profile and localization of matrix metalloproteinases (MMPs) and their tissue inhibitors (TIMPs) in human heart valves. J Heart Valve Dis 2002;11:875-880

26. Durbin AD, Gotlieb AI. Advances towards understanding heart valve response to injury. Cardiovascular pathol 2002;11:69-77

27. Eddahibi S, Adnot S, Frisdal E, et al. Dexfenfluramine-associated changes in 5-hydroxytyptamine transporter expression and development of hypoxic pulmonary hypertension in rats. J pharmacol Exp Ther 2001;297:148-154

28. Elangbam C, Wehe JG, Barton JC, et al. Evaluation of glycosaminoglycans content and 5-hydroxytryptamine 2B receptor in the heart valves of sprague-dawley rats with spontaneous mitral valvulopathy-a possible exacerbation by dl-amphetamine sulfate in fisher 344 rats. Exp toxicol pathol 2006;58:89-99

29. Falk T, Jonsson L, Olsen LH, Pederson HD. Arteriosclerotic changes in the myocardium, lung, and kidney in dogs with chronic congestive heart failure and myxomatous mitral valve disease. Cardiovascular pathology 2006;15:185-193

30. Fitzgerald LW, Burn TC, Brown BS, et al. Possible role of valvular serotonin 5-HT (2B) receptors in the cardiopathy associated with fenflulamine. Mol Pharmacol 2000;57-75-81

31. Glesby MJ, Pyeritz RE. Association of mitral valve prolapse and systemic abnormalities of connective tissue. A phenotypic continuum. J Am Med Assoc 1989;262:523-528

32. Griffith LG, Boon J, Orton EC. Evaluation of techniques and outcomes of mitral valve repair in dogs. J Am Vet Med Assoc 2004;224:1941-1945

33. Gotlieb AI, Rosenthal A, Kazemain P. Valvular interstitial cell wound repair. FASEB J 1999;A508-413

34. Gustafsson BI, Tommeras K, Nordrum I, et al. Long-term serotonin administration induces heart valve disease in rats. Circulation 2005;111:1517-1522

35. Hafizi S, Taylor PM, Chester AH, et al. Mitogenic and secretory responses of human valve interstitial cells to vasoactive agents. J of Heart Valve Dis 2000;9:454-458

36. Haggstrom J, Hanson K, Karlberg BE, et al. Effects of long term treatment with enalapril or hydralazine on the renin-angiotensin-aldosterone system and fluid

balance in dogs with naturally acquired mitral valve regurgitation. Am J Vet Res 1996;57:1645-1652

37. Hey ED. Extracellular matrix. J Cell Biol 1981;91:205s-223s

38. Hiroi J, Kimura K, Aikawa M, et al. Expression of a nonmuscle myosin heavy chain in glomerular cells differentiates various types of glomerular disease in rats. Kidney Int 1996;49:1231-1241

39. Jian B, Jie Xu, Jeanne C, et al. Serotonin mechanisms in heart valve disease I: serotonin-induced up-regulation of transforming growth factorβ1 via G-protein signal transduction in aortic valve interstitial cells. Am J Pathol 2002;161:2111-2121

40. Johnson RJ, Floege J, Yoshimura A, et al. The activated mesangial cell: a glomerular 'myofibroblast'. J Am Soc Nephrol 1992;2:S190-S197

41. Karlstam E, Haggstrom J, Kvart C, et al. Pulmonary artery lesions in cavalier King Charles spaniel. Vet Rec 2000;147:166-167

42. Kammerer U, Kapp M, Gassel AM, et al. A new rapid immunohistochemical staining technique using the envision antibody complex. J Histochem Cytochem 2001;49:623-630

43. Kittleson MD. Myxomatous atrioventricular valvular degeneration. I*n* Kittleson MD ed. Small animal cardiovascular medicine, 1st edition, St. Louis: Mosby, 1998;297-318

44. King BD, Clark MA, Baba N, et al. Myxomatous mitral valves: collagen dissolution as the primary defect. Circulation 1982; 66:288 -296

45. Kogure K. Pathology of chronic mitral valvular disease in the dog. Jpn J Vet Sci 1980;42:323-335

46. Krane SM, Byrne MH, Lemaitre V, et al. Different collagenase gene products have different roles in degradation of type I collagen. J Biol Chem 1996;271:28509-28515

47. Kuro-o M, Nagai R, Nakahara K, et al. cDNA cloning of a myosin heavy chain isoform in embryonic smooth muscle and its expression during vascular development and in arteriosclerosis. J Biol Chem 1991;266:-3768-3773

48. Kvat C, Haggstrom J. Acquired Valvular Heart valve disease. In Ettinger S, Feldman E, ed. Textbook of veterinary internal medicine. 5th edition. Philadelphia: WB Saunders, 2000;787-800

49. Kvart C, Haggstrom J, Pederson HD, et al. Efficacy of enalapril therapy for prevention of congestive heart failure in dogs with myxomatous valve disease and asymptomatic mitral regurgitation. J Vet Intern Med 2002;16:80-88

50. Larsen K, Tuffvessen E, Malmstrom J, et al. Presence of activated mobile fibroblast in bronchoalveolar lavage from patient with mild asthma. Am J Respir Crit Care Med 2004;170(10):1049-1056

51. Launays JM, Birrauxs G, Bondouxs D, et al. Ras involvement in signal transduction by the serotonin 5-HT2B receptor. J Biol Chem 1996;271:3141-3147

52. Lester W, Rosenthal A, Granton B, Gotlieb AI. Porcine mitral valve interstitial cells in culture. Lab Invest 1988;59:710-719

53. Lester WM, Dmaji AA, Tanka M, Gedeon I. Bovine mitral valve organ culture: Role of interstitial cells in repair of valvular injury. J Mol Cell Cardiol 1992:24;43-53

54. Leysen JE. 5-HT2 receptors. Curr Drug Targets CNS Neurol Disord 2004;3:11-26

55. Liu AC, Joag VR, Gotlieb AI. The emerging role of valve interstitial cell phenotypes in regulating heart valve pathobiology. Am J Pathol 2007;171(5):1407-1408

56. Mekontso-Dessap A, Brouri F, Pascal O, et al. Deficiency of the 5-hydroxytryptamine transporter gene leads to cardiac fibrosis a valvulopathy in mice. Circulation 2006;113:81-89

57. Merryman WD, Youn I, Lukoff HD, et al. Correlation between heart interstitial cell stiffness and transvalvular pressure: implications for collagen biosynthesis. Am J Physiol Heart Circ Physiol 2006;290:H224-H231

58. Mow T, Pedersen HD. Increased endothelin receptor density in myxomatous canine mitral valve leaflets. J Cardiovasc Pharmacol 1999;34:254-260.

59. Mow T, Pedersen HD. No expression of angiotensin II receptors and angiotensin-converting enzyme in myxomatous canine mitral valve leaflets. An autoradiographic study. J Vet Med A 1999;46:465-472

60. Mulholland DL and Gotlieb AI. Cell biology of valvular interstitial cells. Can J Cardiol 1996;12(3)231-236

61. Nebigil CG, Launay J-M, Hickel P, et al. 5-hydroxytryptamine 2B receptor regulates cell-cycle progression: cross talk with tyrosine kinase pathways Proc Natl Acad Sci USA 2000;97:2591-2596

62. Nebigil C, Hickel P, Messaddeq N, et al. Ablation of serotonin 5-HT_{2B} receptors in mice leads to abnormal cardiac structure and function. Circulation 2001;103:2973-2979

63. Olsen LH, Fredholm M, Pederson HD. Epidemiology and inheritance of mitral valve prolapse in Dachshunds. Journal of Veterinary Internal medicine 1999;13:448-456

64. Olsen LH, Mortensen K, Martinussen T, et al. Increased NADPH-diaphorase activity in canine myxomatous mitral valve leaflets. J Comp Path 2003;129:120-130

65. Orton CE, Hackett TB, Mama K, et al. Technique and outcome of mitral valve replacement in dogs. J Am Vet Med Assoc 2005;226(9):1508-1511

66. Oyama MA, Chittur SV. Genomic expression patterns of mitral valve tissues from dogs with degenerative mitral valve disease. J Vet Res 2006;67:1307-131

67. Pedersen HD, Mow T. Hypomagnesemia and mitral valve prolapse in Cavalier King Charles spaniels. Zentralbl Veterinarmed A. 1998 Dec;45(10):607-614

68. Pederson HD. Diagnosis canine myxomatous mitral valve disease. Waltham focus 2000;10(1):3-9

69. Perry GJ, Wei CC, Hankes GH, et al. Angiotensin II receptor blockade does not improve left ventricular function and remodeling in subacute mitral regurgitation in the dog. J Am Coll Cardiol 2002;39(8):1374-1379

70. Powell DW, Mifflin RC, Valentich JD, et al. Myofibroblasts I. Paracrine cells important in health and disease. Am J Physiol 1999;277:C1-C9

71. Rabkin E, Aikawa M, Stone JR, et al. Activated interstitial myofibroblasts express catabolic enzymes and mediate matrix remodeling in myxomatous heart valves. Circulation 2001;104:2522-2532

72. Rabkin E, Hoerstrup SP, Aikawa M, et al. Evolution of cell phenotype and extracellular matrix in tissue-engineered heart valves during in-vitro maturation and in-vivo remodeling. J Heart Valve Dis 2002;11:308-314

73. Rabkin-Aikawa E, Farber M, Aikawa M, Schoen FJ. Dynamic and reversible changes of intersititial cell phenotype during remodeling of cardiac valves. J Heart Valve Dis 2004;13(5) 841-847

74. Rajamannan NM, Caplice N, Anthikad F, et al. Cell proliferation in carcinoid valve disease: a mechanism for serotonin effects. J Heart Valve Dis 2001;10:827-831

75. Roberts AB and Sporn MB. Transforming growth factor β. In Clark RA, ed. The Molecular and Cellular Biology of Wound Repair. New York: Plenum Press, 1996; 275-308

76. Ronnov-Jessen L, Peterson OW. A function for filamentous α-sma: retardation of motility in fibroblasts. J Cell Biol 1996;134:67-80

77. Rothman RB, Baumann MH, Savage JE, et al. Evidence for possible involvement of $5HT_{2B}$ receptors in the cardiac valvulopathy associated with fenfluramine and other serotonergic medications. Circulation 2000;102:2836-2841

78. Roy A, Brand NJ, Yacoub MH. Molecular characterization of interstitial cells isolated from human heart valves. J Heart Valve Dis 2000;9:459-464

79. Sari Y, Zhou FC. Serotonin and its transporter on proliferation of fetal heart cells. Int J Devl Neuroscience. 2003;21:417-424

80. Schmitt-Graff A, Desmouliere A, Gabbiani G. Heterogeniety of myofibroblast phenotypic features: an example of fibroblastic cell plasticity. Virchows Arch 1994;425:3-24

81. Schurch, Seemayer TA, Gabbiani G. The myofibroblast: a quarter century after its discovery. Am J Surg Path 1998;73:1000-1012

82. Serini G and Gabbiani G. Mechanisms of myofibroblast activity and phenotypic modulation. Exp Cell Res 1999;250:273-283

83. Sisson D, Kvart C, Drake PG. Acquire valvular heart disease in dogs and cats. In Fox PR, Sisson D, Moise NS, ed. Text book of canine and feline cardiology. 2nd edition. Philadelphia: W.B. Saunders, 1998;536-555

84. Shiojima I, Aikawa M, Suzuki J, et al. Embryonic smooth muscle myosin heavy chain SMemb is expressed in pressure-overloaded cardiac fibroblasts. Jpn Heart J 1999;40:803-818

85. Soini Y, Satta J, Maatta M, Autio-Harmainen A. Expression of MMP2, MMP9, MT-1 MMP, TIMP1 and TIMP2 mRNA in valvular lesions of the heart. J Pathol 2001;194:225-331

86. Stetler-Stevenson WG. Dynamics of matrix turnover during pathologic remodeling of extracellular matrix. Am J Pathol 1996;148:1345-1350

87. Stricklin GP, Jeffrey JJ, Roswit WT, et al. Human skin procollagenase:mechanism of activation by organomercurials and trypsin. Biochemistry 1983;22:61-68

88. Suzuki J, Isobe M, Aikawa M, et al. Nonmuscle and smooth muscle myosin heavy chain expression in rejected cardiac allografts: a study in rat and monkey models Circulation 1996;94:1118-1124

89. Swenson L, Haggstrom J, Kvart C. Juneja RK. Relationship between parental cardiac status in Cavalier King Charles spaniels and prevalence and severity of chronic valvular disease in offsprings. J Am Vet Med Assoc 1996;208:2009-2012

90. Tamura K, Jones M, Yamada I, Ferrans VJ. Wound healing in the mitral valve. J Heart Valve Dis 2000;9:63

91. Taylor PM, Allen SP, Yacoub MH. Phenotypic and functional characterization of interstitial cells from human heart valves, pericardium and skin. J Heart Valve Dis 2000;9:150-158

92. Taylor PM, Batten P, Brand NJ, et al. The cardiac valve interstitial cell. Int J Biochem Cell Biol 2003;35:113-118

93. The COVE study group. Controlled clinical evaluation of enalapril in dogs with heart failure. J Vet Intern Med 1995;9:243-252

94. The IMPROVE study group. Acute and short term hemodynamic, echocardiographic and clinical effects of enalapril maleate in dogs with naturally acquired heart failure. J Vet Intern Med 1995;9:234-242

95. The SOLVD investigators. Effect of enalapril on mortality and development of heart failure in asymptomatic patients with reduced left ventricular ejection fractions. N Engl J Med 1992;327(10):685-691

96. Togashi M, Tamura K, Nitta T, et al. Role of Matrix metalloproteinase and their tissue inhibitor of metalloproteinases in myxomatous change of cardiac floppy valves. Pathol Int 2007;57:251-259

97. Tomasek JJ, Gabbiani G, Hinz B, et al. Myofibroblasts and mechano-regulation of connective tissue remodeling. Nat Rev Mol Cell Biol 2002;3(5):349-363

98. Towbin H, Staehelin T, Gordon J. Electrophoretic transfer of proteins from polyacrylamide gels to nitrocellulose sheets: procedure and some applications Proc Natl Acad Sci 1979;76(9):4350-4354

99. Uechi M, Sasaki T, Ueno K, et al. Cardiovascular and renal effects of carvedilol in dogs with heart failure. J Vet Med Sci 2002;64(6):469-475

100. Wakefield LM, Smith DM, Flanders KC, Sporn MB. Latent transforming growth factor-beta from human platelets. A high molecular weight complex containing precursor sequences. J Biol Chem 1988; 263:7646-7654

100. Walker GA, Masters KS, Shah DN, et al. Valvular myfibroblast activation by transforming growth factor β: Implications for pathological extracellular matrix remodeling in heart valve disease. Circ Res 2004;95:253-260

101. Whitney JC. Observation on the effect of age on the severity of heart valve lesions in the dog. J Small Anim Pract 1974;15:511-522

102. Wordsworth P, Ogilvie D, Akhras F, et al. Genetic segregation analysis of familial mitral valve prolapsed shows no linkage to fibrillar collagen genes. Br Heart J 1989;61(3):300-306

103. Xu J, Jian B, Chu R, et al. Serotonin mechanisms in heart valve disease II: The 5-HT_2 receptors and its signaling pathway in aortic valve interstitial cells. Am J Pathol 2002;161:2209-2218

104. Zimmerman SA, Orton CE. Canine heart valve interstitial cell phenotypic and functional properties of normal and myxomatous valves. Proceeding of the 22nd Annual ACVIM Forum 2004:871

CHAPTER 3

HYPOTHESES AND OBJECTIVES

The hypotheses of this dissertation were:

Hypothesis 1: Transformation of valve interstitial cells occurs in canine myxomatous mitral valve tissues with a particular pattern of distribution that depends on the stage of degeneration. To address the hypothesis 1, the study objectives were.

Objective 1.1: To investigate the transformation of valve interstitial cells in canine myxomatous mitral valves.

Objective 1.2: To correlate the valve interstitial cell transformation to disease severity.

Hypothesis 2: Serotonin and transforming growth factor β1 (TGFβ1) signaling are associated with canine myxomatous mitral valve disease. To address hypothesis 2, the study objective was addressed.

Objective 2.1: To examine the expression of target proteins including receptors and effector proteins involved in serotonin and TGFβ1 signaling transduction in mitral valves of normal dogs and dogs affected by late stage of myxomatous degenerative mitral valve disease.

CHAPTER 4

INTERSTITIAL CELLS FROM DOGS WITH NATURALLY-OCCURRING MYXOMATOUS MITRAL VALVE DISEASE UNDERGO PHENOTYPE TRANSFORMATION

Myxomatous degeneration is a non-inflammatory pathological condition of cardiac valves characterized by interstitial cell proliferation, disruption of the collagenous and elastin matrix architecture, and accumulation of glycosaminoglycan (Devereux, 1995; Fontana et al, 1991; King et al, 1982; Kogure, 1980). Myxomatous degeneration is closely associated with the mitral valve prolapse (MVP) syndrome in humans (Braunwald, 1997). Estimates of the prevalence of MVP range from 3% to 5% of the population (Devereux, 1988; Savage et al, 1983; Levy and Savage, 1963). MVP is an important cause of mitral regurgitation in humans (Savage et al, 1983; Guy et al, 1980). Myxomatous degeneration of the mitral valve is also a naturally occurring disease of domesticated dogs accounting for 40% of heart disease in this species (Buchanan, 1999). The prevalence of myxomatous mitral valve disease in dogs 9-years or older is reported to be as high as 20 to 25% (Delweiler and Patterson, 1965). Several authors have documented the similarities between human and canine myxomatous mitral valve degeneration based on functional and pathologic criteria (Pederson and Haggstrom, 2000; Pomerance and Whitney, 1970; Pensinger, 1965).

Interstitial cells are thought to maintain normal heart valve architecture through balanced synthesis and degradation of extracellular matrix (Mulholland and Gotlieb, 1996; Dreger et al, 2002; Taylor et al, 2003). Several lines of investigation suggest that interstitial cells are phenotypically plastic and transdifferentiate to mediate developmental and pathologic processes within cardiac valves (Rabkin et al, 2001; Rabkin et al, 2002; Rabkin-Aikawa et al, 2004; Tamura et al, 2000; Durbin and Gotlieb, 2002; Messier et al, 1994; Black et al, 2005). Interstitial cells from normal human mitral valves exhibit a quiescent fibroblastic phenotype, whereas interstitial cells from human myxomatous mitral valves demonstrate an "activated myofibroblast" phenotype identified by expression of smooth muscle α-actin, desmin, and non-muscle (embryonic) heavy chain myosin (Rabkin et al, 2001). "Activated myofibroblasts" strongly express several catabolic enzymes and are now implicated as mediators of developmental and pathologic remodeling processes in cardiac valves (Rabkin et al, 2001; Rabkin et al, 2002; Rabkin-Aikawa et al, 2004; Tamura et al, 2000).

Because of the recognized similarity in microscopic pathology between canine and human myxomatous mitral valve disease, the hypothesis that interstitial cells from dogs with naturally-occurring myxomatous mitral valve disease undergo phenotypic transformation similar to that described for human myxomatous mitral valves was addressed. The further hypothesis that if transformed interstitial cells mediate the myxomatous pathology, there should be close correlation between phenotypic transformation and valve pathology as the disease progresses was also created. To address these hypotheses, immunohistochemistry was performed on mitral valves from normal dogs and dogs with 3 stages of myxomatous mitral valve disease based on gross pathologic criteria.

MATERIALS AND METHODS

Tissue Collection

Mitral valves were collected postmortem from dogs that died naturally or underwent euthanasia for reasons unrelated to this study. Mitral valves were collected from apparently normal dogs that died for reasons unrelated to cardiovascular disease, had no cardiac murmur at the time of death, and showed no evidence of mitral valve disease on gross postmortem examination. Mitral valves were collected from dogs with degenerative mitral valve disease and were classified as early-, intermediate-, or late-stage disease based on gross postmortem criteria (Kogure, 1980).

Normal: Thin and translucent leaflets with no nodular thickening on leaflet edge. Chordae tendineae not thickened, elongated, or ruptured.

Early-stage: Small discrete nodules present along the edge of valve leaflets. Chordae tendineae not thickened, elongated, or ruptured.

Intermediate-stage: Thickening and nodules extend over entire rough zone of the valve leaflet margin. Annular portion of leaflet less affected. Chordae tendineae thickened in their proximal portion and mildly elongated. Chordae tendineae rupture may be present.

Late-stage: Entire valve leaflet severely thickened. Chordae tendineae thickened and elongated. Rupture of secondary or primary chordae tendineae usually present.

The thickness of valve leaflet margin was measured with calipers. Tissues were fixed with 10% formalin for 24 hours at room temperature, embedded in paraffin, cut into 4 μm sections, and mounted on glass slides. Each valve was stained with modified Movat

pentachrome stain (American Mastertech Scientific). Valves were evaluated for morphologic changes including glycosaminoglycan (GAG) accumulation, disruption of collagen bundles, elastin fragmentation, and loss of normal valve architecture.

Immunohistochemistry

Immunohistochemistry was performed to determine the cytoskeletal phenotype, collagenase expression, presence of endothelial or inflammatory cells, and proliferation index. Primary monoclonal antibodies for cytoskeletal phenotyping were directed against vimentin, smooth muscle α-actin, desmin, smooth muscle myosin heavy chain (SMMS-1) (Dako Carpenteria, CA, USA), and non-muscle (embryonic) heavy chain myosin (SMemb) (Abcam, Cambridge, MA, USA) (Aikawa, 1998). Monoclonal antibodies against matrix metalloproteinase-1 (MMP-1) and matrix metalloproteinase-13 (MMP-13) (Calbiochem, San Diego, CA, USA) were used to determine collagenase expression. Presence of inflammatory cells was determined by staining with monoclonal antibodies to CD-68 (macrophages) and CD-45 (T-cells). Endothelial cells were demonstrated by a monoclonal antibody to CD-31 (PECAM-1) (Paranya et al, 2001). Interstitial cells in active phases of the cell cycle were identified by monoclonal anti-Ki-67 antigen (Dako Carpenteria, CA, USA) (Gerdes et al, 1984). Tissue sections of canine small intestine served as a positive control for Ki-67 staining (Hu et al, 2006)

Immunohistochemistry staining was performed on an automated staining machine. Tissues were pretreated with an antigen retrieval solution at 95□C for 20 minutes. (Target retrieval solution S1699, Dako). Tissue sections were incubated sequentially with 0.03% hydrogen peroxide containing 0.031 mol/L sodium azide for 5 minutes, primary monoclonal

antibody for 30 minutes, peroxidase-conjugated goat anti-mouse antibody solution for 30 minutes, and 3,3'-diaminobenzidine for 5 minutes at room temperature. For non-muscle myosin immunohistochemistry, incubation with alkaline phosphatase-conjugated goat anti-mouse antibody solution for 30 minutes was substituted and followed by incubation with fast red for 5 minutes at room temperature. Sections were counterstained with Mayer's hematoxylin for 6 minutes and mounted. Negative controls for each tissue were created by substituting universal negative control for N-series mouse antibodies (Dako, Carpenteria, CA, USA) for primary monoclonal antibodies. Double immunohistochemical staining against α-actin and MMP-1 or MMP-13 was performed.

Quantitative Analysis

Stained sections were photographed at 400x magnification by using a digital camera (AxioCam MRc5) and image analysis system (Axiovision). Five images were randomly taken of each valve layer for each tissue sample and stored. Quantitative analysis of cell density and positive staining for α-actin, non-muscle myosin, MMP-1 and MMP-13 were performed by manual counting. The mean number of total cells and positive cells per 40x power field was calculated for each leaflet layer and each disease stage. Difference in cell counts either leaflet layer or stages of degeneration were determined by one-way ANOVA. Pair-wise comparisons were made with the Fisher least significant difference test. The normality of data was tested by Ryan-Joiner test. Values of $p < 0.05$ were considered significant.

RESULTS

Animals

Mitral valves were collected from 4 normal dogs and 4 dogs each with early-, intermediate-, and late-stage of myxomatous mitral valve disease (16 dogs total). Normal dogs had a median age 3.5 yrs (range 1 - 6 yrs) and were younger ($p < 0.05$) than dogs with degenerative mitral valve disease. Median ages were 10.5 yrs (range 9 – 13 yrs), 12 yrs (range 9 – 13 yrs), and 11.5 yrs (range 11 – 13 yrs) for dogs with early-, intermediate-, and late-stage degenerative mitral disease, respectively. Cause of death or euthanasia was related to mitral valve disease in 3 dogs with late-stage disease and 1 dog with intermediate-stage disease. Cause of death was unrelated to cardiovascular disease in all other dogs. Mean weight was 22.9 ± 7.3 kg and was not different between groups. Gender distribution was 10 females and 6 males. Thirteen breeds of dog were represented in the study with no breed of dog represented more than twice. The summary data regarding body weight, gender, age, cause of death, and breed of dogs are presented in Table 4.1.

Table 4.1: The summary data regarding body weight, gender, age, cause of death, and breed of dogs

Dog	Stage	Age (year)	Weight (kg)	Sex	Breed	Cause of death
1	Normal	1	20.04	MI	Australian heeler	Car accident (D)
2	Normal	6	10.92	MC	West highland	Lymphosarcoma (E)
3	Normal	4	30.69	FS	Labrador retriever	Car accident (E)
4	Normal	3	28.67	FI	German shorthair	Car accident (E)
5	Early	9	17.14	FS	Cocker spaniel	Adenocarcinoma (E)
6	Early	11	25.05	MC	Shepherd mixed	Hemangiosarcoma (E)
7	Early	13	16.67	FS	Australian shepherd	Mammary gland adenoma (E)
8	Early	10	31.06	MC	Labrador retriever	Lymphosarcoma (E)
9	Intermediate	13	26.52	FS	Greyhound	Leiomyoma (E)
10	Intermediate	17	13.34	FS	Keeshond	Gastric lymphoma (E)
11	Intermediate	11	28.50	MC	Greyhound	MVD (E)
12	Intermediate	9	30.96	MC	Golden retriever	Gastric dilatation vulvulus (E)
13	Late	12	13.60	FS	Mixed	Hepatocellular carcinoma (D)
14	Late	13	19.00	FS	Cocker spaniel	MVD (D)
15	Late	11	21.93	FS	Australian shepherd	MVD (E)
16	Late	11	32.90	FS	Mixed	MVD (E)

MI indicates male intact; MC, male castrated; FI, female intact; FS, female sprayed; MVD, degenerative mitral valve disease; D, Died; E, euthanasia.

Valve Morphology and Histology

Mitral valves exhibited gross morphological change compatible with normal valves or myxomatous degeneration with early-, intermediate-, and late-stage disease (Fig.4.1). Septal leaflet thickness was statistical different ($p < 0.01$) between normal (0.55±0.24 mm), early- (1.18±0.14 mm), intermediate- (2.14±0.23 mm), and late-stage (3.13±0.09 mm) disease (Fig. 4.2).

Movat pentachrome-stained sections of normal canine mitral valves revealed 3 well-defined leaflet layers (Fig. 4.3A). The *lamina atrialis* was covered by endothelium on the valve surface, and contained interstitial cells with well organized parallel layers of elastin. The *lamina spongiosa* was rich in GAG and contained loosely arranged collagen fibers. The *lamina fibrosa* contained dense organized bundles of collagen and a smooth continuous layer of endothelium on its ventricular surface. Interstitial cells were present in all layers of valve stroma. Histopathologic changes in early-stage valve degeneration (Fig. 4.3B) occurred predominately in the *lamina atrialis* where interstitial cell density appeared increased and in the *lamina spongiosa* where early nodular GAG accumulation accounted for increased leaflet thickness (Fig. 4.3B). Mild disruption of elastin and collagen bundles was evident in the *lamina atrialis* and *lamina fibrosa*, respectively. Valve leaflets with intermediate-stage degeneration showed increased cellular density in all valve layers, but especially in subendocardial *lamina atrialis*. Increased GAG accumulation was more prominent and evenly distributed throughout the *lamina spongiosa* (Fig. 4.3C). Elastin fibers were fragmented and collagen bundles were disrupted and poorly organized in the *lamina atrialis* and *lamina fibrosa,* respectively. In late-stage valve degeneration, pathologic changes were exacerbated and distinct lamina architecture was largely abolished (Fig. 4.3D).

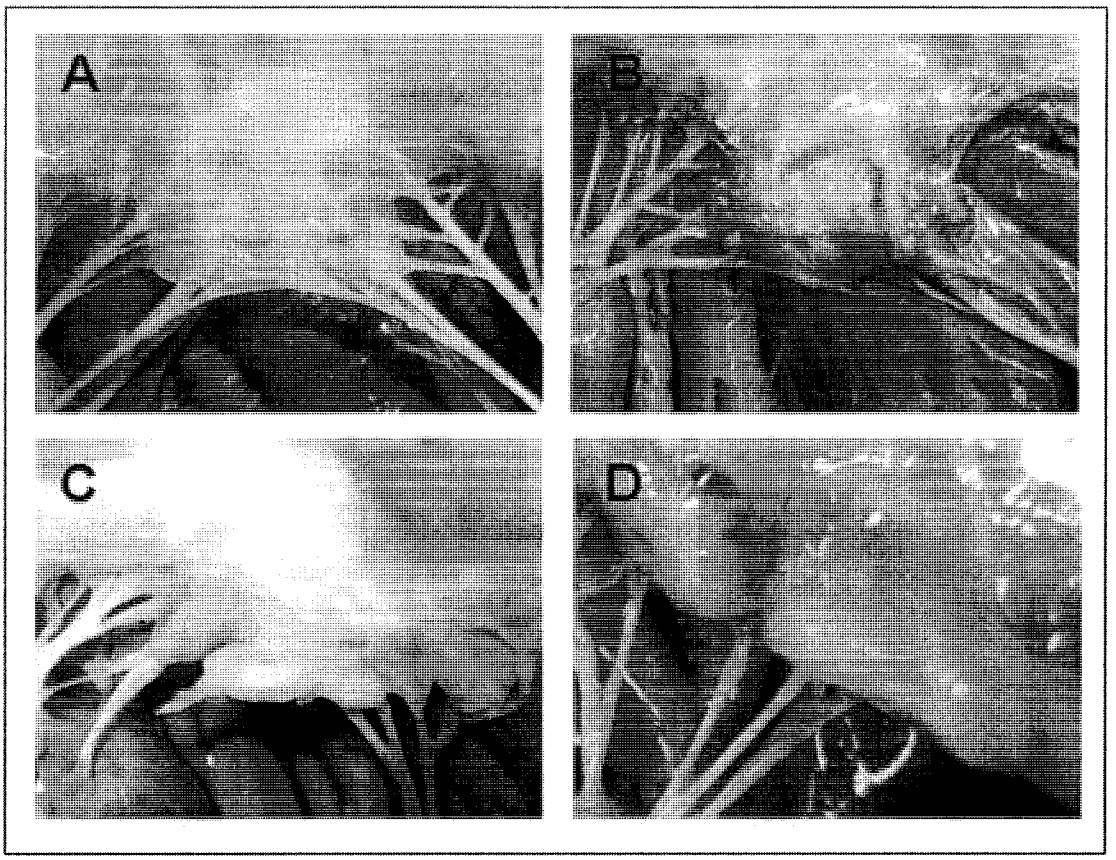

Figure 4.1: Morphology of normal and myxomatous canine mitral valves. (A) Normal canine mitral valve had thin translucent leaflets and intact chordal structure. (B) Early-stage degeneration of canine mitral valves showed mild nodularity and thickening of leaflet margin (i.e. rough zone). Chordal structure was intact. (C) Intermediate-stage myxomatous mitral valves showed thickening of leaflet margin with the annular portion of leaflet less affected. Structural changes in chordal apparatus were present including a ruptured chordae tendineae. (D) Late-stage myxomatous mitral valves showed severe thickening and distortion of valve leaflet. Elongation and rupture of chordae tendineae was present (not shown).

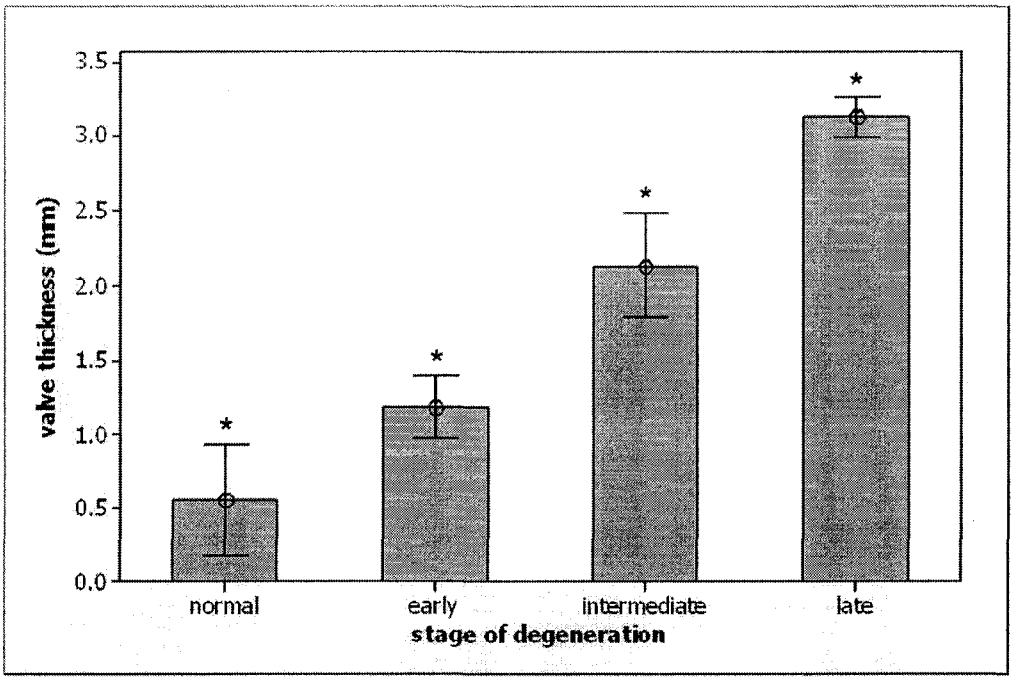

Figure 4.2 Valve leaflet thickness was different ($p<0.05$) between normal, early-, intermediate-, and late- stage degenerative mitral valves from dogs.

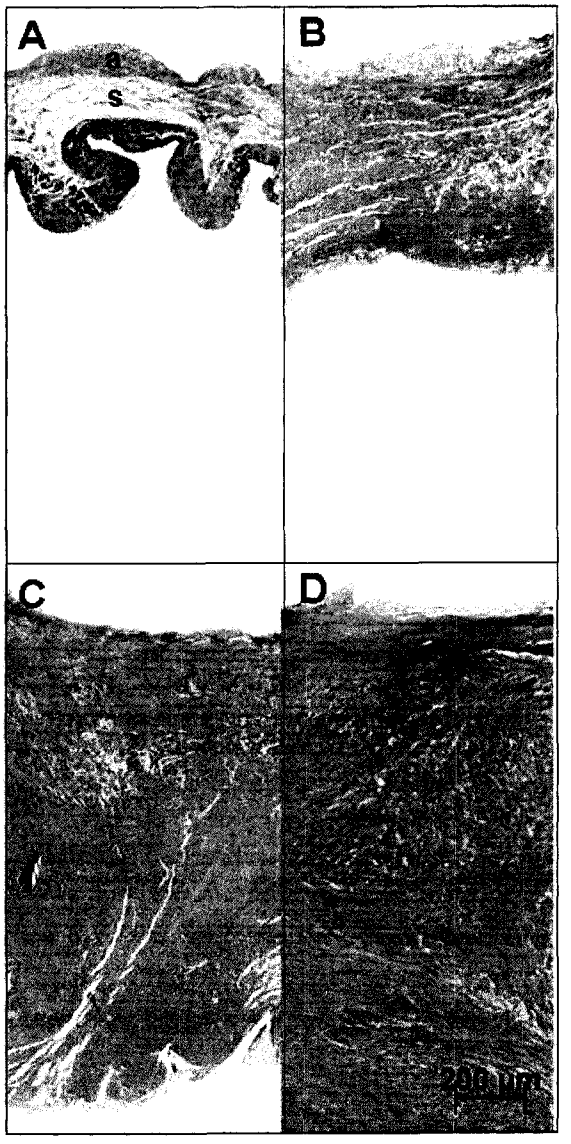

Figure 4.3: Movat pentachrome photomicrographs (collagen - yellow; glycosaminoglycan - blue-green, elastin - black) of normal and myxomatous canine mitral valves. Original magnification x25. (A) Normal mitral valve leaflet. The *lamina atrialis* (a), *lamina spongiosa* (s), and *lamina fibrosa* (f) were readily identified. (B) Early-stage myxomatous mitral valve. (C) Intermediate-stage myxomatous mitral valve. (D) Late-stage myxomatous mitral valve (full thickness of leaflet not shown).

Immunohistochemistry

Immunohistochemistry

Canine interstitial cells (> 95%) in normal and myxomatous mitral valves were positive for vimentin. Smooth muscle cells, identified by positive staining for smooth muscle α-actin and smooth muscle heavy chain myosin, were found near the atrial surface of the leaflet in normal and myxomatous mitral valves. Smooth muscle cells was more prominent at the base of the leaflet toward the annulus and thinned to a 1 or 2 cell thick layer toward the free edge of the leaflet. Normal mitral interstitial cells were negative for α-actin or desmin; whereas myxomatous interstitial cells became positive for smooth muscle α-actin and desmin, but remained negative for smooth muscle heavy chain myosin (Fig 4.4). Smooth muscle α-actin or desmin positive interstitial cells first appeared in the subendocardial *lamina atrialis* in early-stage disease, extended more deeply into the *lamina atrialis* and *lamina spongiosa* in late-stage disease, and tended to occur in "cellular clusters" rather than being dispersed throughout the matrix. Staining patterns for α-actin and desmin were virtually identical on sequential sections. The number of α-actin positive cells increased with disease severity, especially in the *lamina atrialis* (Table 4.2). Interstitial cells from normal mitral valves were negative for non-muscle (embryonic) myosin, whereas interstitial cells from myxomatous mitral valves were positive for non-muscle (embryonic) myosin (Fig. 4.5). Positive staining for non-muscle (embryonic) myosin correlated with disease severity, was dispersed throughout the matrix, and occurred in all valve layers (Table 4.2).

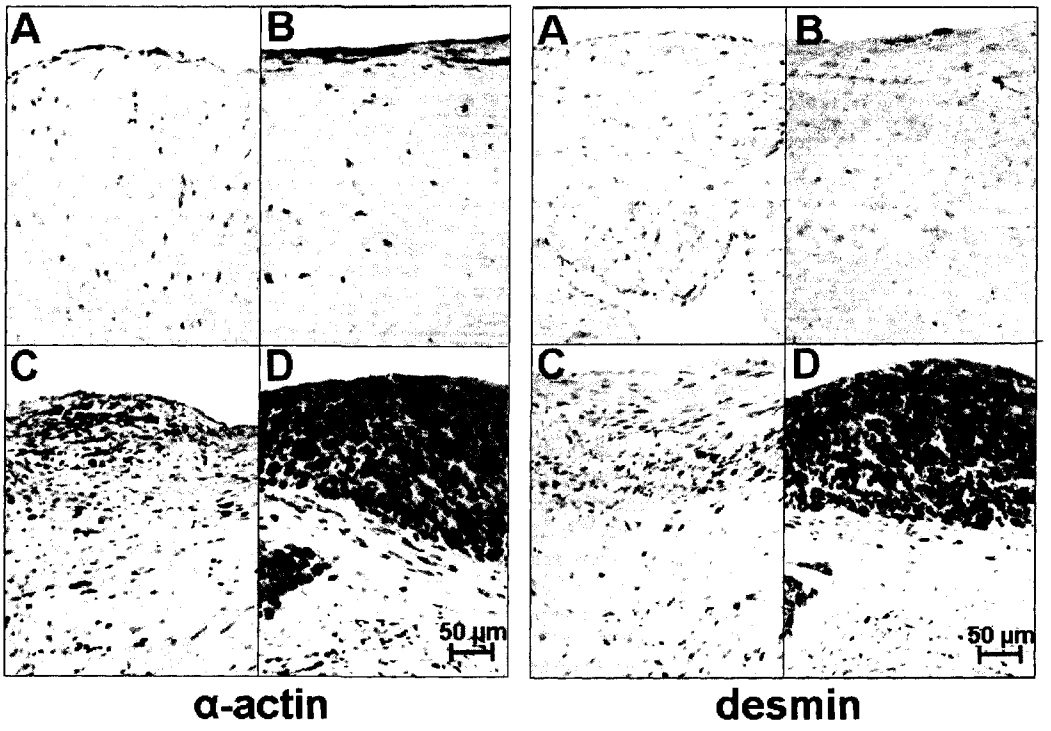

Figure 4.4: Smooth muscle α-actin and desmin immunohistochemistry of normal and myxomatous canine mitral valves. Original magnification x100. (A) Normal mitral valve. (B) Early-stage myxomatous mitral valve. (C) Intermediate-stage myxomatous mitral valve. (D) Late-stage myxomatous mitral valve. α-actin and desmin positive cells first appeared in the subendothelial region the *lamina atrialis*, extended more deeply into the deeper layers of leaflets in late-stage disease.

Table 4.2: Mitral Valve Immunohistochemistry: Number of interstitial cells staining positive for smooth muscle α-actin, non-muscle (embryonic) heavy chain myosin, matrix metalloproteinase-1 (MMP-1) and -13 (MMP-13) in normal and myxomatous canine mitral valves.

	Normal (n=4)	Early (n=4)	Intermediate (n=4)	Late (n=4)
α-actin				
Atrialis	1.0 ± 0.5^{a}	$12.2\pm2.9^{b,1}$	$33.7\pm6.9^{c,1}$	$61.0\pm5.3^{d,1}$
Spongiosa	0.9 ± 0.3^{a}	$4.8\pm1.9^{b,2}$	$7.2\pm2.7^{bc,2}$	$8.1\pm1.2^{c,2}$
Fibrosa	0.8 ± 0.5^{a}	$2.9\pm1.1^{b,2}$	$3.5\pm2.3^{bc,2}$	$4.6\pm0.5^{c,2}$
Non-muscle myosin				
Atrialis	0.8 ± 0.6^{a}	$5.8\pm1.2^{b,1}$	$9.9\pm1.5^{c,1}$	$19.1\pm2.3^{d,1}$
Spongiosa	1.1 ± 0.3^{a}	$6.1\pm0.9^{b,1}$	$10.8\pm2.3^{c,1}$	$15.5\pm0.6^{d,2}$
Fibrosa	1.2 ± 0.8^{a}	$4.2\pm0.4^{b,2}$	$5.3\pm1.0^{bc,2}$	$5.6\pm0.9^{c,3}$
MMP-1				
Atrialis	$3.7\pm0.8^{a,1}$	$24.4\pm2.2^{b,1}$	$42.7\pm2.3^{c,1}$	$58.5\pm2.3^{d,1}$
Spongiosa	$4.4\pm0.7^{a,2}$	$10.8\pm0.6^{b,2}$	$12.4\pm1.8^{b,2}$	$10.5\pm2.1^{b,2}$
Fibrosa	$2.4\pm0.3^{a,1}$	$5.6\pm0.7^{b,3}$	$7.8\pm1.6^{c,3}$	$6.3\pm1.3^{c,3}$
MMP-13				
Atrialis	3.9 ± 0.6^{a}	$13.9\pm0.9^{b,1}$	$28.3\pm2.6^{c,1}$	$40.9\pm1.8^{d,1}$
Spongiosa	3.3 ± 1.5^{a}	$7.5\pm0.9^{b,2}$	$8.3\pm0.6^{b,2}$	$11.5\pm2.8^{c,2}$
Fibrosa	2.4 ± 0.4^{a}	$5.1\pm1.1^{b,3}$	$4.0\pm0.3^{b,3}$	$4.1\pm1.1^{c,3}$

Values are mean number of positive-staining cells per 40x field ± S.D. Different letters within a row indicate significant difference between stages of degeneration ($p<0.05$). Different numbers within a column indicate significant differences between layers of mitral valve leaflet ($p<0.05$).

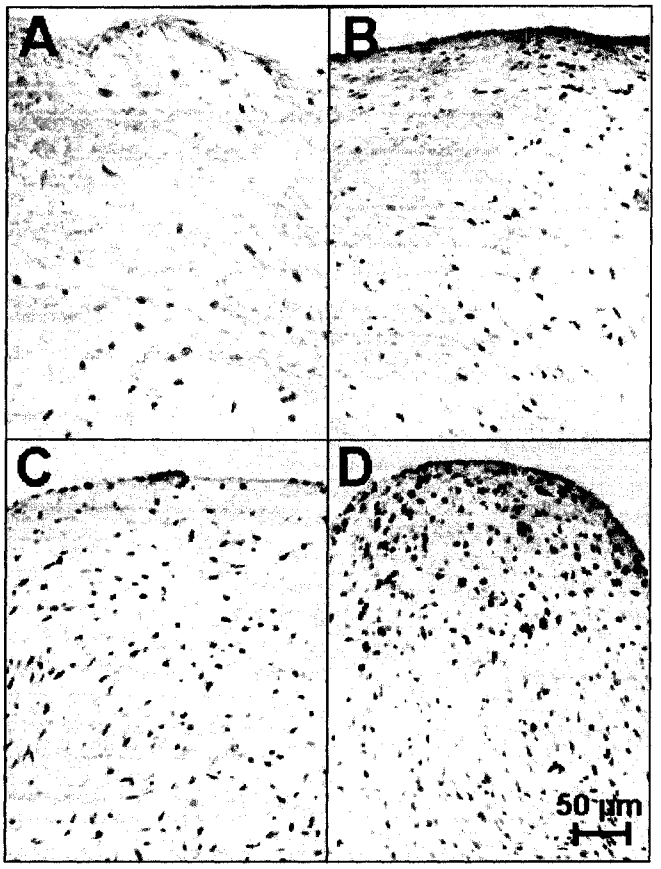

Figure 4.5: Non-muscle (embryonic) heavy chain myosin (SMemb) immunohistochemistry of normal and myxomatous canine mitral valves. Original magnification x100. (A) Normal mitral valve. (B) Early-stage myxomatous mitral valve. (C) Intermediate-stage myxomatous mitral valve. (D) Late-stage myxomatous mitral valve. Positive staining for SMemb correlated to disease severity, was dispersed throughout matrix and occurred in all valve layers.

Immunohistochemical staining for MMP-1 and MMP-13 was light and sparsely distributed throughout all layers of normal canine mitral valves. In early-stage mitral degeneration, clusters of MMP-1 and MMP-13 positive cells appeared first in the subendocardial *lamina atrialis* in regions of positive α-actin and desmin staining (Fig. 4.6). In later stages of disease, MMP positive staining was dispersed throughout the *lamina spongiosa* and *lamina fibrosa* and correlated with disease severity (Table 4.2). Double immunohistochemical staining for α-actin and MMP-1 or MMP-13 (Fig. 4.7) demonstrated that MMP expression was not restricted to α-actin positive cells.

Normal mitral valves had a continuous monolayer of thin CD-31 positive endothelial cells on the valve surfaces (Fig. 4.8). In myxomatous mitral valves, CD-31 positive cells were absent from portions of the valve surface. Loss of CD-31 staining cells occurred on both the atrial and ventricular surfaces and was progressive with disease stage. CD-68 (macrophage) or CD-45 (T-cell) positive cells were only very sparsely present in both normal and myxomatous canine mitral valves.

Cellularity and Ki-67 Proliferation

Total interstitial cellularity increased in myxomatous mitral valves (Table 4.3). Increases in cell number in the *lamina atrialis* accounted for most of the increase in total interstitial cellularity. Positive staining for Ki-67 was nearly undetectable in normal and early-stage myxomatous mitral valves and was only sparsely present (< 0.05 % of interstitial cells), primarily in the *lamina atrialis,* in intermediate- and late-stage myxomatous mitral valves (Fig. 4.9).

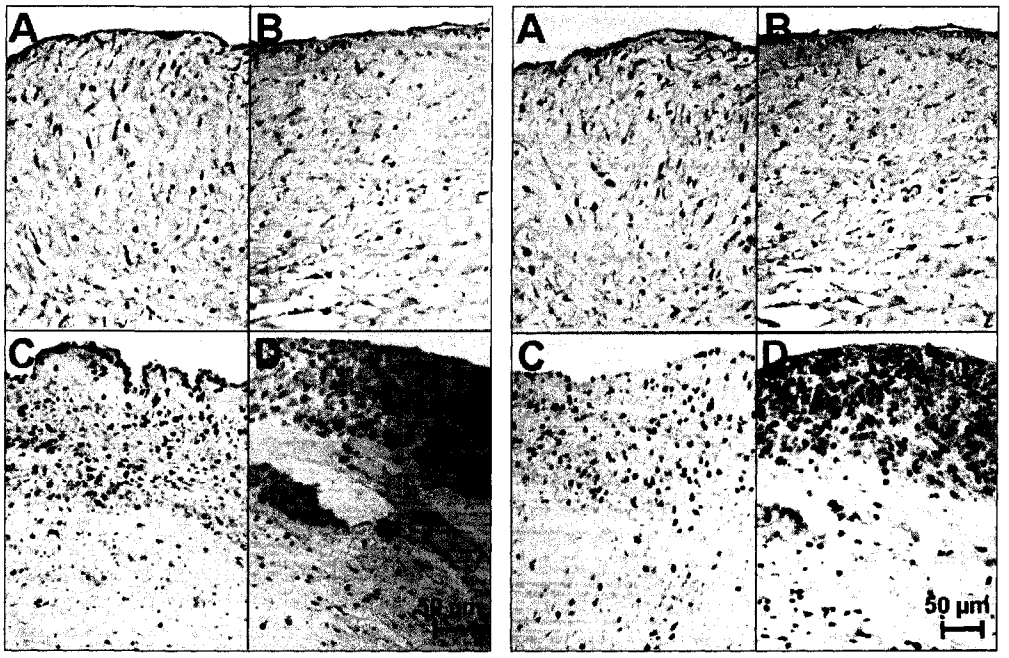

Figure 4.6: MMP-1 and MMP-13 immunohistochemistry of normal and myxomatous canine mitral valves. Original magnification x100. (A) Normal mitral valve. (B) Early-stage myxomatous mitral valve. (C) Intermediate-stage myxomatous mitral valve. (D) Late-stage myxomatous mitral valve. MMP positive staining were dispersed throughout the valve leaflet and correlated with disease severity.

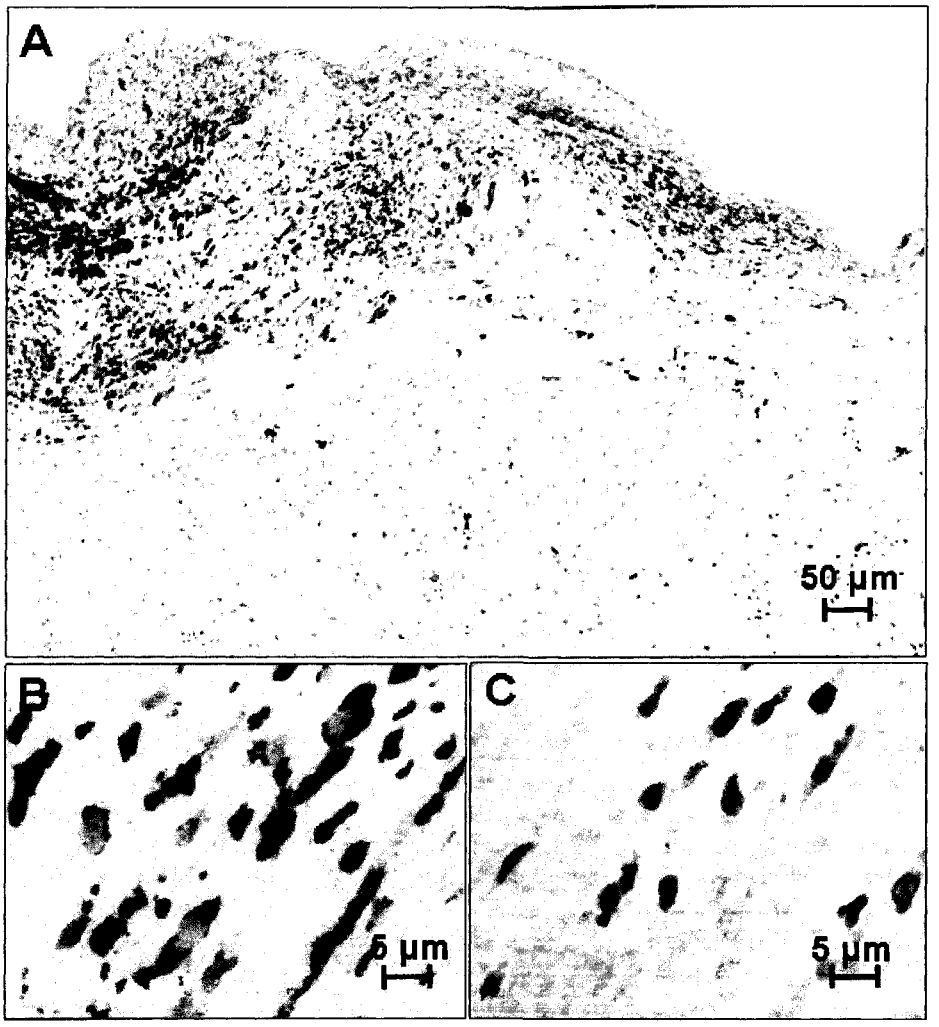

Figure 4.7: Double immunohistochemical stain for smooth muscle α-actin (red) and MMP-13 (brown) of a canine myxomatous mitral valve (A). Original magnification x50. Interstitial cells in the *lamina atrialis* (B) showing positive staining for both α-actin and MMP-13. Original magnification x400. Interstitial cells in *lamina fibrosa* layer (C) showing positive staining for MMP-13 only. Original magnification x400. Double immunohistochemical staining for α-actin and MMP-13 demonstrated that MMP expression was restricted to α-actin positive cells.

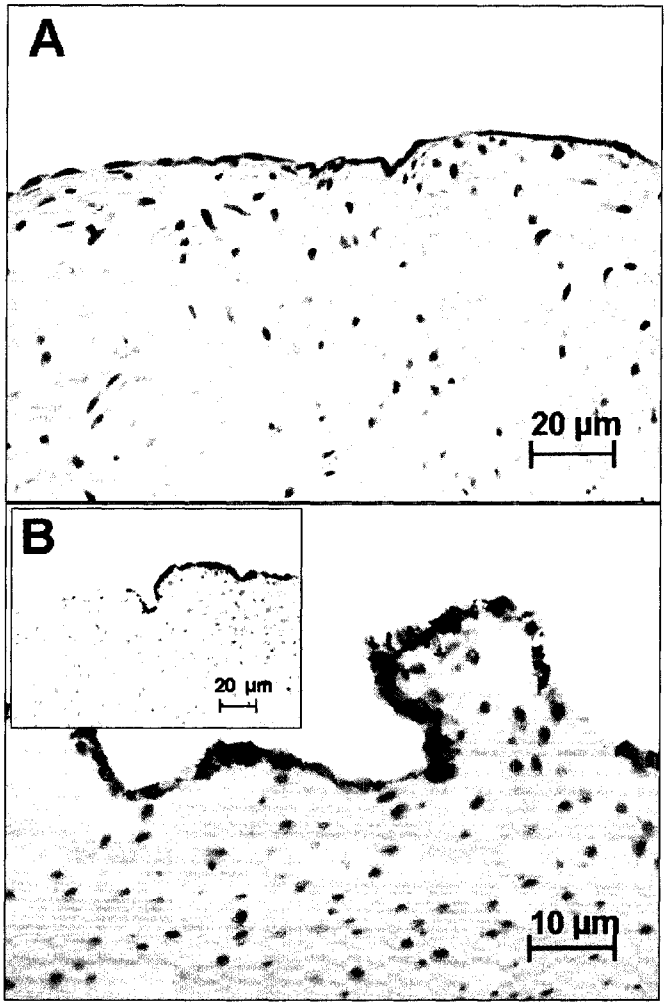

Figure 4.8: Endothelial cell maker, CD-31, immunohistochemistry of a normal (A) and intermediate-stage myxomatous (B) mitral valve. Original magnification x100. Normal mitral valves had a continuous monolayer endothelial cells. In myxomatous mitral valves, endothelial cells were absent from portions of the valve surface.

Table 4.3: Total interstitial cell density and cell density of *lamina atrialis, lamina spongiosa, lamina fibrosa* from normal and early-, intermediate-, and late-stage myxomatous canine mitral valves.

	Normal	Early	Intermediate	Late
Atrialis	10.50 ± 2.65^{a}	$36.77\pm6.10^{b,1}$	$54.65\pm4.55^{c,1}$	$81.65\pm7.83^{d,1}$
Spongiosa	14.65 ± 2.41^{a}	$17.83\pm1.66^{b,2}$	$19.53\pm2.67^{b,2}$	$20.72\pm1.78^{b,2}$
Fibrosa	13.38 ± 4.03	10.40 ± 2.28^{2}	14.50 ± 2.38^{2}	16.95 ± 4.53^{2}
Total	38.58 ± 3.17^{a}	65.95 ± 4.13^{b}	86.23 ± 5.17^{c}	119.32 ± 5.87^{d}

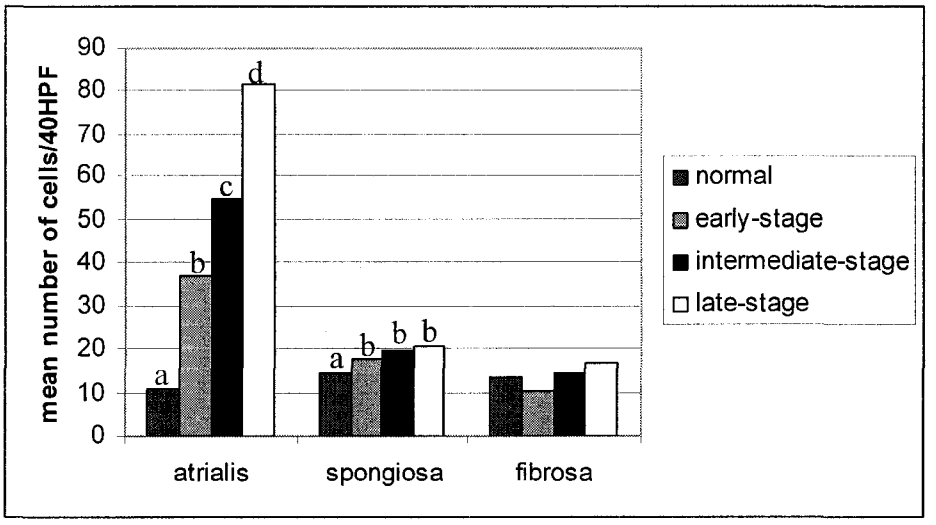

Values are mean number of cells per 40x field ± S.D. Different letters within a row indicate significant difference between stages of degeneration ($p<0.05$). Different numbers within a column indicate significant differences between layers of mitral valve leaflet ($p<0.05$).

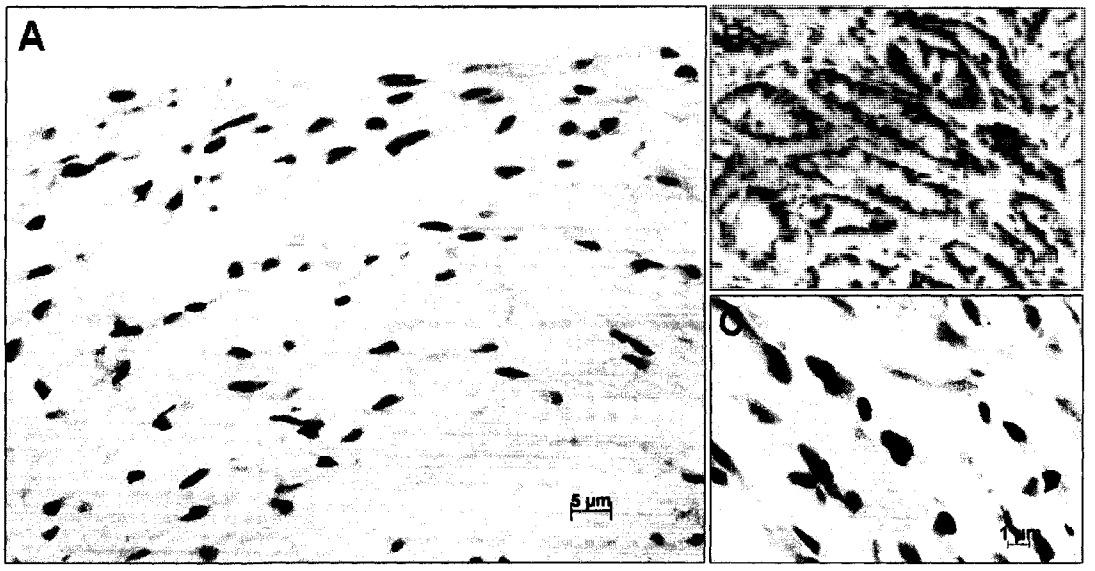

Figure 4.9: Immunohistochemistry for proliferation marker, Ki-67, showing only sparse positive staining in a late-stage myxomatous canine mitral valve (A & C) Original magnification x100 and x400, respectively. Small intestine (B) served as a positive control. Original magnification x100.

DISCUSSION

Normal canine interstitial cells were uniformly positive for vimentin, but were not immunoreactive to smooth muscle α-actin, desmin, or non-muscle (embryonic) myosin. Thus, a majority of canine mitral interstitial cells were concluded to have a quiescent fibroblastic phenotype (Rabkin et al, 2001). A few cells near the atrial surface of normal valves were classified as differentiated smooth muscle cells based on positive for both smooth muscle α-actin and smooth muscle myosin (Aikawa et al, 1998). These findings consistent with those reported for normal human mitral valves (Rabkin et al, 2001).

Interstitial cells from canine myxomatous valves showed progressive positive staining for α-actin and desmin, but remained negative for smooth muscle myosin. As a result, canine myxomatous interstitial cells fulfilled criteria for transdifferentiation to a myofibroblasts in a manner similar to that described for human myxomatous interstitial cells (Rabkin et al, 2001). Transformed myofibroblasts expressed both α-actin and desmin based on identical staining patterns on sequential histological sections. This was an apparent difference from human mitral valve myofibroblasts which were found to express either α-actin or desmin, but not necessarily both. A clear pattern of progression for myofibroblast transformation was identified by examining mitral valves at various stages of disease. Myofibroblasts first appeared in the subendocardial *lamina atrialis* in early-stage disease and spread progressively across the *lamina atrialis* and into the *lamina spongiosa* in later stages of disease. Myofibroblastic interstitial cells formed "cellular clusters" rather than being randomly dispersed throughout the matrix. This pattern of progression for interstitial cell myofibroblast transformation was a new finding that was not reported in human myxomatous valves (Rabkin et al, 2001).

Normal canine interstitial cells did not express non-muscle (embryonic) myosin, but myxomatous interstitial cells showed positive staining that increased with disease severity. These findings were again consistent with results for human mitral valves (Rabkin et al, 2001), however the expression pattern clearly differed from α-actin and desmin expression in that non-muscle myosin expression was dispersed throughout all leaflet layers and did not occur in cellular clusters. Non-muscle (embryonic) myosin (SMemb) is an isoform of the myosin heavy chain that is expressed in embryonic smooth muscle cells, but not normal adult smooth muscle cells (Aikawa et al, 1998). Non-muscle myosin expression occurs in neointimal cells after vascular injury and is currently considered a marker of mesenchymal cell activation and proliferation (Aikawa et al, 1998). Based on these criteria, valve interstitial cells expressing non-muscle myosin are classified as having an "activated" mesenchymal cell phenotype.

Metalloproteases (MMP) represent a family of zinc-dependent endoproteases that play an important role in extracellular matrix remodeling in many tissues including heart valves (16). Expression of interstitial collagenases, MMP-1 and MMP-13, was increased in canine myxomatous mitral valves compared to normal mitral valves. This finding was in agreement with findings in human myxomatous mitral valves which demonstrated increased expression of these and other catabolic matrix enzymes (Rabkin et al, 2001). MMP expression, based on both staining intensity and number of positive cells, correlated with progression from early- to late-stage myxomatous disease. Co-localization demonstrated that MMP expression was increased in areas of myofibroblast transformation, but also extended beyond these areas. The pattern of MMP expression appeared to closely match the expression pattern for non-muscle myosin.

Current understanding suggests that "activated myofibroblasts" mediate developmental, adaptive, and pathologic remodeling processes within cardiac valves (Rabkin et al, 2001; Rabkin et al, 2002; Rabkin-Aikawa et al, 2004). If this is true then it is reasonable to expect that phenotype transformation would correlate with disease stage or severity, and this was the case in canine myxomatous mitral valves. However, our results suggest that there may be two distinct types of interstitial cell phenotype transformation. "Myofibroblast transformation" characterized by expression of α-actin and desmin; and mesenchymal cell "activation" characterized by expression of non-muscle myosin. Both phenotype patterns correlated with disease severity, but differed in their time course and spatial distribution. Myofibroblast transformation began very near the atrial valve surface of the valve and was largely confined to that area in early-stage disease. One possible interpretation of this finding is that triggering signals near the valve surface cause myofibroblast transformation that in turn mediates pathologic events throughout the valve via paracrine and autocrine mechanisms. Alternatively, expression of α-actin or desmin could be a cellular response designed to stabilize abnormal stress or strain near the valve surface. Several lines of evidence suggest that α-actin expression by interstitial cell changes in respond stress or strain loading on the cell (Giles et al, 2007; Weston and Yoganathan, 2001; Merryman et al, 2006a). Further, valve interstitial cells have been known for some time to contract in response to vasoconstrictor agents (Messier et al, 1994). More recent studies have demonstrated that interstitial cell contraction in response to vasoconstrictors can translate into measurable biomechanical changes in the valve leaflet (Kershaw et al, 2004; Merryman et al, 2006b). Thus, it is currently not clear whether α-actin expression represents a specific

cellular response to an abnormal microenvironment or hallmarks a fundamental alteration in the functional phenotype of interstitial cells.

On the other hand, mesenchymal cell "activation", identified by expression of non-muscle myosin, was closely correlated with both the spatial distribution and time course of pathologic changes within the valve. From that standpoint, non-muscle myosin might be a more appealing candidate marker hallmarking a change in the functional phenotype of interstitial cells. The very similar patterns of expression for MMP and non-muscle myosin support this notion. It remains to be determined whether the apparently different patterns of expression for α-actin and non-muscle myosin actually represent different phenotypic transdifferentiation processes, and what implications for interstitial cell function they might carry.

Endothelial cell dysfunction has been implicated in the pathogenesis of cardiac valve diseases including myxomatous disease (Leask et al, 2003). The loss of endothelial cells from the leaflet surfaces of myxomatous valves observed in this study has been reported previously in both canine (Corcoran et al, 2004) and human (Stein et al, 1989) myxomatous mitral valves. Whether endothelial denudation plays a causative role in myxomatous pathology or merely represents a late injury associated with turbulent blood flow can not be resolved by this study. It is interesting that changes observed in early-stage disease, including interstitial cell proliferation and myofibroblast transformation, occurred first in subendocardial regions very near the leaflet surface. Platelet adhesion to areas of endothelial denudation has been documented in canine myxomatous mitral valves (Corcoran et al, 2004) and it is possible to imagine that factors released from platelets, including serotonin, could contribute to transdifferentiation of interstitial cell phenotype.

In conclusion, phenotype transformation occurs in interstitial cells from dogs with myxomatous mitral valve disease and is remarkably similar to that already described for human myxomatous mitral valve disease. Studying canine mitral valves at different disease stages suggested close correlation between phenotype transformation and valve pathology, and identified two different patterns of interstitial cell phenotype transdifferentiation. Myxomatous mitral valve disease in dogs may be a natural model for studying the sequence of triggering signals for and functional consequences of interstitial cell phenotype transformation.

REFERENCES

1. Aikawa M, Rabkin E, Voglic SJ, Shing H, Nagai R, Schoen FJ, Libby P. Lipid lowering promotes accumulation of mature smooth muscle cells expressing smooth muscle myosin heavy chain isoforms in rabbit atheroma. Circ Res 1998;83(10):1015-1026
2. Black A, French AT, Dukes-McEwan J, Corcoran BM. Ultrastructural morphologic evaluation of the phenotype of valvular interstitial cells in dogs with myxomatous degeneration of the mitral valve. Am J Vet Res 2005;66:1408-1414
3. Braunwald E. Valvular heart disease. In Braunwald E, ed. Heart disease. A Textbook of Cardiovascular Medicine, 5th ed. Philadelphia: WB Saunders, 1997;1007-1072
4. Buchanan JW. Prevalence of cardiovascular disorders. In Fox PR, Sisson D, Moise NS, ed. Textbook of Canine and Feline Cardiology, 2nd edition, Philadelphia: WB Saunders, 1999; 457-470
5. Corcoran BM, Black A, Anderson H, et al. Identification of surface morphologic changes in the mitral valve leaflets and chordae tendineae of dogs with myxomatous degeneration. Am J Vet Res 2004;65:198-206
6. Delweiler DK, Patterson DF. The prevalence and types of cardiovascular disease in dogs. Ann NY Acad Sci 1965;127:481-516
7. Devereux RB. Mitral valve prolapse and severe mitral regurgitation. Circulation 1988; 78:234-236
8. Devereux RB. Recent developments in the diagnosis and management of mitral valve prolapse. Curr Opin Cardiol 1995;10:107-116

9. Dreger SA, Taylor PM, Allen SP, Yacoub MH. Profile and localization of matrix metalloproteinases (MMPs) and their tissue inhibitors (TIMPs) in human heart valves. J Heart Valve Dis 2002;11:875-880

10. Durbin AD, Gotlieb AI. Advances towards understanding heart valve response to injury. Cardiovasc Path 2002;11:69-77

11. Fontana ME, Sparks EA, Boudoulas H, Wooley CF. Mitral valve prolapse and the mitral valve prolapse syndrome. Curr Probl Cardiol 1991;16:309-375

12. King BD, Clark MA Baba N, Kilman JW, Wooley CF. "Myxomatous" mitral valves: collagen dissolution as the primary defect. Circulation 1982;66:288-296

13. Kogure K. Pathology of chronic mitral valvular disease in the dog. Jpn J Vet Sci 1980; 42:323-335

14. Levy D, Savage DD. Prevalence and clinical features of mitral valve prolapse. Am Heart J 1963; 113:1281

15. Gerdes J, Lemke H, Baisch H, Wacker HH, Schwab U, Stein H. Cell cycle analysis of a cell proliferation-associated human nuclear antigen defined by the monoclonal antibody Ki-67. J Immunol 1984;133:1710-1715

16. Giles BR, Balachandran K, Sucosky P, Yoganathan AP. Site-specific biological responses of porcine aortic valve to cyclic stretch. Proceedings 4th biennial meeting of the society for heart valve disease 2007; 110

17. Guy FC, MacDonald RPR, Fraser DB, Smith ER. Mitral valve prolapse as a cause of hemodynamically important mitral regurgitation. Can J Surg 1980;23:166-170

18. Hu R, Khor TO, Shen G, et al. Cancer chemoprevention of intestinal polyposis in ApcMin/+ mice by sulforaphane, a natural product derived from cruciferous vegetable. Carcinogenesis 2006;27(10):2038-2046

19.

20. Kershaw JD, Misfeld M, Sievers HH, Yacoub MH, Chester AH. Specific regional and directional contractile responses of aortic cusp tissue. J Heart Valve Dis 2004; 13:798-803

21. Leask RL, Jain N, Butany J. Endothelium and valvular diseases of the heart. Microscopy Res and Technique 2003;60:129-137

22. Merryman WD, Youn I, Lukoff HD, Krueger PM, Guilak F, Hopkins RA, Sacks MS. Correlation between heart valve interstitial cell stiffness and transvalvular pressure: implications for collagen synthesis. Am J Physiol 2006a; 290:H224-H231

23. Merryman WD, Haung HYS, Scheon FJ Sacks MS. The effects of cellular contraction on aortic valve leaflet flexural stiffness. J Biomechanics 2006b;39:88-96

24. Messier RH, Bass BL, Aly HM, Jones JL, Domkowski PW, Wallance RB, Hopkins RA. Dual structural and functional phenotypes of the porcine aortic valve interstitial population: characteristics of the leaflet myofibroblast. J Surg Res 1994; 57:1-21

25. Mulholland DL, Gotlieb AI. Cell biology of valvular interstitial cells. Can J Cardiol 1996;12 231-236

26. Paranya G, Vineberg S, Dvorin E, et al. Aortic valve endothelial cells undergo transforming growth factor-β-mediated and non-transforming growth factor-β-mediated transdifferentiation *in vitro*. Am J Pathol 2001;159(4):1335-1343

27. Pedersen HD, Haggstrom J. Mitral valve prolapse in the dog: a model of mitral valve prolapse in man. Cardiovas Res 2000;47:234-243

28. Pensinger RR. Comparative aspects of mitral valve disease in dogs. Ann NY Acad Sci 1965;118:525

29. Pomerance A, Whitney JC. Heart valve changes common in man and dog: a comparative study. Cardiovasc Res 1970;4:61-66

30. Rabkin E, Aikawa M, Stone JR, Fukumoto Y, Libby P, Scheon FJ. Activated interstitial myofibroblasts express catabolic enzymes and mediate matrix remodeling in myxomatous heart valves. Circulation 2001;104:2525-2532

31. Rabkin E, Hoerstrup SP, Aikawa M, Mayer JE, Schoen FJ. Evolution of cell phenotype and extracellular matrix in tissue-engineered heart valves during in-vitro maturation and in-vivo remodeling. J Heart Valve Dis 2002;11:308-314

32. Rabkin-Aikawa E, Farber M, Aikawa M, Schoen FJ. Dynamic and reversible changes of interstitial cell phenotype during remodeling of cardiac valves. J Heart Valve Dis 2004;13:841-847

33. Savage DD, Devereux RB, Garrison RJ, et al. Mitral valve prolapse in the general population.1. Epidemiologic features: The Framingham Study. Am Heart J 1983;106:577-578

34. Stein PD, Wang CH, Riddle JM, Riddle JM, Sabbah HN, Magilligan DJ, Hawkins ET. Scanning electron microscopy of operatively excised severely regurgitant floppy mitral valves. Am J Cardiol 1989;64(5):392-394

35. Tamura K, Jones M, Yamada I, Ferrans VJ. Wound healing in the mitral valve. J Heart Valve Dis 2000;9:53-63

36. Taylor PM, Batten P, Brand NJ, Thomas PS, Yacoub MH. The cardiac valve interstitial cell. International J Biochem Cell Biol 2003; 35:113-118

37. Weston MW, Yoganathan AP. Biosynthetic activity in heart valve leaflets in response to *in vitro* flow environments. Ann Biomed Engin 2001; 29:752-763

CHAPTER 5

POSSIBLE INVOLVEMENT OF SEROTONIN AND TRANSFORMING GROWTH FACTOR β SIGNALINGS IN CANINE MYXOMATOUS DEGENERATIVE MITRAL VALVE DISEASE

Serotonin or 5-hydroxytryptamine is a monoamine neurotransmitter normally synthesized in central nervous system and enterochromaffin cells in the gastrointestinal tract. Serotonin is involved in regulating function in several organ systems. In the cardiovascular system, serotonin has a role in regulating blood pressure and cardiac function. Actions of serotonin are mediated depending on the interaction of serotonin and numerous cognate receptor subtypes. At present, there are at least 15 receptor subtypes belong to 4 classes including $5HT_{1/5}$, $5HT_2$, $5HT_3$, and $5HT_{4/6/7}$ (Hoyer et al, 1994). Among these receptor subtypes, serotonin 2B receptor ($5HT_{2B}R$) is the predominant subtype found in human (Nebigil et al, 2000) and canine heart (Bonaventure et al, 2005). It has been reported that $5HT_{2B}R$ subtype is involved with regulation of cardiovascular development and function (Nebigil et al, 2001) as well as development of valvular fibroplasia in humans treated with serotonergic drugs (Rothman et al, 2000) and affected by carcinoid tumor, an enterochromaffin cell tumor which secretes large amount of serotonin (Robiolio et al, 1995).

Studies in cell cultures have shown mitogenic effects of serotonin on several cell types (Seuwen et al, 1988; Nemecek et al, 1986; Takamura et al, 1989; Pakula et al, 1994) including valve interstitial cells (Rajamannan et al, 2001). The serotonin mediated mitogenic effect has been reported to involve with both $5HT_{2B}R$ and the mitogen-activated protein kinases/extracellular signaling-regulation kinases (MAPK/ERK) pathways (Nebigil et al, 2000). The effect of serotonin in activation MAPK/ERK signaling has also described in cultured sheep aortic valve interstitial cells. (Xu et al, 2002) Serotonin signaling has been closely linked with the transforming growth factor β1 (TGFβ1) signaling pathway (Jian et al, 2002). The activation of this TGFβ1 signaling pathway generally contributes to the transcription of target proteins involved in cell function regulation including cell proliferation, migration and differentiation.

Myxomatous mitral valve disease is the most common heart valve disease in dogs. Approximately 75% of dogs suffering from heart diseases are affected by myxomatous mitral valve disease (Detweiler and Patterson, 1965). The common microscopic lesions of canine myxomatous valve disease include deposition and destruction of extracellular matrix (ECM) and accumulation of valve interstitial cells in subendothelial regions. These pathologic lesions are similar to those described in human heart valve diseases mediated by serotonergic drugs and carcinoid tumors (Ferrans and Roberts, 1976; McDonald et al, 2002). Because of the similarity of lesions between canine myxomatous mitral valve disease and serotonin induced human heart valve diseases as well as roles of serotonin signaling described in valve interstitial cell cultures (Xu et al, 2002; Jian et al, 2002), the hypothesis that serotonin signaling and its closely associated signaling pathways including MAPK/ERK and TGFβ1 are associated with the evidence of myxomatous mitral valve disease in dogs was created. To

address this hypothesis, the expression of serotonin, ERK1/2 proteins and TGFβ1 signaling pathways were examined in canine normal and myxomatous mitral valves.

MATERIALS AND METHODS

Tissue Collection

Mitral valves were collected postmortem from dogs that died for reasons other than cardiac disease. Myxomatous mitral valves were obtained postmortem from dogs with gross pathologic and histopathologic evidence of myxomatous disease. Myxomatous mitral valves were classified as having late-stage disease based on previously reported criteria (Disatian et al, 2008). Leaflet thickness was measured with calipers.

Immunohistochemistry

Mitral valves were fixed in 10% buffered formalin, embedded in paraffin, cut at 4 μm, and mounted on glass slides. Tissue slides underwent deparaffinization, rehydration, and antigen unmasking with citrate buffer (pH 6) at 95° C for 20 minutes. Immunohistochemical staining was performed using an automated staining machine (Dako, Carpenteria, CA, USA). Sections were pre-incubated with 0.03% hydrogen peroxide containing 0.031 mol/L sodium azide for 5 minutes to block endogenous peroxidase activity. Primary antibody was applied and incubated for 30 minutes. Sections were incubated with peroxidase-conjugated goat anti-mouse or anti-rabbit immunoglobulin (Envision+; Dako) for 30 minutes. Slides were rinsed in Tris-buffered saline after each incubation step. Peroxidase activity was visualized with 3,3'-diaminobenzidine solution fleshly prepared in 0.05 M Tris-HCl buffer (pH 7.6) containing 0.01 M sodium azide and 0.006% hydrogen peroxide.

Sections were counterstained with Mayer's hematoxylin for 6 minutes and mounted with toluene solution.

Primary antibodies were mouse monoclonal antibodies to α-smooth muscle actin (Dako), $5HT_{2B}R$ (BD Biosciences Pharmingen, San Jose, CA, USA), tryptophan hydroxyalse 1 (Sigma-Aldrich, St.Louis, MO, USA), serotonin transporter (Advanced targeting system, San Diego, CA, USA), total ERK1/2 (MBL, Woburn, MA, USA), phosphorylated ERK1/2 (Upstate, Temecula, CA, USA), latency associated peptide (LAP) TGFβ1 (R&D systems, Minneapolis, MN, USA), CD-31 (PECAM1; Dako) and rabbit polyclonal antibodies to TGFβ1 receptor I (Santa Cruz Biotechnology, Santa Cruz, CA, USA), and TGFβ1 receptor II (Santa Cruz Biotechnology). Tissue sections treated with universal negative control for N-series mouse or rabbit antibodies (Dako) provided controls for antibody specificity.

Western Blot Analysis

Mitral valves for Western blot analysis were stored at -80°C until used. Four mitral valves from each group were pooled and manually homogenized in a solution for extracting water-soluble protein (10mM Tris HCl, 1mM dithiothreitol, 2mM $MgCl_2$, 10mM KCl, 100KIU/ml aprotinin, pefabloc 0.5mM, 134mM non-detergent sulfobetaines (NDSB) 256) and lipid-soluble protein (10mM Tris HCl, 1mM dithiothreitol, 2mM $MgCl_2$, 10mM KCl, 100KIU/ml aprotinin, pefabloc 0.5mM, 134mM non-detergent sulfobetaines 256, 1% w/v n-Dodecyl-β-D-Maltose). After centrifugation at 17,000 g at 4°C for 20 minutes, supernatants were concentrated by Centricon® centrifugal filter device (Millipore, Bedford, MA, USA) and retained for analysis. Protein concentration of the supernatant was evaluated using the DC Protein Assay (Bio Rad, Hercules, CA, USA). 40 μg of protein extract from normal and myxomatous mitral valves were combined with SDS sample buffer (Invitrogen) containing

2-Mercaptoethanol and heated at 85 °C for 2 minutes. Protein samples were then loaded on 4-12% Tris-glycine polyacrylamide gels and electrophoresed in Tris-glycine SDS running buffer at 125 V for 90 minutes using an XCell SureLock™ Mini-Cell system (Invitrogen Carlsbad, CA, USA). Protein standards (MagicMark™ Western Protein Standards; Invitrogen) were used for estimating the size of detected proteins. After electrophoresis, proteins were transfer into nitrocellulose membrane (15x15 cm, 0.2 μm pore size; Invitrogen) using XCell II Surelock Minicell blotting system Blot Module (Invitrogen) at 25 V for 90 minutes. Membranes were incubated sequentially in 1% bovine serum albumin blocking solution at room temperature for 30 minutes, primary antibody diluted in a solution of Tris-buffer saline containing 0.01% Tween-20 (TBS-T) and 1% instant nonfat dried milk at 4°C overnight, and secondary antibody for 1 hour at room temperature. Primary antibodies used in Western blot analysis were the same as those used for immunohistochemistry. Western blot analysis with mouse monoclonal anti-α-tubulin (Abcam, Cambridge, MA, USA) was run as a protein loading control. Membranes were rinsed with TBS-T for 10 minutes three times prior to and between incubations. After washing with TBS-T, antibody detection was accomplished with freshly prepared chemiluminescent reagent (Supersignal West Femto; Piece, Rockford, IL, USA). Signals were demonstrated using a CCD camera (BioChemi; UVP, Upland, CA, USA). To confirm the consistency of results, western blot analyses were performed at least twice on two separate pooled protein extractions of normal and myxomatous mitral valves. Data of PROTEIN EXTRACT #1 and #2 are summarized in Table 5.1a and 5.1b, respectively.

Table 5.1a Data of PROTEIN EXTRACT #1

protein	valve	Weight (g)	Volume (μl)	Concentration (μg/μl)	% yield
Water-soluble	normal	0.852	1400	3.13	0.51
	degenerative	1.102	1500	3.08	0.42
Lipid-soluble	normal	0.852	700	2.84	0.23
	degenerative	1.102	800	2.96	0.22

Table 5.1b Data of PROTEIN EXTRACT #2

Protein	valve	Weight (g)	Volume (μl)	Concentration (μg/μl)	% yield
Water-soluble	normal	0.91	1400	3.48	0.54
	degenerative	1.028	1500	3.86	0.56
Lipid-soluble	normal	0.91	700	2.45	0.18
	degenerative	1.028	800	2.81	0.22

RESULTS

Animals

Mitral valves were collected from dogs with normal (n=13) and late-stage myxomatous (n=13) mitral valves. Median age of normal and myxomatous mitral valve dogs was 4 years (range 1-9 years) and 14 years (range 9-15 years), respectively. Cause of death was related to myxomatous mitral valve disease in 4 dogs of myxomatous valve group. Death was not directly related to cardiovascular disease in other dogs. Fourteen of 26 dogs were pure-bred. No breed of dog was represented more than twice in the myxomatous valve group. Data from dogs with normal and myxomatous mitral valves for immunohistochemical and Western blot studies are summarized in Table 5.2 and 5.3, respectively. Valve leaflet thickness was greater ($p<0.05$) for myxomatous mitral valves (2.33±0.16 mm) compared to normal mitral valves (0.60±0.04 mm).

Table 5.2: Data from dogs with normal and myxomatous degenerative mitral valves for immunohistochemical study

Dog	valve	Age (year)	Valve thickness (mm)	Sex	Breed	Cause of death
1	Normal	6	0.64	MI	Labrador retriever	Laryngeal paralysis
2	Normal	7	0.62	MC	Collie	Cranial nerve deficiency
3	Normal	4	0.67	MI	Bull dog	Hit by car
4	Normal	2	0.58	MI	Mixed	Cocaine toxicosis
5	Normal	5	0.57	MC	Scottish terrier	Lymphoma
6	degenerative	15	2.28	MC	CKCS	MVD
7	degenerative	9	2.23	FS	Weimaraner	Hepatic carcinoma
8	degenerative	13	2.04	MC	Basset hound	Lymphoma
9	degenerative	14	2.52	MC	Mixed	Arthritis
10	degenerative	11	2.56	MC	Great dane	Degenerative myelopathy

MI indicates male intact; MC, male castrated; FS, female sprayed; MVD, degenerative mitral valve disease; CKCS, Cavalier King Charles spaniel

Table 5.3 Data from dogs with normal and myxomatous degenerative mitral valves for Western blot study

PROTEIN EXTRACT#1

Dog	Stage	Age (year)	Valve thickness (mm)	Sex	Breed	Cause of death
1	Normal	9	0.57	FS	Golden retriever	Abdominal mass
2	Normal	2	0.64	FS	Labrador retriever	Hepatitis
3	Normal	3	0.57	FS	Boxer	Hit by car
4	Normal	3	0.62	MC	mixed	Melanoma
5	Degenerative	13	2.16	FS	Labrador retriever	Hemangiosarcoma
6	Degenerative	14	2.36	FS	Mixed	Splenic mass
7	Degenerative	14	2.26	FS	shelter	Neuropathy
8	Degenerative	14	2.56	FS	Cocker spaniel	MVD

MC, male castrated; FS, female spayed; MVD, degenerative mitral valve disease

PROTEIN EXTRACT#2

Dog	Stage	Age (year)	Valve thickness (mm)	Sex	Breed	Cause of death
1	Normal	3	0.54	FS	Mixed	Hit by car
2	Normal	6	0.55	FS	Siberian huskey	Cystitis
3	Normal	1	0.65	FS	Mixed	Parvoviral infection
4	Normal	4	0.54	FS	Standard poodle	Immune hemolytic anemia
5	degenerative	14	2.47	FS	Mixed	Inflammatory bowel disease
6	degenerative	13	2.23	FS	Cocker spaniel	MVD
7	degenerative	13	2.27	FS	Mixed	MVD
8	degenerative	14	2.34	MC	Mixed	Hemangiosarcoma

MC, male castrated; FS, female spayed; MVD, degenerative mitral valve disease

α-Smooth Muscle Actin and CD-31

As reported previously, interstitial cells from normal canine mitral valves were negative for α-smooth muscle actin (except for a thin layer of subendothelial smooth muscle cells), whereas interstitial cells from myxomatous valves showed intense α-smooth muscle actin staining that was particularly focused in the *lamina atrialis* layer (Fig. 5.1). Immunohistochemistry staining for the endothelial cell marker, CD-31, confirmed presence of intact endothelial layers on the atrial and ventricular surfaces of normal mitral valves. CD-31 staining of myxomatous valves demonstrated patchy areas of endothelial denudation on both valve surfaces (Fig. 5.2).

Serotonin Signaling

Immunohistochemistry revealed positive staining for the serotonin 2B receptor ($5HT_{2B}R$) in both valve endothelial and interstitial cells of normal and myxomatous canine mitral valves (Fig. 5.3). However, Western blot analysis demonstrated that $5HT_{2B}R$ expression was increased in myxomatous mitral valves compared to normal mitral valves (Fig. 5.4). Immunohistochemistry revealed strong positive staining for the serotonin transmembrane transporter (SERT) in both endothelial and interstitial cells of normal mitral valves. SERT immunohistochemistry staining was markedly diminished in myxomatous interstitial cells, but was maintained in endothelial cells from myxomatous mitral valves (Fig. 5.5). Western blot analysis confirmed that SERT expression was decreased in myxomatous compared to normal mitral valves suggesting a decreased capacity for myxomatous interstitial cells to internalize and metabolize serotonin (Fig. 5.4).

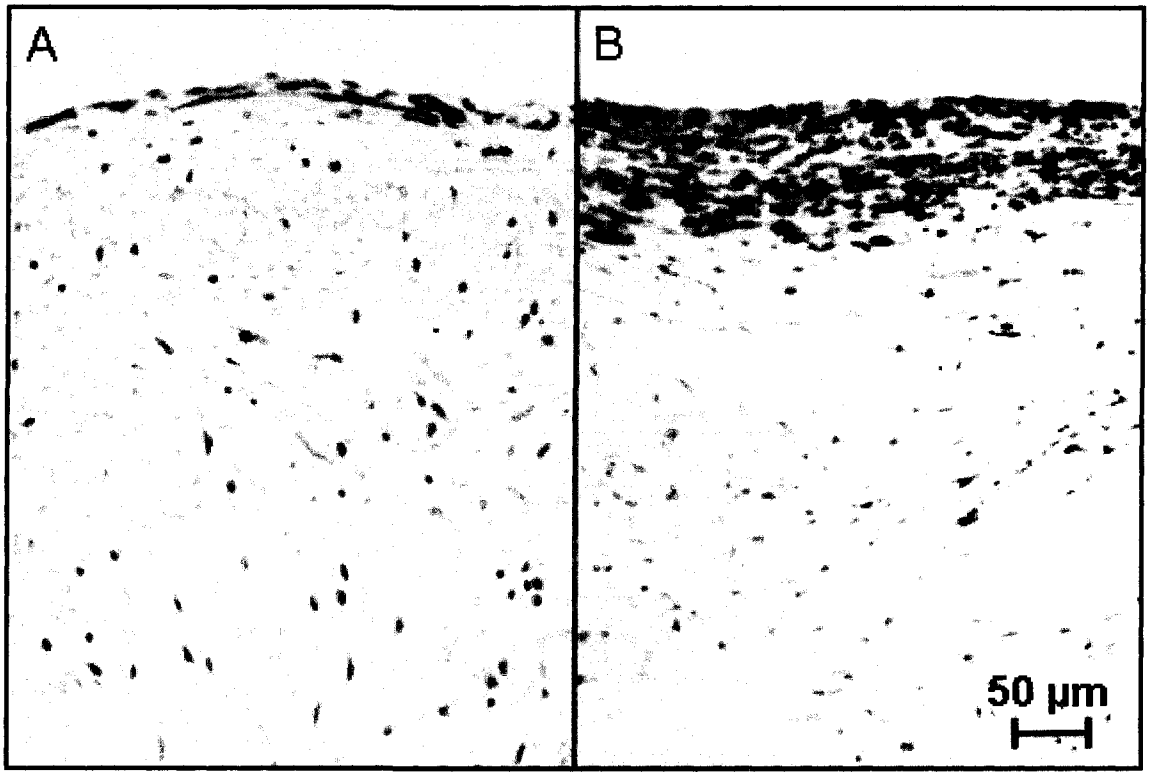

Figure 5.1: Immunohistochemistry of canine normal (A) and myxomatous mitral valves (B) to α-smooth muscle actin (α-actin). Original magnification x100. α-actin positive cells increased and accumulated as clusters within the *lamina atrialis* of myxomatous mitral valve leaflets.

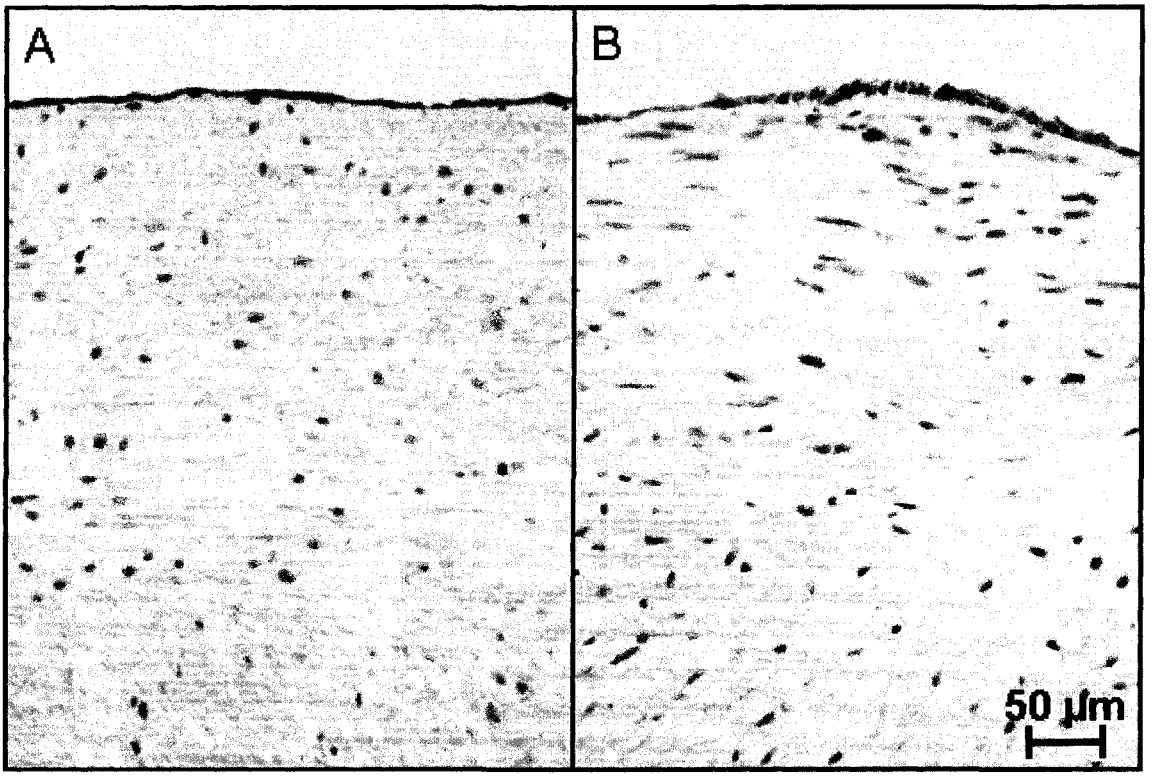

Figure 5.2: Immunohistochemistry of canine normal (A) and myxomatous mitral valves (B) to CD-31. Original magnification x100. Illustration demonstrates valve endothelial cell linings on normal and myxomatous mitral valves.

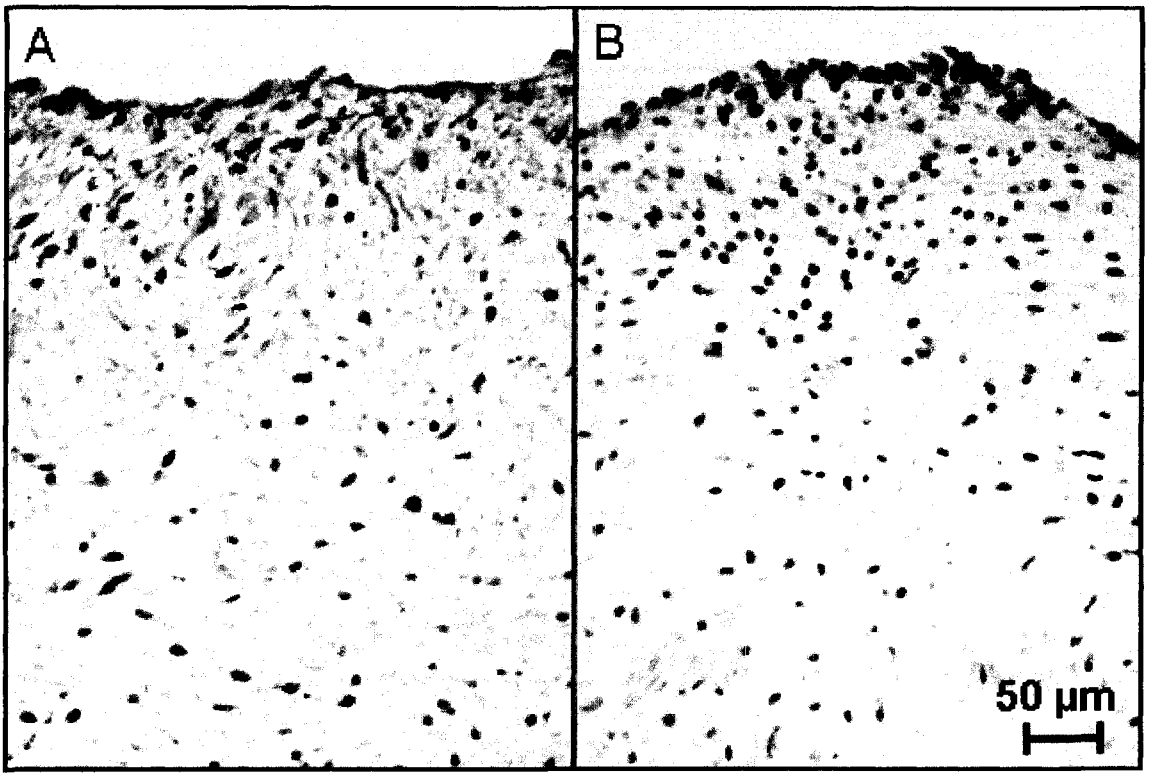

Figure 5.3: Immunohistochemistry of canine normal (A) and myxomatous mitral valves (B) to serotonin 2B receptor ($5HT_{2B}R$). Original magnification x100. Both valve endothelial and interstitial cells were expressed $5HT_{2B}R$ in canine normal and myxomatous mitral valves.

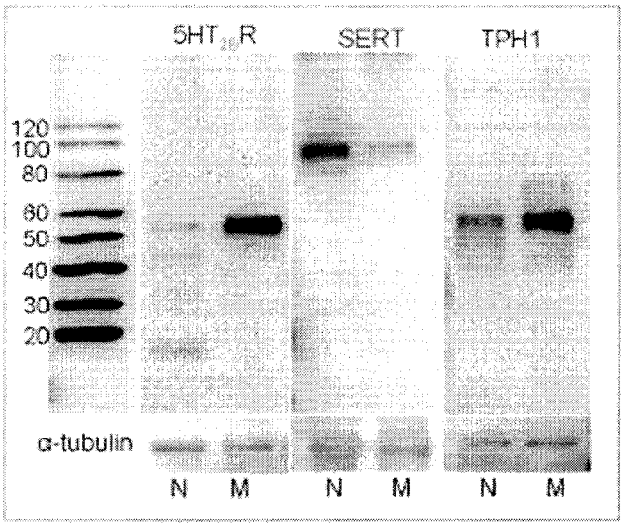

Figure 5.4: Western blot analysis of normal (lane N) and myxomatous (lane M) canine mitral valves for serotonin 2B receptor ($5HT_{2B}R$), serotonin transporter (SERT), and tryptophan hydroxylase 1 (TPH1). Loading control analysis of α-tubulin shown for each protein. $5HT_{2B}R$ and TPH1 expressions were up-regulated, but SERT expression was down-regulated in canine myxomatous mitral valves compared to normal mitral valves.

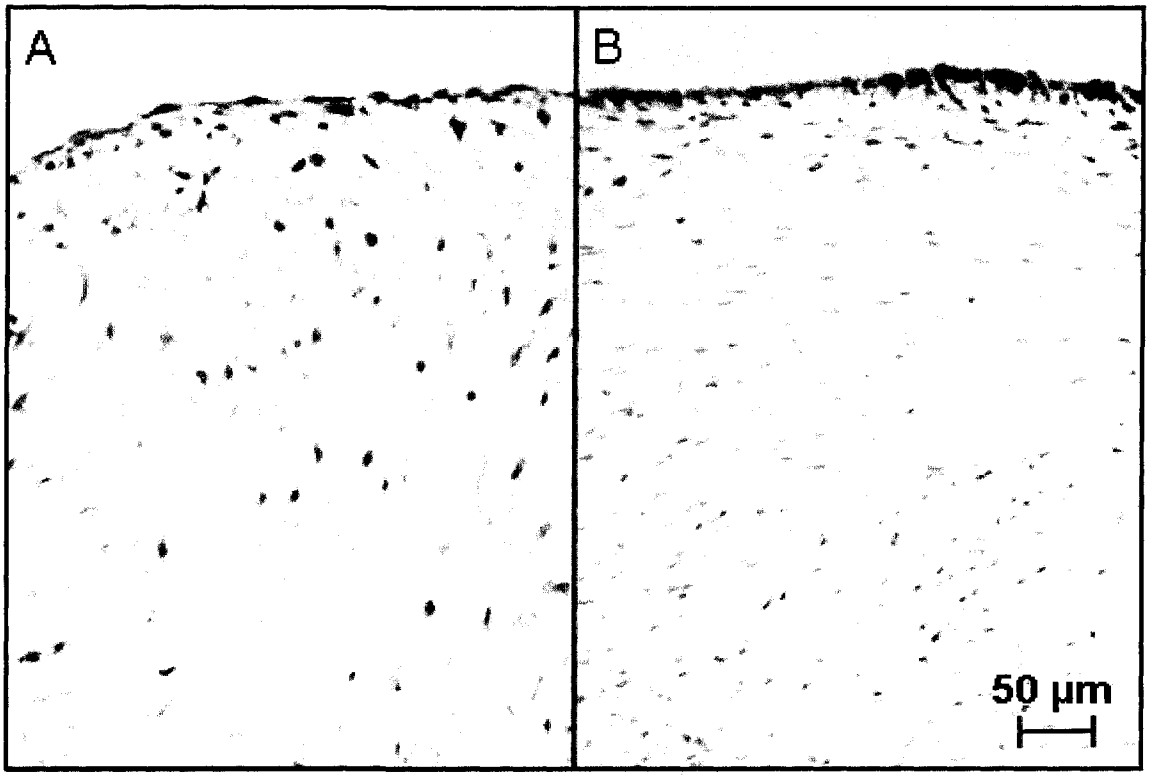

Figure 5.5: Immunohistochemistry of canine normal (A) and myxomatous mitral valves (B) to serotonin transmembrane transporter (SERT). Original magnification x100. SERT expression decreased in canine myxomatous mitral valves.

Immunohistochemical staining for tryptophan hydroxylase 1 (TPH1) appeared increased in both endothelial and interstitial cells of myxomatous valves compared to the same cells of normal valves (Fig. 5.6). Western blot analysis confirmed increased expression of TPH1 in myxomatous compared to normal valves suggesting an increased capacity for local tissue serotonin synthesis in canine myxomatous mitral valves (Fig. 5.4).

Total and Phosphorylated ERK 1/2

Extracellular signal regulated kinases 1 and 2 (ERK 1/2) are in the family of MAP kinases and have been shown to be phosphorylated in cultured aortic valve interstitial cells in response to serotonin. Total ERK 1/2 were not apparently different between normal and myxomatous mitral valves, whereas phosphorylated ERK 1/2 (pp ERK 1/2) were increased in myxomatous mitral valve on both immunohistochemistry and Western blot analysis (Fig 5.7, 5.8, and 5.9). This finding is consistent with enhanced serotonin activation of cells from myxomatous valves.

Transforming Growth Factor β1 Signaling

Transforming growth factor β1 (TGFβ1) is released as an inactive complex known as latent TGFβ1 and is comprised of active TGFβ1 and latency associated peptide (LAP). Thus, analysis with monoclonal antibody against LAP reflects expression of latent TGFβ1. (Tsang et al, 1995). Immunohistochemistry staining for latent TGFβ1 as well as TGFβ1 receptors I (TGFβ1 RI) and II (TGFβ1 RII) was increased in myxomatous compared to normal mitral valves (Fig. 5.10, 5.11, and 5.12). Increased straining for these peptides appeared in the *lamina atrialis* layer similar to increased α-actin staining; however, positive staining to these peptides also dispersed throughout the *lamina spongiosa* and *lamina fibrosa*

in myxomatous valves (Fig 5.1). Increased expression of α-actin, latent TGFβ1, TGFβ1 RI, and TGFβ1 RII in myxomatous valves was confirmed on Western blot analysis (Fig 5.13)

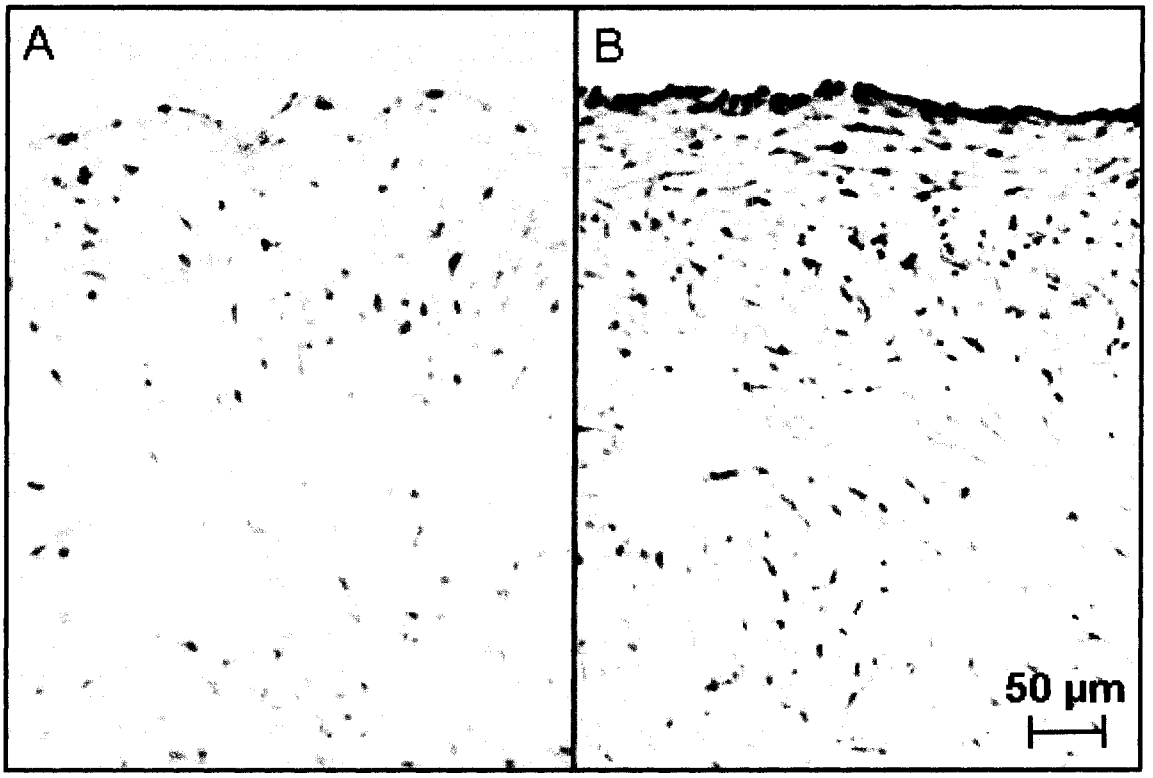

Figure 5.6: Immunohistochemistry of canine normal (A) and myxomatous mitral valves (B) to tryptophan hydroxylase 1 (TPH1). Original magnification x100. TPH1 expression increased in canine myxomatous mitral valves.

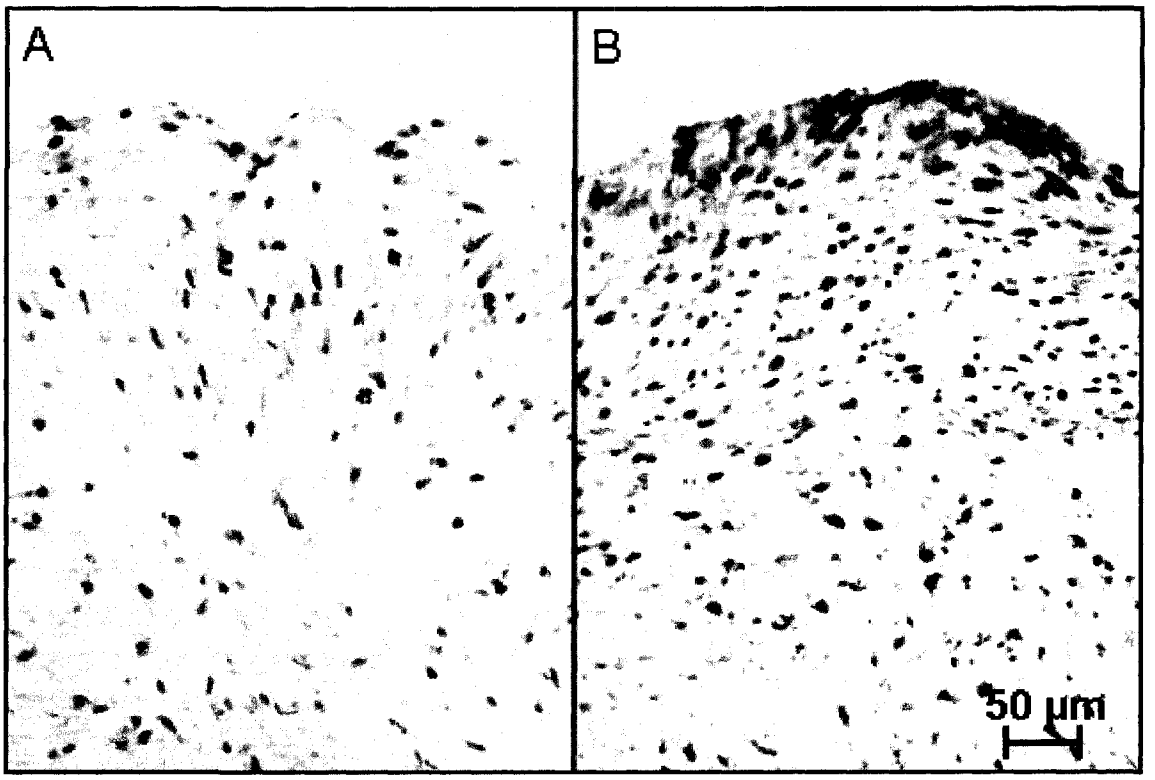

Figure 5.7: Immunohistochemistry of canine normal (A) and myxomatous mitral valves (B) to total extracellular signaling regulated kinases 1 and 2 (total ERK1/2). Original magnification x100. Non-phosphorylated and phosphorylated ERK1/2 (total ERK1/2) were present in both normal and myxomatous mitral valves.

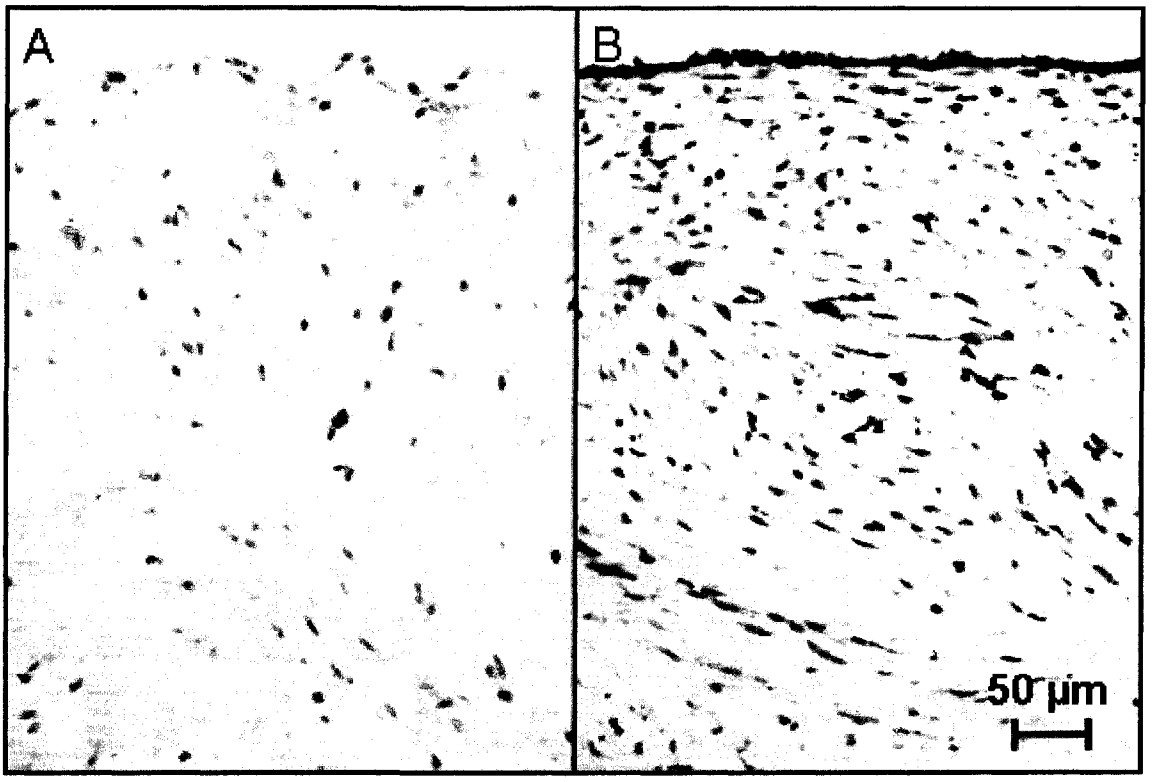

Figure 5.8: Immunohistochemistry of canine normal (A) and myxomatous mitral valves (B) to phosphorylated extracellular signaling regulated kinases 1 and 2 (PP ERK1/2). Original magnification x100. The phosphorylation of ERK1/2 increased in canine myxomatous mitral valves.

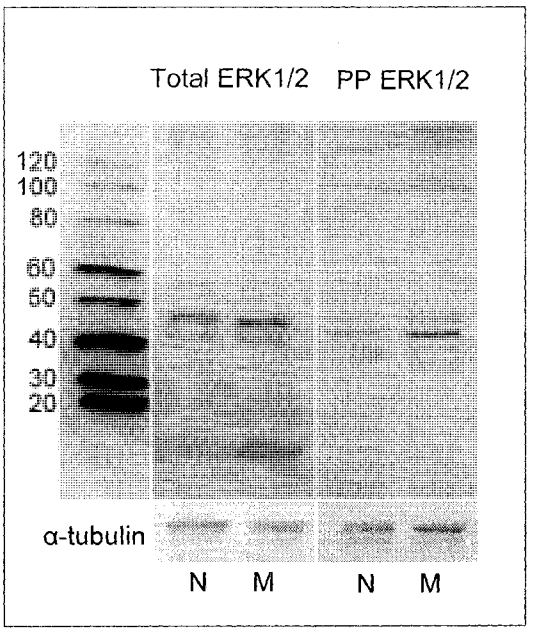

Figure 5.9: Western blot analysis of normal (lane N) and myxomatous (lane M) canine mitral valves for 42 and 44 kDa total extracellular signaling-regulated kinases 1 and 2 (total ERK1/2) and phosphorylated ERK1/2 (PP ERK1/2). Loading control analysis of α-tubulin shown for each protein. Total ERK1/2 were not apparently different between normal and myxomatous mitral valves, whereas ppERK1/2 increased in myxomatous mitral valves.

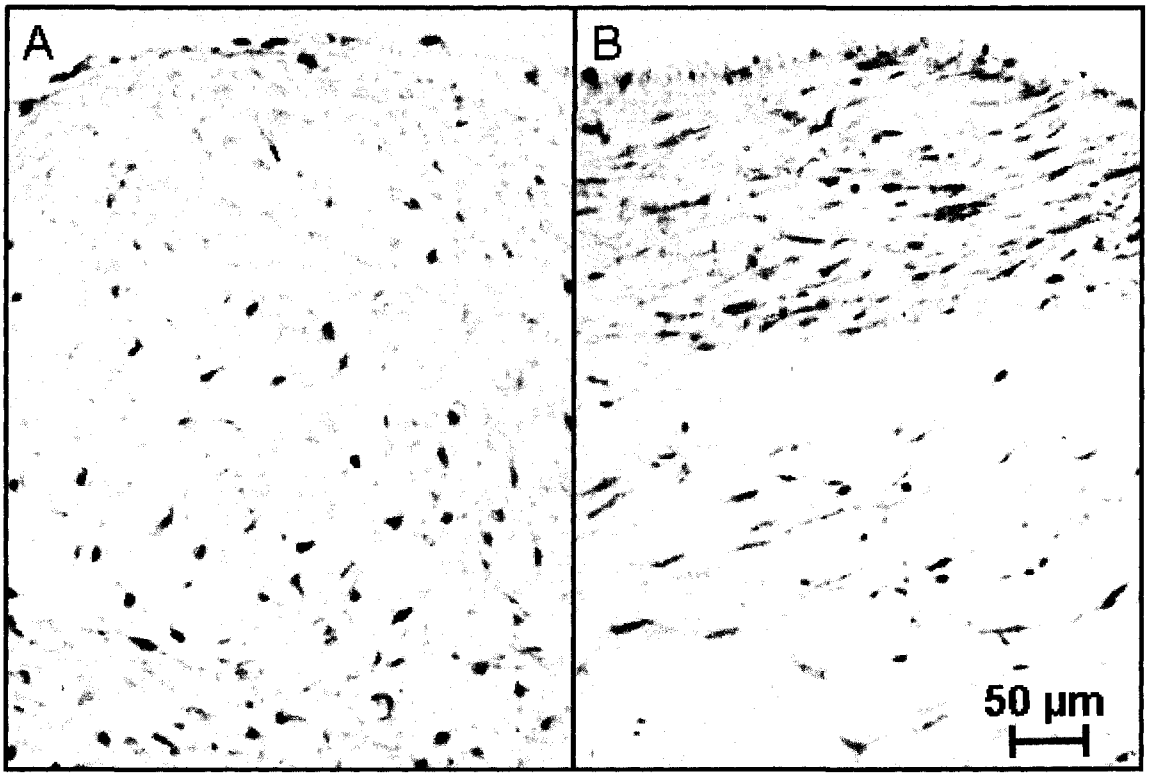

Figure 5.10: Immunohistochemistry of canine normal (A) and myxomatous mitral valves (B) to latent transforming growth factor β1 (latent TGFβ1). Original magnification x100. Latent TGFβ1 expression increased in myxomatous mitral valves.

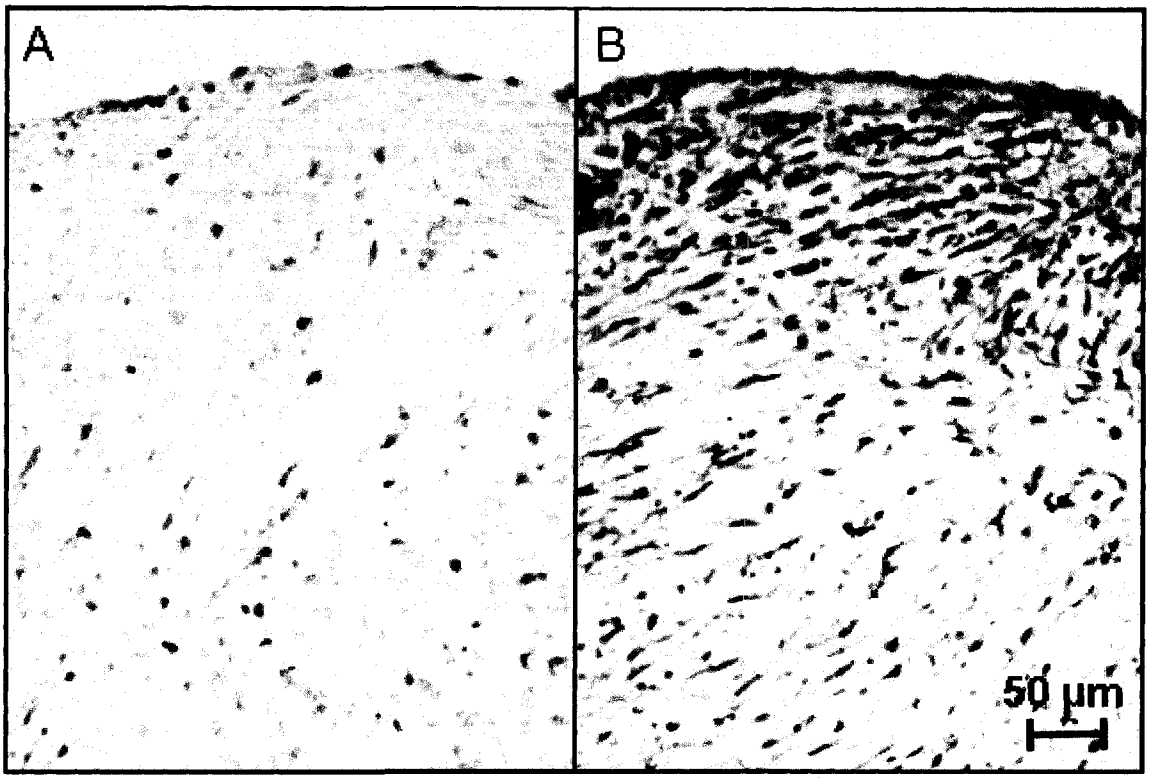

Figure 5.11: Immunohistochemistry of canine normal (A) and myxomatous mitral valves (B) to TGF β1 receptor I (TGFβ1 RI). Original magnification x100. TGF β1 RI expression increased in canine myxomatous mitral valves.

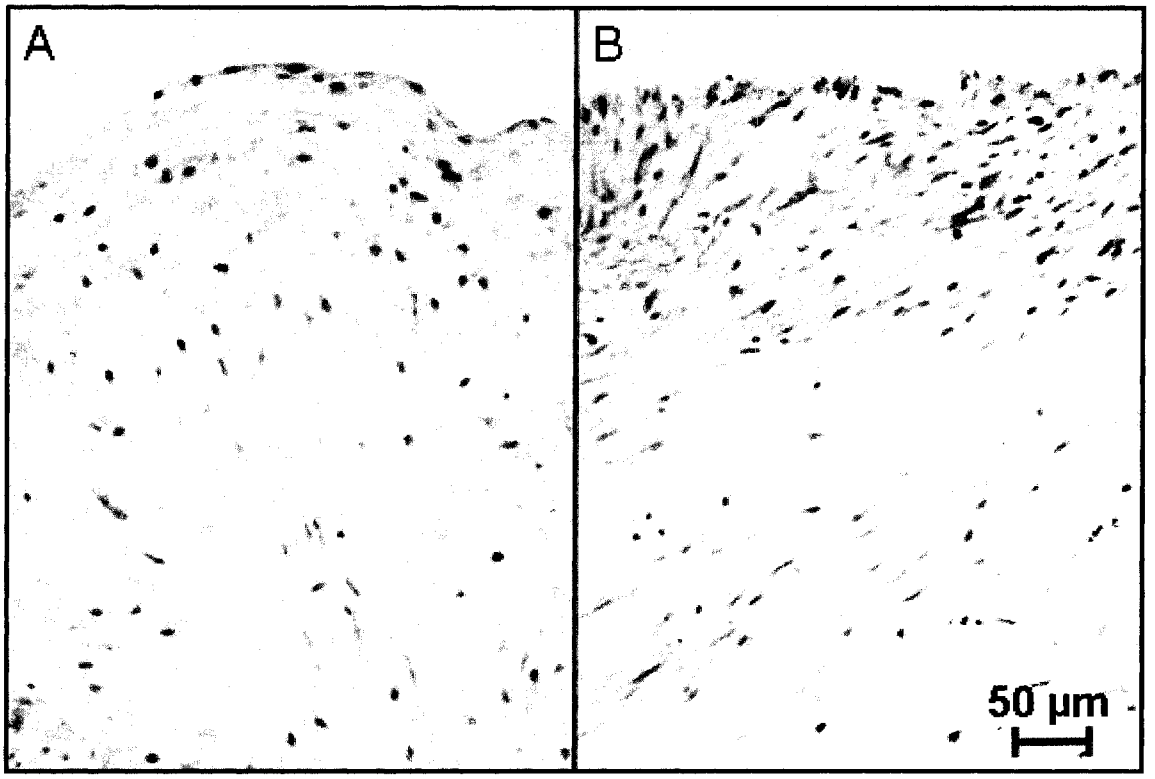

Figure 5.12: Immunohistochemistry of canine normal (A) and myxomatous mitral valves (B) to TGF β1 receptor II (TGFβ1 RII). Original magnification x100. TGF β1 RII expression increased in canine myxomatous mitral valves.

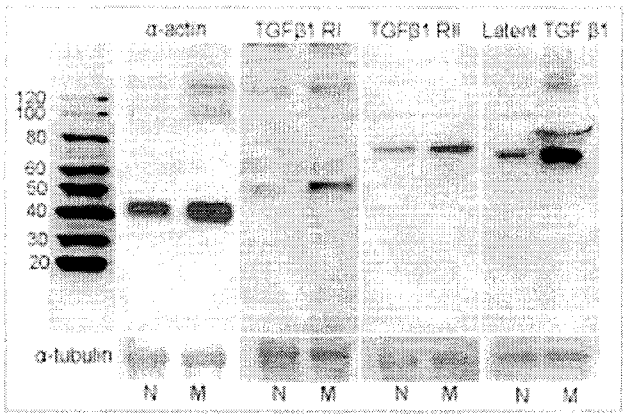

Figure 5.13: Western blot analysis of normal (lane N) and myxomatous (lane M) canine mitral valves for α-smooth muscle actin (α-actin), latent transforming growth factor β1 (latent TGFβ1), TGFβ1 receptors I (TGFβ1 RI) and II (TGFβ1 RII). Loading control analysis of α-tubulin shown for each protein. The expression of α-actin, latent TGFβ1, TGFβ1 RI and TGFβ1 RII increased in canine myxomatous mitral valves.

DISCUSSION

A role of serotonin in mediating heart valve diseases has been reported in humans with carcinoid tumors (Rajamannan et al, 2001) and those receiving serotonergic drugs (Rothman et al, 2000) as well as in rats supplemented with serotonin (Gustafsson et al, 2005). Serotonin 2B receptor ($5HT_{2B}R$) has been reported to be involved with the development of carcinoid and serotonergic induced heart valve diseases in humans (Rothman et al, 2000; Fitzgerald et al, 2000) and spontaneous myxomatous valve disease in rats (Elongbam et al, 2006). Because lesions of canine myxomatous mitral valve disease are similar to those described in serotonin induced heart valve diseases in humans, we speculated that $5HT_{2B}R$ and serotonin signaling transduction may be involved with pathogenesis of canine myxomatous mitral valve disease. In present study, we demonstrated that valve endothelial cells and valve interstitial cells expressed $5HT_{2B}R$ suggesting that both cell types have potential to respond to serotonin signaling. Western blot analysis showed up-regulation of $5HT_{2B}R$ protein in myxomatous valves compared to normal valves implying an alteration of serotonin signaling in diseased valves and suggesting a crucial role of $5HT_{2B}R$ in the development of canine myxomatous mitral valve disease. The different distribution pattern of valve interstitial cells expressed for $5HT_{2B}R$ and α-actin suggests that α-actin or myofibroblast interstitial cells are not the only phenotype that reflects the $5HT_{2B}R$ expression in dogs affected with myxomatous mitral valve disease. In other words, both fibroblast and myofibroblast phenotypes have a capability to respond to serotonin signaling and may take part in pathogenesis of canine myxomatous mitral valve disease.

Mitogen activated protein kinases (MAPK) represent a family of serine-threonine kinases which can be activated by several factors and be involved in the cell proliferation and

differentiation (Cobb, 1999). There are 3 major subfamilies of (MAPK) including extracellular signal regulated kinases (ERK), c-Jun N-terminal protein kinase (JNK) and p38 MAPK (p38). ERK are the most commonly activated kinases in signal transduction pathways of the mammalian cells. ERK1/2 are effector proteins in ERK signaling pathway that have function in transduction signal from the cell surface to the nucleus. To activate this signaling pathway, ERK1/2 generally need to be phosphorylated by their upstream activators. By immunohistochemistry and Western blotting, we showed an up-regulation of the phosphorylated ERK1/2 protein in myxomatous mitral valves compared to normal valves suggesting the association of MAPK/ERK signaling and the degenerative process. A previous study in cultured sheep aortic interstitial cells demonstrated that ERK1/2 are downstream signaling molecules from the serotonin receptor (Xu et al, 2002). The up regulation of both $5HT_{2B}R$ and phosphorylated ERK1/2 in diseased mitral valves implies an association of serotonin signaling and ERK1/2 phosphorylation. Signal pathways from serotonin receptors to ERK1/2 have not been fully elucidated yet. It has been speculated that these pathways may vary among cell types and species (Crow et al, 2001). Several components have been implicated in the pathway from serotonin receptors to ERK1/2 including src (Nebigil et al, 2000) superoxide anions and protein kinase C (PKC) (Grewel et al, 1999). Both src and PKC have been shown to be involved in serotonin induced ERK1/2 activation in cultured sheep aortic valve interstitial cells (Xu et al, 2002). Further investigations are required to elucidate whether src and/or PKC are involved in ERK1/2 stimulation *in vivo*. ERK signaling has been reported for involvement in cell proliferation (Lee et al, 2001). Our previous study (Disatian et al, 2008) showed that myxomatous valves contained higher cell density than normal valves. We suspected that an increase in number of

interstitial cells within diseased valves may occur secondary to an activation of serotonin-ERK signaling pathways.

Serotonin synthesis is controlled by tryptophan hydroxylase (TPH). Two isoforms of TPH have been classified including TPH1, an isoform mostly expressed in periphery tissues and TPH2, an isoform executively expressed in central nervous system. The expression of TPH1 was found in canine mitral valves indicating that interstitial cells themselves are capable of producing serotonin in a paracrine/autocrine fashion. An increase TPH1 in interstitial cells and valve endothelial lining myxomatous leaflets suggests a role of these cells as a source of serotonin during the diseased process. Because the distribution pattern of TPH1 was not restricted to cells expressing α-actin, both fibroblast and myofibroblast interstitial cells are the source of serotonin within canine heart valves.

Normally, serotonin is largely produced from enterochromaffin cells in the gut and stored in platelets for release. The relationship between high levels of serotonin in circulation and development of heart valve diseases has been reported in patients affected with carcinoid tumors suggesting an endocrine effect of serotonin on pathogenesis (Kema et al, 1992). To date, evidence that circulating serotonin concentrations mediated with myxomatous mitral valve disease in dogs has not been demonstrated. Thus, the endocrine serotonin mechanism in canine myxomatous mitral valve disease is currently unclear. As mentioned previously, platelets are the major storage of serotonin in circulation which may act as a carrier to transport the serotonin into the diseased valve. Platelets may be attracted to damaged valve surfaces or an area of valve endothelial cell denudation as at a wound site. Serotonin released from these platelets may activate serotonin signaling transduction by interacting with its receptor within the valve leaflet ultimately leading to myxomatous mitral valve disease. The

possible role of platelets as a transporter of serotonin in diseased mitral valve is unknown and requires additional studies.

Serotonin transmembrane transporter (SERT) is a monoamine transporter protein that transports serotonin from the extracellular fluid into cells using a sodium/chloride dependent co-transport process. After uptake into the cell, internalized serotonin is either degraded by enzymes such as monoamine oxidases or accumulated in vesicles. In neuronal system, SERT has a major function of reducing the serotonin concentration in the synaptic area by facilitating intracellular processing of serotonin after receptor interactions (Bohm et al, 1997). We demonstrated that SERT was expressed by both valve endothelial cells and interstitial cells. Immunohistochemistry and Western blot analysis review an apparent decrease in SERT expression within myxomatous valves compared to normal valves. That decrease in SERT expression may enhance the effect of serotonin signaling by decreasing serotonin processing into cells contributing to persistent interactions between serotonin and its receptor. This suggestion is supported by a previous study demonstrating that SERT deficient mice develop cardiac fibrosis and valvulopathy (Mejontso-Dessap et al, 2006). A function for SERT as a protector against the deleterious effect of serotonin has also been proposed in kidney (Pizzinat et al, 1999) and liver (Ruddell et al, 2006). In contrast to valve interstitial cells, the expression of SERT in valve endothelial cells of myxomatous valves was not apparently decreased suggesting SERT on valve endothelial cells may have another function in diseased mitral valves. Further studies are required to determine the exact role of SERT in canine valve endothelial and interstitial cells.

TGFβ1 is normally released as an inactive or latent form which is comprised of the mature TGFβ1 and latency associated peptide (LAP). Valve interstitial cells in both normal

and myxomatous valves expressed latent TGFβ1 suggesting a role for TGFβ1 synthesis in normal valve maintenance. The up-regulation of latent TGFβ1 in myxomatous valves suggests that increased TGFβ1 production may play a role in the degenerative disease process. Both TGFβ1 RI and RII were expressed in canine mitral valves indicating a potential for response of canine valve interstitial cells to TGFβ1 signaling. Enhanced expression of TGFβ1 receptors was found in myxomatous valves compared to normal controls suggesting a role for TGFβ1 signaling in canine myxomatous mitral valve disease. Previous studies in cultured valve interstitial cells demonstrated that TGFβ1 can mediate valve interstitial cells transformation from fibroblast phenotype into myofibroblast phenotype (Walker et al, 2004). Interestingly, expression of TGFβ1 receptors, latent TGFβ1 and α-actin were increased in the *lamina atrialis* of myxomatous valves. This concomitant expression suggests a role of TGFβ1 signaling in valve interstitial cell transformation to myofibroblast phenotype. It has also been reported previously that TGFβ1 signaling is involved in extracellular matrix (ECM) production. An effect of TGFβ1 in stimulating ECM production has been shown in cultured sheep aortic valve interstitial cells (Xu et al, 2002). A possible for TGFβ1 in altered ECM production in canine myxomatous valves has not yet been previously demonstrated. An association between serotonin signaling and TGFβ1 production has been reported in cultured sheep aortic valve interstitial cells (Xu et al, 2002). The up-regulation of serotonin and TGFβ1 receptors as well as latent TGFβ1 in canine degenerative mitral valves implies the association and cooperative roles of these two signaling pathways in canine myxomatous mitral valve disease.

In conclusion, up-regulation of $5HT_{2B}$ and TGFβ1 receptors as well as an apparent increase in serotonin and TGFβ1 local synthesis suggests a role for these mediators in the

pathogenesis of canine myxomatous degenerative mitral valve disease. Down-regulation of SERT may augment serotonin signaling and further contribute to development of myxomatous mitral valve disease in dogs. Up-regulation of phosphorylated ERK1/2 indicates an involvement of ERK signaling pathway in the degenerative process. This study provides evidence for autocrine/paracrine signaling pathways in pathogenesis of canine myxomatous degenerative mitral valve disease. Further studies focusing on specific triggering mechanisms for increased serotonin and TGFβ1 signaling may provide further insight into pathogenesis of canine myxomatous mitral valve disease.

REFERENCES

1. Bohm S, Grady E, Bunnett N. Regulatory mechanisms that modulate signaling by G-protein-coupled receptors. Biochem J 1997;322:1-18
2. Bonaventure P, Nepomuceno D, Miller K, et al. Molecular and pharmacological characterization of serotonin 5-HT_{2A} and 5-HT_{2B} receptor subtypes in dog. Eur J Pharmacol 2005;513(3):181-192
3. Cobb MH. MAP kinase pathways. Prog Biophys Mol Biol 1999;71:479-500
4. Crow T, Xue-Bian JJ, Siddiqi V, Neary JT. Serotonin activation of the ERK pathway in Hermissenda: contribution of calcium-dependent protein kinase C. J neutochem 2001;78:358-364
5. Detweiler D, Patterson D. The prevalence and types of cardiovascular disease in dogs. Ann NY Acad Sci 1965;127:481-516
6. Disatian S, Zimmerman S, Orton CE. Interstitial cells from dogs with naturally-occurring myxomatous mitral valve disease undergo phenotype transformation. J Heart Valve Disease. 2008 "in press"
7. Elongbam CS, Wehe JG, Barton JC, et al. Evaluation of glycosaminoglycans content and 5-hydroxytryptamine 2B receptor in the heart valves of Sprague-Dawley rats with spontaneous mitral valvulopathy: a possible exacerbation by dl-amphetamine sulfate in Fischer 344 rats. Exp Toxicol Pathol 2006; 58(2-3):89- 99
8. Ferrans VJ, Roberts WC. The carcinoid endocardial plaque: an ultrastructural study. Hum Pathol 1976;7-387-409

9. Fitzgerald LW, Burn TC, Brown BS, et al. Possible role of valvular serotonin 5-HT_{2B} receptors in the cardiopathy associated with fenfluramine. Mol Pharmacol 2000;57(1):75-81

10. Grewel JS, Muhkin YV, Garnovskaya MN, et al. Serotonin 5-HT2A receptor induces TGF-β1 expression in mesangial cells via ERK: proliferation and fibrotic signals. Am J Physiol 1999;276:F922-F930

11. Gustafsson BI, Tommeras K, Nordrum I, et al. Long-term serotonin administration induces heart valve disease in rats. Circulation 2005;111:1517-1522

12. Hoyer D, Fozard JR, Saxena PR, et al. International union of pharmacology classification of receptors for 5-hydroxytryptamine (serotonin). Pharmacol Rev 1994;46:157-203

13. Jian B, Xu J, Savani R, et al. Serotonin mechanisms in heart valve disease I: Serotonin induced upregulation of TGF-β1 via G-protein signal transduction in aortic valve interstitial cells. Am J Pathol 2002;161:2207-2216

14. Kema IP, Meijer WG, Meiborg G, Ooms B, Willemse PH, de Vries EG. Improved diagnosis of carcinoid tumors by measurement of platelet serotonin. Clin Chem. 1992;38:534-540

15. Lee SL, Simon AR, Wang WW, Fanburg BL. H202 signals 5-HT induced ERK MAP kinase activation and mitogenesis of smooth muscle cells. Am J Physiol 2001;281:L646-L652

16. McDonald PC, Wilson JE, Gao M et al. Quantitative analysis of human heart valves-does anorexigen exposure procedure a distinctive morphological lesion? Cardiovasc Pathol 2002;11:251-62

17. Mekontso-Dessap A, Brouri F, Pascal O, et al. Deficiency of the 5-hydroxytryptamine transporter gene leads to cardiac fibrosis and valvulopathy in mice. Circulation 2006;113:81-89

18. Nebigil CG, Launay JM, Hickel P, Tournois C, Maroteaux L. 5-hydroxytryptamine 2B receptor regulates cell-cycle progression: cross talk with tyrosine kinase pathways. Proc Natl Acad Sci USA 2000;97:2591-2596

19. Nebigil CG, Hickel P, Messaddeq N, et al. Ablation of serotonin 5-HT_{2B} receptors in mice leads to abnormal cardiac structure and function. Circulation 2001;103:2973-2979

20. Nemecek MM, Coughlin SR, Handley DA, Moskowitz MA. Stimulation of aortic smooth muscle cell mitogenesis by serotonin. Proc Natl Acad Sci USA. 1986;83:674-678

21. Pakula R, Willerson JT, Benedict CR. Mitogenic effect of serotonin on vascular endothelial cells. Circulation 1994;90:1919-1926

22. Pizzinat N, Girolami JP, Parini A, Pecher C, Ordener C. Serotonin metabolism in rat mesangial cells: involvement of serotonin transporter and mono amine oxidase A. Kidney Int 1999:56:1391-1399

23. Rajamannan NM, Caplice N, Anthikad F, et al. Cell proliferation in carcinoid valve disease: a mechanism for serotonin effects. J Heart Valve Dis 2001;10:827-831

24. Robiolio PA, Rigolin VH, Wilson JS, et al. Carcinoid heart disease: correlation of high serotonin levels with valvular abnormalities detected by cardiac catheterization and echocardiography. Circulation 1995; 92:790-795

25. Rothman RB, Baumann MH, Savage JE, et al. Evidence fro possible involvement of 5-HT2B receptors in the cardiac valvulopathy associated with fenfluramine and other serotonergic medications. Circulation 2000;102:2836-2841

26. Ruddell RG, Oakley F, Hussain Z, et al. A role for serotonin (5-HT) in hepatic stellate cell function and liver fibrosis. Am J Pathol 2006:169(3):861-876

27. Seuwen K, Magnaldo I pouyssegur J. Serotonin stimulates DNA synthesis in fibroblasts acting through 5-HT1B receptors coupled to a Gi-protein. Nature 1988;335:254-256

28. Takuwa N, Ganz M, Takkuwa Y, Sterzel RB, Rasmussen H. Studies of the mitogenic effect of serotonin in rat renal mesangial cells. Am J Physiol 1989;257:F431-F439

29. Tsang ML, Zhou L, Zheng BL, et al. Characterization of recombinant soluble human transforming growth factor-beta receptor type II (rhTGF-beta sRII). Cytokine 1995;7(5):389-397

30. Walker GA, Masters KS, Shah DN, Anseth KS, Leinwand LA. Valvular myofibroblast activation by transforming growth factor β: Implications for pathological extracellular matrix remodeling in heart valve disease. Circ Res 2004;95:253-260

31. Xu J, Jian B, Chu R, et al. Serotonin mechanisms in heart valve disease II: The 5-HT_2 receptors and its signaling pathway in aortic valve interstitial cells. Am J Pathol 2002;161:2209-2218

CHAPTER 6

CONCLUSIONS AND FUTURE DIRECTIONS

The present study demonstrated that in canine myxomatous degenerative mitral valves, valve interstitial cells transform into at least into 2 phenotypes including: 1) *myofibroblast phenotype* (desmin and α-actin positive) and 2) *activated mesenchymal phenotype* (non-muscle myosin positive). The transformation of valve interstitial cells into these two phenotypes correlated with disease progression. These two phenotypes had different patterns of distribution. *Myofibroblast phenotype* accumulated mainly in clusters in the atrialis layer of the leaflet; whereas, *activated mesenchymal phenotype* was dispersed throughout the valve stroma in a more random fashion. Expression of collagenases (MMP-1 and MMP-13) was increased in, but not restricted to the myofibroblast phenotype. The distribution pattern of the *activated mesenchymal phenotype* more closely matched the pattern of valve interstitial cell expression of collagenases (MMP-1 and MMP-13). However, collagenase expression was also not restricted to the activated mesenchymal phenotype. For this reason, we suspect that both the non-transformed phenotype and the transformed phenotype have a role in ECM remodeling during the disease process. The exact role of the *quiescent phenotype, myofibroblast phenotype,* and *activated mesenchymal phenotype* remains unclear. Further studies using laser microdissection technique with functional genomic and/or proteomic downstream analysis might provide further understanding in gene and/or protein expression profiles of each valve interstitial cell phenotype. The information

derived from functional genomic and proteomic analysis might provide insights into the actual molecular circumstance within each valve interstitial cell phenotype contributing to a better understanding in pathogenesis of canine myxomatous mitral valve disease.

Mechanisms and factors responsible for valve interstitial cell transformation remain still uncertain. The present study demonstrated a possible association between TGFβ1 receptors and α-actin expressions suggesting the relationship between TGFβ1 signaling and valve interstitial cell transformation into myofibroblast phenotype. Further studies using canine mitral valve organ cultures or animal models supplemented with TGFβ1 will help to elucidate the potential role of TGFβ1 signaling in mediating valve interstitial cell transformation. Effects of other factors such as mechanical stretch on valve interstitial cell transformation should also be investigated. A study using mitral valve organ tissue cultures incubated in a device with different levels of stretch may provide better understanding of the influences of mechanical stretch on transformation of valve interstitial cell.

The present study demonstrated that cell density within canine myxomatous mitral valves increases with disease progression. However, the proliferative rate is only mildly increased in all stages of myxomatous degeneration. It is possible that cell proliferation may gradually occur over a long period of time during the disease process. Further cells may live longer secondary to a decreased apoptosis rate. Additional experiments investigating apoptosis of valve interstitial cell within canine myxomatous mitral valves might confirm this suggestion.

The involvement of serotonin, MAPK/ERK, and TGFβ1 signaling pathways in canine myxomatous mitral valve disease was demonstrated by an increased expression of $5HT_{2B}$ receptor, phosphorylated ERK1/2 and TGFβ1 receptors within degenerative valves.

Investigations should be done to elucidate the specific roles of these signaling pathways in the development of myxomatous degenerative disease in dogs might provide further insight into the pathogenesis of this disease.

This study demonstrated an increased potential for autocrine/paracrine serotonin synthesis in canine myxomatous degenerative disease valves. Effects of the endogenous serotonin on pathogenesis might be confirmed by experiments with TPH1 gene disruption.

An augmented latent TGFβ1 expression implies an increase of TGFβ1 synthesis in myxomatous valves. The latent form of TGFβ1 needs to be activated into the mature form before it is able to bind and has effects on its receptor. To date, mechanisms of TGFβ1 activation *in vivo* are unclear. Previous studies in several cell types have demonstrated that TGFβ1 is activated *in vitro* by MMP. A study investigating the association between MMP activity and the expression of mature form of TGFβ1 might provide a better standing about mechanisms of TGFβ1 activation *in vivo*.

Finally, a decrease expression of serotonin transporter (SERT) was found within diseased valves suggesting a role of decreased SERT in canine myxomatous degenerative disease. Experiments investigating the specific roles of SERT in canine valves both in normal and pathologic conditions should be undertaken. An *in vitro* study in VIC culture investigating SERT uptake of serotonin in cultured VIC as well as an expression and activity of degradation enzymes such as monoamine oxidase within VIC might provide to understanding more about a role of SERT on VIC in protecting heart valves from effect of serotonin signaling.

Data on valve interstitial cell phenotypes and signaling pathways involved in naturally-occurring canine myxomatous mitral valve disease presented in these studies will

be useful for future studies elucidating the pathogenesis of canine myxomatous mitral valve disease. Ultimately, the development the new therapeutic approaches for that disrupt the pathogenesis and progression of myxomatous mitral valve disease in dogs is the ultimate goal of these studies.

APPENDIX

PROTOCOLS

Tissue collection

Entire mitral valve complex (valve annulus, leaflets, chordae tendineae, and papillary muscles) with attached aortic valve were collected from septal (anterior) leaflet (Figure A1). Tissue samples were fixed with 10% formalin for 24 hours at room temperature and then mounted in paraffin and cut into 4 μm sections.

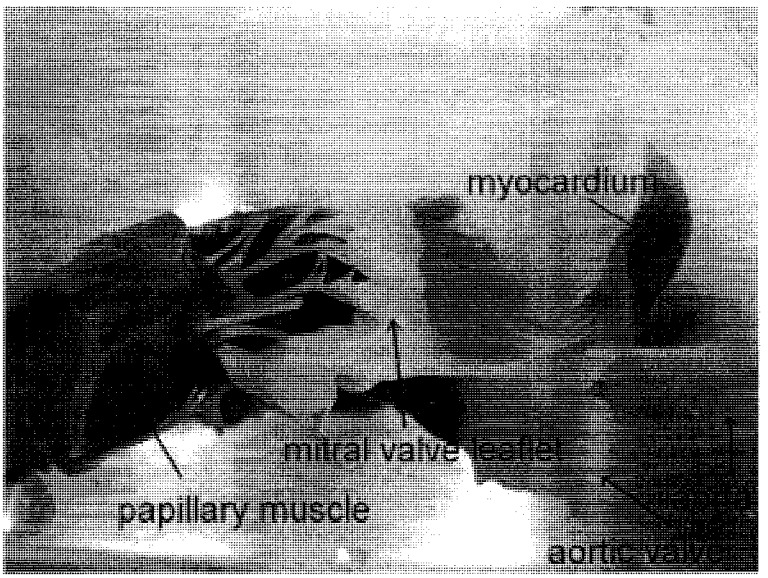

Figure A1: Entire mitral valve complex tissue samples.

Russell-Movat Pentachrome staining

Reagents and solutions

10% alcoholic hematoxylin

Universal iodine solution

5% sodium thiosulfate

1% alcian blue solution

1% gracial acetic acid

Alcoholic saffron solution

10% ferric chloride

2% ferric chloride

3% glacial acetic acid

Crocein scarlet acid

5% phosphotunstic acid

Verhoeff's elastic satin (prepare by mixing 20 ml of 10% alcoholic hematoxyllin, 20 ml of reagent alcohol, 20 ml of 10% ferric chloride and 20 ml of universal iodine solution)

Staining protocol

1. Deparafinize slides using xylene and hydrate through alcohols.
2. Rinse slides in deionized water.
3. Place slide in Verhoeff's Elastic Stain for 15 to 20 minutes.
4. Rinse slides in running tap water for 5 minutes, flowed by deionized water.
5. Differentiate sections in 2% ferric chloride until elastic fibers are sharply defined.
6. Rinse slides in deionized water and place in 5% sodium thiosulfate for 1 minute.
7. Rinse slides in running tap water for 5 minutes.

8. Place slides in 3% glacial acetic acid for 3 minutes.
9. Place slides directly in 1% alcian blue solution for 15 minutes or until mucins are blue.
10. Rinse slides in warm running tap water for 1 minute, then rinse in deionized water.
11. Place slides in crocein scarlet acid fuchsin for 2 minutes.
12. Rinse slides with deionized water 3 times 2 minutes each.
13. Dip slides 5 times in 1% glacial acetic acid.
14. Place slides in 2 changes of 5% phosphotunstic acid for 2 minutes each.
15. Dip slides 5 times in 1% gracial acetic acid.
16. Dehydrate slides in ethyl alcohol 3 times 2 minutes each.
17. Place slides in alcoholic saffron solution for 15 minutes.
18. Dehydrate slides in fresh absolute alcohol 3 times 2 minutes each.
19. Incubate slides in xylene 3 times 2 minutes each
20. Coverslip using toluene solution.

Result

Elastic fibers, nuclei: black

Collagen: yellow

Mucins: blue to green

Muscle: red

Fibrinoid: intense red

Immunohistochemical Assay

Reagents and Solutions

Tris buffered saline (TBS)

Working solution: Tris-base 10 mM, NaCl 150 mM, pH 7.6

To prepare 1000 ml 10x stock solution, dissolved Tris base 12.2 g and NaCl 87.75 g in 1000 ml deionized water. Adjust pH with concentrated HCl.

To prepare working solution, dilute 1 part of 10x stock solution in 9 part of deionized water.

Target retrieval solution (S1699, Dako)

Citrate buffer, pH6,10x concentrated

Immunohistochemical system

1. Dako EnVision™+ Horse radish peroxidase (HRP) System
2. Dako EnVision™ Doublestain System
3. Dako LSAB+ Alkaline phosphatase (AP) System

N-Universal negative control mouse reagent

Cocktail of mouse IgG_1, IgG_{2a}, IgG_{2b}, IgG_3, and IgM

Antibody diluent

Tris-HCl buffer containing stabilizing protein and 0.015 mol/L sodium azide

Mouse monoclonal antibodies

Antibody	Clone	Company	Concentration
smooth muscle α actin	1A4	Dako	1:25
Vimentin	3B4	Dako	1:200
Desmin	D33	Dako	1:50
Smooth muscle myosin heavy chain	SMM1	Dako	1:50
Non-muscle myosin heavy chain	3H2	Abcam	1:1000
MMP-1	IM35L	Calbiochem	2.5 µg/ml
MMP-13	IM44L	Calbiochem	5 µg/ml
macrophages	CD68	Dako	1:20
T-cell	CD45	Dako	1:10
Ki-67	MIB-1	Dako	1:100
CD31	PECAM-1	Dako	1:20

Immunohistochemistry protocol using EnVision+ HRP System

1. Paraffin embedded tissues are deparafinized, and rehydrated in descending grades of alcohol.
2. Sections are heated with antigen retrieval solution at 95°C for 20 minutes and leaved to cool down at room temperature for 20 minutes.
3. Slides are washed in deionized water for 3 minutes and TBS for 3 minutes.
4. Slides are loaded into the autostainer and stained automatically by using following protocol:

   - wash slides with 1xTBS twice 2 minutes each

- block endogenous peroxidase by 0.03% hydrogen peroxide containing sodium azide for 5 minutes

- wash slides with 1xTBS twice 2 minutes each

- incubate slides in primary antibody diluted with antibody diluent or negative control reagent for 30 minutes

- wash slides with 1xTBS twice 2 minutes each

- incubate slides in peroxidase labeled polymer conjugated to goat anti-mouse immunoglobulins in Tris-HCl buffer for 30 minutes

- wash slides with 1xTBS twice 2 minutes each

- incubate slides with 3,3'diaminobenzidine chromogen in pH 7.5 hydrogen peroxide solution for 5 minutes

- wash slides with deionized water for 2 minutes

- wash slides with TBS for 2 minutes

- counterstain slides with Mayer's hematoxylin for 6 minutes

- wash slides with TBS for 2 minutes

- wash slides with deionized water for 2 minutes

5. Slides are dehydrated with 70% alcohol, 100% alcohol and Hemo-de
6. Slides are mounted with and coverslipped with toluene solution, a nonaqueous permanent mounting media.

Immunohistochemical protocol using LSAB+ AP System

1. Paraffin embedded tissues are deparafinized, and rehydrated in descending grades of alcohol.
2. Sections are heated with antigen retrieval solution at 95°C for 20 minutes and leaved to cool down at room temperature for 20 minutes.
3. Slides are washed in deionized water for 3 minutes and TBS for 3 minutes.
4. Slides are loaded into the autostainer and stained automatically by using following protocol:

- wash slides with 1xTBS twice 2 minutes each

- block endogenous peroxidase by 0.03% hydrogen peroxide containing sodium azide for 5 minutes

- wash slides with 1xTBS twice 2 minutes each

- incubate slides in primary antibody diluted with antibody diluent or negative control reagent for 30 minutes

- wash slides with 1xTBS twice 2 minutes each

- incubate slides in Biotinylated link universal (anti-rabbit, anti-mouse, and anti-goat immunoglobulins) in phosphate buffer saline for 15 minutes

- wash slides with 1xTBS twice 2 minutes each

- incubate slides in Streptavidin conjugated to alkaline phosphatase in Tris buffered saline for 15 minutes

- wash slides with 1xTBS twice 2 minutes each

- incubate slides with fast red for 10 minutes

- wash slides with deionized water for 2 minutes

- wash slides with TBS for 2 minutes

- counterstain slides with Mayer's hematoxylin for 6 minutes

- wash slides with TBS for 2 minutes

-wash slides with deionized water for 2 minutes

5. Slides are dehydrated with 70% alcohol, 100% alcohol and Hemo-de
6. Slides are mounted with and coverslipped with a faramount aqueous mounting medium, an aqueous permanent mounting media.

Double immunohistochemical staining

1. Paraffin embedded tissues are deparafinized, and rehydrated in descending grades of alcohol.
2. Sections are heated with antigen retrieval solution at 95°C for 20 minutes and leaved to cool down at room temperature for 20 minutes.
3. Slides are washed in deionized water for 3 minutes and TBS for 3 minutes.
4. Slides are loaded into the autostainer and stained automatically by using following protocol:

- wash slides with 1xTBS twice 2 minutes each

- block endogenous peroxidase by 0.03% hydrogen peroxide containing sodium azide for 5 minutes

- wash slides with 1xTBS twice 2 minutes each

- incubate slides in primary antibody diluted with antibody diluent for 30 minutes

- wash slides with 1xTBS twice 2 minutes each

- incubate slides in peroxidase labeled polymer conjugated to goat anti-mouse immunoglobulins in Tris-HCl buffer for 30 minutes

- wash slides with 1xTBS twice 2 minutes each

- incubate slides with 3,3'diaminobenzidine chromogen in pH 7.5 hydrogen peroxide solution for 5 minutes

- wash slides with deionized water for 2 minutes

- wash slides with TBS for 2 minutes

- incubate slides in doublestain blocking reagent for 3 minutes

- wash slides with TBS for 2 minutes

- incubate slides in primary antibody diluted with antibody diluent for 30 minutes

- wash slides with TBS for 2 minutes

- incubate slides in alkaline phosphatase labeled polymer conjugated to goat anti-rabbit and goat anti mouse immunoglobulin in phosphate buffered for 30 minutes

- wash slides with TBS for 2 minutes

- incubate with fast red in naphthol solution in Tris buffer for 5 minutes

- wash slides with deionized water for 2 minutes

- wash slides with TBS for 2 minutes

- counterstain slides with Mayer's hematoxylin for 6 minutes

- wash slides with TBS for 2 minutes

- wash slides with deionized water for 2 minutes

5. Slides are mounted with and coverslipped with aqueous permanent mounting media.

Controls: Negative control slides are subjected to the same experiment conditions, but a universal control for N-series mouse antibodies is used instead of the primary antibodies.

Tissue samples preparation

Reagents and solutions

Phosphate buffered saline (PBS)

Working solution: 1.3 M NaCl, 70 mM NaH_2PO_4, 30 mM NaH_2PO_4, pH 7.4

To prepare 1 liter of 10X stock PBS solution, dissolve 76.0 g NaCl, 12.46 mM NaH_2PO_4, 4.68 g NaH_2PO_4 in 800 ml of deionized water. Then, adjust pH of solution to 7.4 with 1 N HCl. Finally, adjust volume to 1 liter with deionized water.

To prepare working solution, dilute 1 part of 10x stock solution in 9 part of deionized water.

Tissue freezing solution

Working solution: 15% Dimethyl sulfoxide (DMSO), 85% Dulbecco's modified eagle's medium (DNEM)

To prepare 100 ml of working solution, combine 15 ml of DMSO and 85 ml of DNEM

Tissue collection protocol

1. Collect septal mitral valve leaflets from fresh canine cadavers.
2. Wash tissues with ice cold PBS 3 times 10 minutes each on a rotary shaker.
3. Place tissues into cryostorage tube containing tissue freezing solution.
4. Freeze tissues rapidly in liquid nitrogen or dry ice.
5. Store tissues in a -80C freezer until use.

Protein extraction

Reagents and solutions

Standard solution

Working solution: 10mM Tris HCl pH 8, 1mM dithiothreitol, 2mM $MgCl_2$, 10mM KCl, 100KIU/ml Aprotinin, 0.5mM Pefabloc

To prepare 100 ml of working solution, mix 10 ml of Tris HCl pH 8, 0.015 g dithiothreitol, 0.04 g $MgCl_2$, 0.075 g KCl, 0.93 ml of aprotinin, 0.012 g pefabloc in 100 ml of nanopure water.

Cytoplasmic protein extraction solution

Working solution: 5mM Tris HCl pH 8, 0.5mM dithiothreitol, 1mM $MgCl_2$, 5mM KCl, 50KIU/ml Aprotinin, 0.25 mM Pefabloc 134 mM non-detergent sulfobetaines (NDSB256)

To prepare 50 ml of working solution, dissolve 1.72 g non-detergent sulfobetaines (NDSB256) in 50 ml of standard solution

Membrane protein extraction solution

Working solution: 5mM Tris HCl pH 8, 0.5mM dithiothreitol, 1mM $MgCl_2$, 5mM KCl, 50 KIU/ml aprotinin, 0.25 mM Pefabloc 134 mM non-detergent sulfobetaines (NDSB256), 1% w/v n-Dodecyl-β-D-Maltose

To prepare 50 ml of working solution, dissolve 1.72 g non-detergent sulfobetaines (NDSB256) and 0.5 g n-Dodecyl-β-Maltose in 50 ml of standard solution.

Protein extraction protocol

1. Weight tissue samples approximately 0.1-0.2 g
2. Use sterile scissors to cut up tissues into small pieces.
3. Incubate samples in 0.5 ml of ice cold cytoplasmic protein extraction solution.
4. Vertex samples for 2-3 seconds and incubate at 4C for 1 hour.
5. Centrifuge samples at 17,000g at 4C for 25 minutes. The supernatant is designated the crude extract of cytoplasmic protein. The pellet is retained for extraction of the membrane bound protein.
6. To wash the pellet, resuspend the pellet with cytoplasmic protein extraction solution and incubate at 4C for 30 minutes. Then, Centrifuge at 17,000g at 4C for 20 minutes.
7. To extract membrane protein, resuspend the pellet with 0.5 ml of ice cold membrane protein extraction solution.
8. Vertex samples for 2-3 seconds and incubate at 4C for 1 hour
9. Centrifuge samples at 17,000g at 4C for 25 minutes. The supernatant is designated the crude extract of membrane protein.

Concentration protein samples protocol

1. Use Centricon® centrifugal filter device to concentrate protein from both crude extracts of cytoplasmic and membrane protein.
2. Centrifuge samples at 6500g at 4C for 1.30 hours.
3. Aliquot concentrated protein extracts with volume of 100 µl and stored in -80 C until use.

DC protein assay

Reagents and solutions

REAGENT A- an alkaline copper tartrate solution

REAGENT B- a dilute foline reagent

REAGENT S

Equipments

Microtiter plates

Eppendorf tubes

Pipets accurately delivering 5 µl, 25 µl, and 200 µl

Microplate reader set to 690 nm

Microplate assay protocol

1. Prepare REAGENT A' by mixing 20 µl of REAGENT S into 1 ml of REAGENT A
2. Prepare 0, 1, 2, 4, 6, 8, 10 mg/ml bovine serum albumin standard solution diluted in cytoplasmic protein extraction solution or membrane protein extraction solution.
3. Pipet 5 µl of standards and samples into a clean, dry microtiter plate.
4. Add 25 µl of REAGENT A' into each well.
5. Add 200 µl REAGENT B into each well.
6. After 10 minutes, absorbances can be read at 690 nm.
7. Plot a curve of values obtained from standards optical density versus µg protein. The concentration of protein samples is calculated from the standard curve.

Gel electrophoresis

Reagents and solutions

MagicMark™ XP Western protein standard

2-mercaptoethanol

Tris-glycine SDS sample buffer

Working solution: Tris HCl 0.5 M, Glycerol 10%, SDS 2%, Bromophenol Blue 0.0025%, pH 6.8

To prepare 20 ml of tris-glycine SDS sample buffer, mixed 0.5 M Tris-HCl, pH 6.8 2.5 ml, glycerol 2.0 ml, 10% (w/v) SDS 4.0 ml and 0.1% bromophenol 0.5 ml in 10.0 ml deionized water. Keep in 4°C until required.

Tris-glycine running buffer

Working solution: Tris-base 25 mM, Glycine 192 mM, SDS 0.1%, pH 8.3

To prepare 1000 ml 10x stock solution, dissolved Tris Base 29 g, Glycine 144 g, and SDS 10 g in 1 liter deionized water.

To prepare working solution, dilute 1 part of 10x stock solution in 9 part of deionized water. 1x running buffer should be pH 8.3. Do not add acid or base to adjust pH.

Equipment

4-12 % Tris-glycine polyacrylamide gel (10 well, 1.5 mm thickness)

XCell SureLock™ MiniCell system

Power supply

Streamer or boiling water bath

Eppendorf tubes

Gel electrophoresis protocol

1. Peel off the tape covering the slot on the back of the gel cassette.
2. Pull the comb out and gently wash the cassette wells with 1x running buffer 3 times. Fill the samples wells with running buffer.
3. Assambly the XCell SureLock™ MiniCell system and insert gel cassettes into the machine.
4. Prepare loading samples by mixing 1 volume of samples with 1 volume of Tris-glycine SDS sample buffer and 1:10 volume of 2-mercaptoethanol: protein samples.
5. Heat samples at 85 ˚C for 2 minutes.
6. Spin down protein samples for 1 second and load samples in to wells using micropipette.
7. Load one well with 5 µl western protein standard.
8. Load all unused wells with Tris-glycine SDS sample buffer.
9. Run gel with 125 V for 90 minutes.

Western blotting protocol

Reagents and solutions

Tris-glycine transfer buffer

Working solution: Tris-base 25 mM, Glycine 192 mM, 20% methanol, pH 8.3

To prepare 1000 ml Tris-glycine transfer buffer, dissolved Tris base 3.03 g and Glycine 14.42 g in methanol 200 ml. Add deionized water to 1000 ml.

Tris buffered saline with Tween 20 (TBST)

Working solution: 10 mM Tris HCl, 150 mM NaCl, 0.01% Tween 20, pH 8.0

To prepare working solution, prepare 1 liter of 1x TBS from the 10x stock add 0.1 ml of Tween 20 to a final concentration of 0.01%.

Blocking solution

Working solution: 5% bovine serum albumin (BSA) in TBST

To prepare working solution: mix 5 ml of 10% (BSA) with 5 ml TBST.

Antibody dilution solution

Working solution: 1% instant nonfat dry milk in TBS

To prepare working solution: dissolve 1 g of instant nonfat dry milk in 100 ml of TBS.

Chemiluminescent reagent

Supersignal West Femto, Piece

Monoclonal antibodies

Antibody	Clone	Company	Concentration
α-smooth muscle actin	1A4	Dako	1:400
$5HT_{2B}R$	A72-1	BD biosciences	2 μg/ml
Tryptophan hydroxylase	WH-3	Sigma-Aldrich	1:500
Serotonin transporter	4A2.2	Advanced targeting system	1:500
Total ERK1/2	ERK7D8	MBL	1 μg/ml
Phosphorylated ERK1/2	12D4	millipore	0.5 μg/ml
LAP TGF β1	27235	R&D system	2 μg/ml
TGFβ1 receptor I	V22	Santa Cruz Biotechnology	1:100
TGFβ1 receptor II	L21	Santa Cruz Biotechnology	1:100

Equipments

Nitrocellulose membrane (15x15 cm, 0.2 μm pore size)

Filter papers

Blotting pads

XCell II Surelock Minicell blotting system Blot Module

Power supply

Plastic box (15x15x2 cm^3)

Rotary shaker

CCD camera

Protein transferring protocol

1. Soak nitrocellulose membrane, filter papers and blotting pads in transfer buffer for 30 minutes
2. Remove the gel from the gel cassette and place it on the wet filter paper. Use a pipette to roll out air bubbles.
3. After wetting the gel, place a wetted sheet of nitrocellulose membrane on top of the gel. Remove air bubbles with a pipette.
4. Place a wetted sheet of a filter paper over the nitrocellulose and roll a pipette over the sandwich to remove any air bubbles.
5. Place soaked blotting pads into the blot module.
6. Place the gel assembly on top of the blotting pads.
7. Add blotting pads on top of the gel assembly, close the blot module.
8. Run the transfer at 25 V for 90 minutes.

Western blotting protocol

1. Wash the nitrocellulose membrane with deionized water 2 times 5 minutes each.
2. Incubate the membrane in the blocking solution for 30 minutes.
3. Incubate the membrane in primary antibody diluted in the antibody dilution solution at 4°C overnight.
4. Wash the membrane with TBST 3 times 10 minutes each.
5. Incubate the membrane in secondary antibody conjugated with horse radish peroxidase diluted in antibody dilution for 1 hour.
6. Wash the membrane with TBST 3 times 10 minutes each.
7. Soak the membrane with the chemiluminescent reagent. Signals are demonstrated using CCD camera.